Upgrading the toolbox for fermentation of crude syngas:

Process characterization for complete carbon usage, cyanide adaption and production of C$_4$ components

zur Erlangung des akademischen Grades eines

DOKTORS DER INGENIEURWISSENSCHAFTEN (DR.-ING.)

der KIT-Fakultät für Chemieingenieurwesen und Verfahrenstechnik des

Karlsruher Instituts für Technologie (KIT)

genehmigte

DISSERTATION

von

Dipl.-Ing. Florian Oswald

aus Ellwangen an der Jagst

Referent: Prof. Dr. rer. nat. Christoph Syldatk

Korreferent: Prof. Dr. Nicolaus Dahmen

Tag der mündlichen Prüfung: 07.12.2018

For Kathrin I. Oswald

Run, you clever boy … and be a Doctor.

Clara Oswald, *Doctor Who*

Declaration

I declare that this thesis represents my own work and that I have written this thesis independently by myself, without the use of other documents or sources beyond those stated in the references.

Karlsruhe, 25th of October 2018

Florian Oswald

Preamble

Parts of this thesis have been published as peer reviewed research articles. They describe the main findings of my work. At the end of any applicable paragraph a reference note states the publication in which the content has been previously published. The text of these paragraphs is partially identical to the content of the publications. Layout, citation style, figures and formatting have been modified and adjusted to the style of this dissertation. Chapters that contain contents of previously published work are as follows:

Chapters with the heading "Elevated pressure for increased mass transfer" and the conclusions contain content of the publication

Oswald, F., Stoll, I. K., Zwick, M., Herbig, S., Sauer, J., Boukis, N. and Neumann, A. Formic Acid Formation by *Clostridium ljungdahlii* at Elevated Pressures of Carbon Dioxide and Hydrogen. *Frontiers in Bioengineering and Biotechnology*. 2018. 6:6. doi: 10.3389/fbioe.2018.00006.

Chapters with the heading "Influence of Cyanide on growth and product formation of *Clostridium ljungdahlii*" and the conclusions contain content of the publication

Oswald, F., Zwick, M., Omar, O., Hotz, E. N. and Neumann, N. Growth and Product Formation of *Clostridium ljungdahlii* in Presence of Cyanide. *Frontiers in Microbiology*. 2018. 9:1213. doi: 10.3389/fmicb.2018.01213.

Chapters with the heading "Process link-up: From syngas to malic acid" and the conclusions contain content of the publication

Oswald, F., Dörsam, S., Veith, N., Zwick, M., Neumann, A., Ochsenreither, K. and Syldatk, C. Sequential Mixed Cultures: From Syngas to Malic Acid. *Frontiers in Microbiology*. 2016. 7:891. doi: 10.3389/fmicb.2016.00891.

Acknowledgements

List of Publications

Peer reviewed original research papers

Henkel, M., Zwick, M., Beuker, J., Willenbacher, J., Baumann, S., Oswald, F., Neumann, A., Sieman-Herzberg, M., Syldatk, C. and Hausmann, R. Teaching bioprocess engineering to andergraduates: Multidisciplinary hands-on training in a one-week practical course. *Biochemistry and Molecular Biology Education*. 2015. 43(2):189-202. doi: 10.1002/bmb.20860.

Oswald, F., Dörsam, S., Veith, N., Zwick, M., Neumann, A., Ochsenreither, K. and Syldatk, C. Sequential Mixed Cultures: From Syngas to Malic Acid. *Frontiers in Microbiology*. 2016. 7:891. doi: 10.3389/fmicb.2016.00891.

Ramaloko, W. T., Koen, N., Polliack, S., Aliyu, H., Lebre, P. H., Mohr, T., Oswald, F., Zwick, M., Zeigler, D. R., Neumann, A., Syldatk, C., Cowan, D. A., De Maayer, P. High Quality Draft Genomes of the Type Strains *Geobacillus thermocatenulatus* DSM 730[T], *G. uzensis* DSM 23175[T] and *Parageobacillus galactosidasius* DSM 18751[T]. *Journal of Genomics*. 2018. 6:20-23. doi: 10.7150/jgen.22986.

Oswald, F., Stoll, I. K., Zwick, M., Herbig, S., Sauer, J., Boukis, N. and Neumann, A. Formic Acid Formation by *Clostridium ljungdahlii* at Elevated Pressures of Carbon Dioxide and Hydrogen. *Frontiers in Bioengineering and Biotechnology*. 2018. 6:6. doi: 10.3389/fbioe.2018.00006.

Oswald, F., Zwick, M., Omar, O., Hotz, E. N. and Neumann, N. Growth and Product Formation of *Clostridium ljungdahlii* in Presence of Cyanide. *Frontiers in Microbiology*. 2018. 9:1213. doi: 10.3389/fmicb.2018.01213.

Infantes, A., Zwick, M., Stoll, I. K., Boukis, N., Oswald, F. and Neumann, A. Syngas Fermentation at Elevated Pressure. *Chemie Ingenieur Technik*. 2018. 90(9):1283-1284. doi: 10.1002/cit.201855330.

Book chapter

Neumann, A., Dörsam, S., Oswald, F. and Ochsenreither, K.. Microbial Production of Value-Added Chemicals from Pyrolysis Oil and Syngas. In: M. Xian (Hrsg.) *Sustainable Production of Bulk Chemicals*. Dordrecht: Springer Science+Business Media. 2016.

Conference talks

Oswald, F., Dörsam, S., Zwick, M., Neumann, A., Ochsenreither, K. and Syldatk, C. Upgrading the Toolbox for Fermentation of (Crude) Syngas. Talk at the annual conference of the VAAM in Jena 2016.

Oswald, F., Dörsam, S., Zwick, M., Neumann, A., Ochsenreither, K. and Syldatk, C. Upgrading the Toolbox for Fermentation of (Crude) Syngas: From Syngas to Malic acid. Talk at the 2nd C1net conference in Nottingham 2016.

Oswald, F., Zwick, M., Omar, O., Hotz, E. N. and Neumann, A. Towards utilization of crude syngas: growth and Product formation of *Clostridium ljungdahlii* in presence of cyanide. Talk at the "Clostridium XV" conference in Munich 2018.

Poster Presentations

Oswald, F., Ochsenreither, K. and Neumann, A. Identification and Heteroloous Expression of Gene Encoding for the Alternariol-*O*-Methyltransferase of *Alternaria alternata.* Poster at the annual conference of the VAAM in Dresden 2014.

Oswald, F. and Neumann, A. Fermentation of crude syngas from the bioliq® plant Karlsruhe. Poster at the 1st C1net conference in Nottingham 2015.

Oswald, F., Zwick, M. and Neumann, A. Impact of Ammonia and Cyanide on Fermentation of (Crude) Syngas. Poster at the annual conference of the VAAM in Jena 2016.

Oswald, F., Zwick, M., Syldatk, C. and Neumann, A. Impact of process parameters and impurities on syngas fermentation with *Clostridium ljungdahlii* and production of malic acid from syngas. Poster at the annual conference of the VAAM in Würzburg 2017.

Oswald, F., Dörsam, S., Zwick, M., Neumann, A., Ochsenreither, K. and Syldatk, C. Upgrading the Toolbox for Fermentation of (Crude) Syngas: From Syngas to Malic acid. Poster at the Himmelfahrtstagung of the DECHEMA 2017.

Abstract

In recent years, synthesis gas, or syngas, industrial exhaust gases and other C_1 molecules came into focus as interesting substrates for the biotechnological production of fuel and bulk chemicals. In this context, syngas is a mixture of hydrogen, carbon monoxide and carbon dioxide, derived from gasification of biomass and organic waste streams, like sewage sludge and municipal waste. Organisms that can be used for syngas fermentation belong to the class of acetogenic bacteria. They have access to a unique pathway of carbon fixation that combines two molecules of CO or CO_2 via subsequent reactions into one molecule of acetyl-CoA. This is called reductive acetyl-CoA pathway or Wood-Ljungdahl-Pathway (WLP). Acetic acid, ethanol, butyric acid, *n*-butanol or 2,3-butandiol are natural products of this metabolic route. One of the model organisms of acetogenic bacteria is *Clostridium ljungdahlii*. Efforts of synthetic biology, genetic engineering and process development focus mainly on enhancing the production of natural C_4 products or introducing new pathways for the production of C_4 and C_6 chemical. However, bioenergetic constrains prevent higher yields of those products, since acetogenic bacteria gain the most energy from the formation of acetic acid or ethanol, which are the preferred products.

One of the limiting steps in syngas fermentation, that is often mentioned, is mass transfer of hydrogen and carbon monoxide from the gaseous phase into the aqueous culture broth. Possible routes of enhancing mass transfer are the increase of gas-liquid interfacial area by increased stirrer speed and/or increased gas feed rate. For production of low value chemicals from syngas, such as ethanol, the increase of mass transfer by means of increased stirrer speed is uneconomic at larger scales. Another possibility would be, to raise the saturation solubility of hydrogen and carbon monoxide, by increasing the partial pressure of these components. However, higher liquid concentrations of hydrogen or carbon monoxide can lead to inhibitory effects and reduce the process efficiency. Though, crude syngas also contains minor constituents like nitric oxides, hydrogen sulfide or hydrogen cyanide, most research groups work with purified or synthetic mixtures of syngas. Working with crude or partially purified syngas could further increase the economics of syngas fermentation, since gas cleaning and conditioning is expensive. Unfortunately, most of the minor constituents of syngas are known catalyst poisons and even though, microorganisms are in general more robust than chemical catalysts, studies with crude cell extract or purified enzymes showed that some of the

impurities in crude syngas inhibit central enzymes of the WLP. Actual data on the effects of gas impurities on whole cells of acetogenic bacteria is scarce.

This thesis investigates the following topics:

- The influence of increasing mass transfer by increasing gas feed rate
- Increased mass transfer by increased system and partial pressure of substrates
- The influence of cyanide on growth and product formation of *C. ljungdahlii*
- Process link-up via sequential mixed culture for production of malic acid

Since mass transfer is considered a main limiting parameter in syngas fermentation, two stirrer set-ups, with one that allows partial recirculation of the headspace gas, have been tested for their mass transfer properties at different stirrer speeds and gas feed rates. It has been found that a stirrer speed of $800 \, min^{-1}$ provides the highest mass transfer coefficients ($k_l a$) for all three gas feed rates. Subsequent batch cultivations in 1.5 L-scale showed, that despite increasing $k_l a$-values with increasing gas feed rate, the substrate conversion efficiency is higher at lower gas feed rates. Increasing the gas feed rate does enhance the mass transfer coefficient, though, the effect is small compared to increasing the stirrer speed and does also reduce the bubble residence time. With less time to be completely absorbed from the gaseous phase, unused substrates leave the bioreactor and are wasted. Here, the stirrer set-up with partial recirculation of the headspace gas allows to reintroduce parts of otherwise wasted substrates. This resulted in better conversion efficiencies despite a lower $k_l a$-value and stresses the importance of gas recirculation for efficient substrate conversion.

Due to the possible drawbacks of increased mass transfer by increased gas feed rate, experiments at elevated substrate pressure should show if this alternative to increasing mass transfer will enhance substrate conversion efficiency. In cooperation during the PhD thesis of Katharina Stoll from the group of Dr. Boukis at IKFT, KIT Campus North, the 1.5 L-scale has been scaled-up to 2.5 L-scale. Levels of absolute system pressures of 1 bar, 4 bar and 7 bar with a constant volumetric mass-flow rate of substrates and constant gas composition over all pressure levels have been investigated. To avoid inhibitory effects by high CO partial pressures, a gas mixture only consisting of CO_2, H_2 and N_2 as a carrier was used. It was shown for the first time, that with increasing substrate pressure growth of *C. ljungdahlii* declined and product formation stagnated, although the gas mixture did not contain carbon monoxide. Furthermore, the product composition shifted from 2.4 % formic acid, 86.5 %

acetic acid and 11.1 % ethanol at atmospheric conditions towards 82.7 % formic acid, 15.6 % acetic acid and 1.7 % ethanol at a total gas pressure of 7 bar. However, since the amount of substance flow rate was kept constant over all pressure stages instead of the gas volume feed rate, the overall product yield and conversion efficiency of the experiments at 7 bar is 7.5 times higher than previously reported.

Cyanide is considered one of the most critical components of crude syngas that need to be removed from the gas stream prior to fermentation. The results in this thesis are the first to show, that *C. ljungdahlii* can be adapted to growth in presence of up to 1.0 mM cyanide under heterotrophic conditions and up to 0.1 mM cyanide under autotrophic conditions. After adaption, maximum growth rate and biomass concentration is unaffected by cyanide up to the indicated concentrations. Product yields from heterotrophic conditions indicate that at 1.0 mM cyanide CODH activity is completely inhibited and the WLP is inactive. This is confirmed by results under autotrophic conditions where no growth could be observed at 1.0 mM cyanide. While the difference in growth is an increasing lag- phase with increasing cyanide concentrations, the product spectrum shifts from 97 % acetic acid and 3 % ethanol at 0 mM cyanide to 20 % acetic acid and 80 % ethanol at 1.0 mM cyanide for cultures growing on fructose and 80 % acetic acid and 20 % ethanol at 0.1 mM cyanide (syngas).

To circumvent the limitations of the production of desirable C_4 or C_6 products from syngas, a process has been developed together with Dr.-Ing. Stefan Dörsam, to produce malic acid from syngas as initial carbon source (see also chapter four of the PhD thesis *Evaluation of Renewable Resources as Carbon Sources for Organic Acid Production with Filamentous Fungi*). The production of malic acid by filamentous fungi like *Aspergillus oryzae* has high yields of product per gram substrate but is commonly limited to sugars as substrate. The process developed together with Dr.-Ing. Stefan Dörsam, shows for the first time, that it is possible to produce malic acid from syngas in a two stage process with acetic acid as linking metabolite. Due to the need of nitrogen limitation in the fungal fermentation stage of this sequential mixed culture, it was necessary to reduce the initial ammonia contend of the syngas fermentation medium. During the syngas fermentation stage, hydrogen and carbon monoxide from the gas stream have been converted to acetic acid (88.9 %) and ethanol (11.1 %) with a yield of 0.86 g g^{-1}. In the fungal fermentation stage, the previously formed acetic acid has been converted to malic acid with a yield of 0.33 g g^{-1}. This resulted in an overall yield of 0.28 gram malic acid per gram hydrogen and carbon monoxide fed to the process.

Zusammenfassung

Synthesegas (Syngas), Industrieabgase und andere C_1-Moleküle haben sich in den letzten Jahren als interessante Substrate für die biotechnologische Produktion von Kraftstoffen und Plattformchemikalien herauskristallisiert. Syngas ist in diesem Zusammenhang eine Mischung aus Wasserstoff, Kohlenmonoxid und Kohlendioxid, welche über Vergasung von Biomasse und organischen Abfällen (z. B. Kommunalabfälle oder Klärschlamm) hergestellt wird. Organismen, die in der Syngas-Fermentation eingesetzt werden können, gehören zur Klasse der acetogenen Bakterien. Diese nutzen einen einzigartigen Stoffwechselweg zur Kohlenstofffixierung in dem zwei Moleküle CO oder CO_2 über sequenzielle Reaktionen zu einem Molekül Acetyl-CoA kondensiert werden. Dieser wird reduktiver Acetyl-CoA Weg oder Wood-Ljungdahl-Stoffwechselweg (WLS) genannt. Natürliche Produkte die aus dem WLS abgeleitet werden können sind Essigsäure, Ethanol, Buttersäure, *n*-Butanol oder 2,3‑Butanidol. *Clostridium ljungdahlii* ist einer der Modelorganismen für acetogene Bakterien. Bisher konzentrieren sich Forschungen der synthetischen Biologie, Gentechnik und Prozessentwicklung hauptsächlich darauf, die Produktion natürlicher C_4-Moleküle eines Organismus zu erhöhen oder neue Stoffwechselwege für C_4- und C_6-Moleküle zu implementieren. Bioenergetische Limitierungen verhindern jedoch die Produktion dieser Zielprodukte mit hohen Ausbeuten. Dies liegt darin begründet, dass acetogene Bakterien bevorzugt Essigsäure oder Ethanol herstellen, da dies einen höheren Energiegewinn für die Zelle bedeutet, als die Produktion von C_4- oder C_6-Molekülen.

Die Limitierung des Massentransfers von Kohlenmonoxid und Wasserstoff von der Gasphase in die Flüssigphase ist einer der Punkte, die häufig im Zusammenhang mit Limitierungen der Syngas-Fermentation in der Literatur genannt werden. Möglichkeiten den Massentransfer zu verbessern sind zum einen die Vergrößerung der Phasengrenzfläche Gas-Flüssig durch erhöhte Rührerdrehzahl und/oder Begasungsrate und zum andern, die Erhöhung der Sättigungskonzentration von Kohlenmonoxid und Wasserstoff durch das Anheben des Partialdruckes. Sollen allerdings Produkte mit geringer Wertschöpfung produziert werden, so hat sich gezeigt, dass die Verbesserung des Massentransfers über Erhöhung der Rührerdrehzahl nicht wirtschaftlich ist. Während die Verbesserung des Massentransfers über die Steigerung der Begasungsrate den Umsatz beeinträchtigen kann, führen höhere Gelöstkonzentrationen von Wasserstoff und Kohlenmonoxid zu Stoffwechselinhibierungen und dadurch zu einer Reduktion der Effizienz des Prozesses.

Da Roh-Syngas neben den genannten Hauptkomponenten auch Verunreinigungen wie Stickoxide, Schwefelwasserstoff oder Blausäure enthält, arbeiten viele Forschergruppen mit gereinigten oder synthetischen Syngas-Mischungen. Jedoch ist die Reinigung von Gas ein kostenintensiver Schritt. Die Möglichkeit ungereinigtes oder nur Teilgereinigtes Syngas einsetzten zu können, würde die Wirtschaftlichkeit jedes Syngas-Fermentationsprozesses verbessern. Leider sind die meisten, der in Roh-Syngas enthaltenen Stoffe, bekannte Katalysatorgifte. Bakterien sind zwar generell robuster gegenüber Katalysatorgiften als chemische Katalysatoren, aber Studien mit Extrakten aus aufgeschlossenen Zellen oder gereinigten Enzymen zeigen, dass manche der Verunreinigungen die zentralen Enzyme des WLS inhibieren. Daten, die den Effekt von Syngas-Verunreinigungen auf ganze Zellen acetogener Bakterien zeigen, sind dagegen nur wenige in der Literatur zu finden.

Im Zuge dieser Doktorarbeit wurden die folgenden vier Themen untersucht:

- Der Einfluss erhöhten Massentransfers durch gesteigerte Begasungsrate
- Verbesserung des Massentransfers durch erhöhen des Systemdrucks und Partialdrucks der Substrate
- Der Einfluss von Cyanid auf Wachstum und Produktbildung von *C. ljungdahlii*
- Prozesskopplung über sequentielle Mischkultur zur Produktion von Äpfelsäure

Hinsichtlich der Massentransfereigenschaften wurden zwei Rührerandordnungen mit drei unterschiedlichen Begasungsraten getestet. Eine ermöglichte die Teilweise Rückführung von Gas aus dem Kopfraum des Reaktors. Es zeigte sich für alle Begasungsraten, dass das Maximum des volumenbezogenen Stoffübergangskoeffizienten ($k_l a$-Wert) bei einer Rührerdrehzahl von $800 \, min^{-1}$ liegt. Über Batch-Kultivierungen im $1,5 \, L$ Maßstab konnte gezeigt werden, dass trotz steigender $k_l a$-Werte mit steigender Begasungsrate, die Konversion von Substraten zu Produkten bei höheren Begasungsraten ineffizienter wird. Der Einfluss der Begasungsrate auf den $k_l a$-Wert ist klein, verglichen mit dem Einfluss der Begasungsrate. Zudem Verringern steigenden Begasungsraten die Verweilzeit der Gasblasen in der Flüssigkeit. Dadurch wird mit steigender Begasungsrate zunehmend ungenutztes Substrat aus dem Reaktor ausgetragen. In diesem Punkt zeigt sich die Rühreranordnung, die eine Teilrückführung von Gas aus dem Kopfraum des Reaktors gestattet, überlegen und erreicht bessere Konversionseffizienten obwohl der $k_l a$-Wert im Vergleich zur anderen Rühreranordnung kleiner ist.

Aufgrund der möglichen Nachteile, die mit einer Steigerung des Massentransfers durch Erhöhung der Begasungsrate verbunden sind, sollen Experimente mit erhöhtem Druck zeigen, ob dies eine Alternative darstellt, um den Massentransfer zu verbessern. Zu diesem Zweck wurden Experimente aus dem 1,5 L Maßstab in den 2,5 L Maßstab hochskaliert und Versuche bei absoluten Systemdrücken von 1 bar, 4 bar und 7 bar, bei ansonsten konstantem volumenbezogenen Massenfluss der Gase und konstanter Gaszusammensetzung, durchgeführt. Um mögliche Inhibierungen durch erhöhte Gelöstkonzentrationen von Kohlenmonoxid zu vermeiden wurde hierfür ein Gasgemisch aus CO_2, H_2 und N_2 verwendet. Für dieses Gasgemisch konnte erstmals gezeigt werden, dass eine direkte Steigerung der Substratpartialdrücke keine Verbesserungen bei Wachstum und Produktbildung zur Folge hat. Im Gegenteil, das Wachstum ging mit steigendem Druck zurück und die Produktbildung stagnierte. Darüber hinaus änderte sich die Produktzusammensetzung von 2,4 % Ameisensäure, 86,5 % Essigsäure und 11,1 % Ethanol bei atmosphärischem Druck zu 82,7 % Ameisensäure, 15,6 % Essigsäure und 1,7 % Ethanol bei einem Systemdruck von 7 bar. Da aber der Massenfluss an Substraten über alle Druckstufen konstant gehalten wurde, war die Produktausbeute und Konversionseffizienz bei 7 bar um den Faktor 7,5 höher, als bisher in der Literatur beschrieben.

Die Literatur betrachtet Cyanid als die kritischste Komponente in Roh-Syngas, die erst aus dem Gasstrom entfernt werden muss, bevor das Gas für die Fermentation eingesetzt werden kann. Die Ergebnisse in dieser Doktorarbeit zeigen jedoch zum ersten mal, dass *C. ljungdahlii* unter heterotrophen Bedingungen an bis zu 1,0 mM Cyanid adaptiert werden kann. Unter autotrophen Bedingungen ist eine Adaptation bis zu 0,1 mM Cyanid möglich. Nachdem die Zellen an Cyanid adaptiert wurden, werden die maximale Wachstumsrate und Biomasse nichtmehr von Cyanid beeinflusst, bis die oben genannten Grenzwerte erreicht sind. Die Ausbeutekoeffizienten aus Versuchen unter heterotrophen Bedingungen zeigen, dass bei einer Cyanidkonzentration von 1,0 mM die Aktivität der Kohlenmonoxiddehydrogenase (CODH) vollständig inhibiert und der WLS inaktiv ist. Die Ergebnisse unter autotrophen Bedingungen bestätigen dies, hier konnte bei einer Cyanidkonzentration von 1,0 mM weder Wachstum noch Produktbildung beobachtet werden. Im Zusammenhang mit der Inhibierung der CODH konnte zudem erstmals beobachtet werden, dass die Produktzusammensetzung sich mit steigender Cyanidkonzentration ändert und mehr Ethanol gebildet wird. Bei 0 mM Cyanid bestehen die Produkte zu 97 % aus Essigsäure und 3 % aus Ethanol während bei 1,0 mM Cyanid die Produktzusammensetzung 20 % Essigsäure und 80 % Ethanol ist (heterotrophe

Kulturen). Unter autotrophen Bedingungen (Wachstum auf Syngas) setzen sich die Produkte in Gegenwart von 0,1 mM Cyanid zu 80 % aus Essigsäure und zu 20 % aus Ethanol zusammen.

Um die Limitierungen bei der Produktion von gewünschten C_4 oder C_6 Molekülen zu umgehen, wurde zusammen mit Dr.-Ing. Stefan Dörsam ein Prozess zur Produktion von Äpfelsäure (2-Hydroxybernsteinsäure) mit syngas als initiale Kohlenstoffquelle entworfen (vgl. Kapitel vier der Doktorarbeit *Evaluation of Renewable Resources as Carbon Sources for Organic Acid Production with Filamentous Fungi*). Die Herstellung von Äpfelsäure mit filamentösen Pilzen, wie zum Beispiel *Aspergillus oryzae*, resultiert in hohen substratbezogenen Ausbeuten. Allerdings sind diese Verfahren bisher auf Zucker als Kohlenstoffquelle limitiert. In Kooperation mit Dr.-Ing. Stefan Dörsam wurde ein zweistufiger Prozess entworfen der es ermöglicht Äpfelsäure aus Syngas herzustellen. Bei dieser sequentiellen Mischkultur ist Essigsäure der Metabolit, der beide Prozessstufen miteinander verbindet. Da die *A. oryzae*-Stufe dieses Prozesses auf Stickstofflimitierung angewiesen ist, war es zunächst notwendig, die Konzentration an Ammoniumchlorid im Medium für die Syngasfermentation so weit zu reduzieren, dass am Ende der Syngas-Stufe kein Ammonium-Stickstoff mehr enthalten ist. Während der Syngasfermentation wurden Wasserstoff und Kohlenmonoxid zu Essigsäure (88,9 %) und Ethanol (11,1 %) umgewandelt. Die Ausbeute lag bei 0,86 g g^{-1}. Aus dieser Mischung wurde während der *A. oryzae*-Stufe des Prozesses die Essigsäure in Äpfelsäure umgewandelt. Hierbei lag die Ausbeute bei 0,33 g g^{-1}. Daraus ergab sich eine Gesamtausbeute von 0,28 Gramm Äpfelsäure pro Gramm eingesetztem Wasserstoff und Kohlenmonoxid. Damit konnte erstmalig gezeigt werden, dass über Verfahrenskopplung höhere Ausbeuten an hochwertigen C_4-Molekülen erreicht werden können.

List of symbols

$\widetilde{M}_{H_2O}$	molar weight of water, g mol^{-1}
$\widetilde{M}_i$	molar mass of I, g mol^{-1}
$\dot{n}_i$	amount of substance flow rate, mol min^{-1}
$\dot{V}_g$	volume flow rate of gas, L min^{-1}
$\widetilde{V}_M$	molal Volume of dissolved gas at normal boiling point, $\text{mL g}^{-1} \text{ mol}^{-1}$
$c_{O_2}^*$	saturation concentration of oxygen in water, mol L^{-1}
c_{O_2}	concentration of oxygen in water, mol L^{-1}
$Y_{P/S}^{**}$	product yield based on overall fed substrates, g g^{-1}
$Y_{P/S}^*$	product yield based on consumed substrates, g g^{-1}
ϕ_{H_2O}	association parameter for i in water, -
Δm_{Sub}	mass of consumed substrates, g
D	inner diameter of reactor, m
d	stirrer diameter, m
$D_{1.5}$	reactor diameter in 1.5 L-scale, m
$d_{1.5}$	stirrer diameter in 1.5 L-scale, m
$D_{2.5}$	reactor diameter in 2.5 L-scale, m
$d_{2.5}$	stirrer diameter in 2.5 L-scale, m
$\boldsymbol{D}_i$	diffusion coefficient of substance i in water, $\text{m}^2 \text{ s}^{-1}$
Δm_{Sub}	mass of consumed substrates, g
e_i	consumption ratio of substance i, -
E_i	ratio of accumulation for substance i, -
g	gravitational force, m s^{-2}
$h_{l,\,1.5}$	filling level in 1.5 L-scale, m

$h_{l,\,2.5}$	filling level in 2.5 L-scale, m
$k_l a$	volumetric mass transfer coefficient, s^{-1}
$l_{S,\,1.5}$	length of the stirrer shaft in 1.5 L-scale, m
$l_{S,\,2.5}$	length of the stirrer shaft in 2.5 L-scale, m
n	stirrer speed, min^{-1}
Ne	Newton number, -
$n_{i,\,R}$	consumed amount of substance of i, mol
p	absolute pressure, bar
P	power consumption of the stirrer, W
Q	Gas-throughput number, -
Re	Reynolds number, -
T	temperature, K
t	time, s
τ_p	time constant of an dissolved oxygen probe, s
υ	superficial gas velocity, $m\,s^{-1}$
V_l	liquid volume of the reactor, L
x_i	mole fraction of substance i, -
β_i	concentration of i, $g\,L^{-1}$
β_i	mass concentration of substance i, $g\,L^{-1}$
ϑ	relative temperature, °C
v	dynamic viscosity of water, $m^2\,s^{-1}$
ρ	density of water, $kg\,m^{-3}$

List of abbreviations

MES	2-(N-morpholino)ethansulfonic acid
TES	Trace element solution
STR	Stirred tank reactor
ORP	Oxidation reduction potential
BLT	Institute of Process Engineering in Life Sciences
GC	Gas chromatograph
FFAP	Free Fatty Acid Phase
MFC	Mass-Flow-Controller
pHICR	pH indicate, control and record
TICR	Temperature indicate control and record
ORPIR	ORP indicate and record
AF	Anti-foam
RMR	Rushton-Marine-Rushton
RRB	Rushton-Rushton-Baffles
ATP	Adenosine triphosphate
WLP	Wood-Ljungdahl-Pathway
Fd	Ferredoxin
CODH/Acs	Carbon monoxide dehydrogenase-acetyl-CoA synthase complex
CODH	carbon monoxide dehydrogenase
SLP	Substrate level phosphorylation
SEM	Scanning electron microscope
CDW	Cell dry weight
IKFT	Institute of Catalysis Research and Technology
OD	Optical density
NH_4-red	NH_4-reduced media
HPF	High pressure fermentation
N/A	No data available
WT	wild type
MFM	Mass-Flow-Meter

Content

1. Introduction

Nowadays most bulk chemicals are still based on fossil fuels like crude oil and natural gas. Due to dwindling resources and climate change, it is necessary to develop sustainable methods to produce industrially relevant chemicals. In recent years, industrial exhaust gases such as steel mill off-gas [Köpke *et al.* 2011] and synthesis gas (syngas), a mixture of H_2, CO and CO_2, deriving from gasification of biomass and waste streams like sewage sludge and municipal waste [Hammerschmidt *et al.*, 2011; Rokni 2015] as well as other C_1 molecules, came into focus as interesting substrates for biotechnological applications [Daniell *et al.* 2012, Bengelsdorf et al. 2013]. Syngas fermentation uses acetogenic bacteria, a class of bacteria using a unique pathway [Müller 2003] to combine two molecules of CO or CO_2 via subsequent reactions into one molecule of acetyl-CoA [Diekert and Wohlfarth 1994]. Natural products of that metabolic pathway are acetic acid, ethanol, butyric acid, butanol or 2,3-butandiol. However, the highest energy gain for acetogenic bacteria is achieved by the formation of C_2 molecules (acetic acid and ethanol) which are therefore the preferred products with reported concentrations of up to 60.3 $g\,L^{-1}$ acetic acid [Kantzow and Weuster-Botz 2016]. Efforts of process development, synthetic biology and genetic engineering focus on an increase in yield of natural C_4 [Fernández-Naveira, *et al.* 2016, Köpke *et al.* 2010, Lewis *et al.* 2007] and C_6 products [Fernández-Naveira *et al.* 2017, Doll *et al.* 2018] and introducing new metabolic routes to new products like acetone [Banerjee *et al.* 2014]. Today however, bioenergetic constrains hamper higher yields of desired products [Bertsch and Müller 2015] and production of C_4 or C_6 products is always accompanied by a 3 to 60-fold higher production of acetic acid or ethanol [Banerjee *et al.* 2014, Fernández-Naveira *et al.* 2017, Doll *et al.* 2018].

One of the limiting steps on the way to higher productivity with gaseous substrates is the mass transfer of sparingly soluble compounds from the gaseous to the liquid phase [Worden *et al.* 1997]. The common approach to enhance gas-liquid mass transfer – the increase of gas-liquid interfacial area by increased stirrer speed or gas feed rate – may not be economically feasible when producing low value products like fuels [Bredwell et al., 1999]. Therefore, Vega *et al.* [1989a, 1989b] and Schmid and Cooney [1986] increased gas-liquid mass transfer of carbon monoxide by increasing the partial pressure. In doing so, they found that immediate increase of pressure results in reduced growth and product formation due to inhibitory effects of CO [Vega *et al.* 1989a, b]. This could be shown to be overcome by a stepwise increase in CO

partial pressure [University of Arkansas 1993]. Cultivation with only carbon dioxide and hydrogen in the gas stream would circumvent inhibition caused by carbon monoxide. For *Acetobacterium woodii*, studies with gas mixtures devoid of carbon monoxide have been conducted by Demler (2012) and Kantzow and Weuster-Botz (2016). They investigate the effect of increased p_{H_2} but leave the effect of carbon dioxide partial pressure out of their consideration. Hence, one part of this thesis focuses on the effects of increased pressure on growth and product formation of *C. ljungdahlii* with a gas mixture devoid of carbon monoxide. Furthermore, this thesis examines the effects of different mass transfer coefficients and stirrer set-ups on substrate consumption with CO containing syngas as substrate. The aim is to investigate if mass transfer limitation can be overcome and whether complete substrate utilization is possible by applying elevated pressure or varying the gas feed rate. Experiments in 1.5 L-scale are used to scale-up process parameters to 2.5 L-scale, where experiments at absolute system pressures of 1 bar, 4 bar and 7 bar are conducted.

Use of syngas in chemical catalysis requires the crude gas to be cleansed of minor constituents to avoid catalyst poisoning. Gas conditioning makes for about 22 % of the total investment costs of biomass to liquid plants (BTL) and 1/3 of the investment costs for gasification alone [Hannula and Kurkela, 2013]. Hence, processes capable of using crude syngas offer an economic advantage over other processes that depend on purified syngas [Ahmed *et al* 2006, Xu *et al*. 2011, Abubackar *et al*. 2011]. In addition to the principal constituents hydrogen, carbon monoxide and carbon dioxide, crude syngas also contains: nitrogen – if air is used as the gasification medium – and variable amounts of C_1 and C_2 hydrocarbons (e. g. methane, ethane, ethylene and acetylene), tar components (e. g. benzene, toluene, xylene and naphthalene), halogens such as hydrogen chloride and hydrogen fluoride, sulfur compounds like hydrogen sulfide, carbonyl sulfide and carbonyl disulfide and nitrogen species such as nitrogen oxides, ammonia and hydrogen cyanide as well as oxygen and reactive oxygen species [Hofbauer et al. 2009]. Feedstock and gasification method impact the concentrations of these minor constituents. Cyanide levels of crude syngas, for example, range from below 25 ppm [Boerrighter et al. 2013] to 2500 ppm [Broer et al. 2015]. Carbon monoxide dehydrogenase and hydrogenase, two important enzymes in the autotrophic metabolism of acetogens, have been shown to be inhibited by many of the above-named impurities [Thauer *et al*. 1974, Ha *et al*. 2007, Grahame and Stadtman 1987, Diekert and Thauer 1978, Anderson *et al*. 1993, Hyman *et al*. 1989, Vega *et al*. 1990, Klasson *et al*., 1992, Hyman and Arp 1988, Krasna and Rittenberg 1954]. Competitive effects and interferences of

inhibition have been described when applying mixtures of catalyst poisons to those enzymes [Thauer *et al.* 1974, Terlesky *et al.* 1986, Grahame and Stadtman 1987, Ensing *et al.* 1989, Hyman *et al.* 1989]. Hence, understanding the effects of syngas impurities is necessary to avoid delays in reaching full-scale production capacity and additional costs when using crude syngas as substrate [Lane 2014]. The removal of gas impurities is named as a crucial point in literature that deals with the usage of syngas or waste gases for syngas fermentation. Many publications describe the effect of minor syngas components on enzymes of the acetogenic metabolism – but those studies usually examine isolated enzymes or cell extracts. So far only few reports can be found in literature about the effects of syngas impurities on growing acetogens, and no reports about the effects of cyanide on growing acetogens exist. Therefore, one part of this thesis investigates the effect of cyanide ions on growth and product formation of *Clostridium ljungdahlii* under heterotrophic and autotrophic conditions in closed serum bottles. Determining a maximum cyanide concentration tolerated by the cells will help in determining whether crude syngas with a certain cyanide load is usable as substrate without further pretreatment.

As described above, production of products with more than two carbon atoms in acetogens faces bioenergetic constrains and is always linked to the by-production of acetic acid or ethanol. To overcome this, different researchers across the globe suggest using the acetic acid or ethanol from syngas fermentation as a substrate to produce other higher-value products [Evonik Industries 2013, Hu *et al.* 2016, Molitor *et al.* 2017, Gildemyn *et al.* 2017, Liebal *et al.* 2018]. Suitable candidates for higher-value products are various dicarboxylic acids – because of their suitability to be used for the synthesis of various polymers – as was summarized by Lee *et al.* [2011]. In 2004, the US Department of Energy selected the C_4 dicarboxylic acids malic acid, fumaric acid and succinic acid to be one of the 12 most important platform chemicals produced from biomass [Werpy and Petersen 2004]. Recently, Liebal *et al.* [2018] reviewed different metabolic routes and process strategies to produce succinic acid. Their outcome is, that the most economic route for succinic acid production is syngas fermentation to acetic acid and conversion of acetic acid to succinic acid by an *E. coli* strain. Malic acid is a C_4 dicarboxylic acid from the list of the US Department of Energy which is still mostly produced from crude oil [Lohbeck *et al.* 2000, Miltenberger 2000]. It can be used for the synthesis of polymers for the food and pharmaceutical industries [Werpy and Petersen 2004], as well as for many other bulk and fine chemicals. Some fungi from the genus *Aspergillus* – like *A. flavus* or *A. oryzae* – produce, under certain stress conditions, sizeable

amounts of malic acid which is secreted to the culture media [Knuf *et al.* 2013]. Ochsenreither *et al.* [2014] showed that *A. oryzae* can convert different carbon sources to malic acid, like glycerol or pentose sugars (i.e. xylose), which are also part of lignocellulosic. The "food or fuel" debate shows the importance to develop a biotechnological route for production of dicarboxylic acids based on sustainable non-food carbon sources. Therefore, the last part of this thesis uses malic acid as an example of broadening the substrate spectrum for production of other biotechnological products beyond glycerol and sugars. This will also expand the final product spectrum from syngas fermentations. By sequential link-up of anaerobic syngas fermentation and aerobic malic acid production, the substrate spectrum is broadened to syngas, which can be obtained from steel mill off-gas [Köpke *et al.* 2011] or by gasification of biomass organic wastes and fossil feedstocks [Neumann 2015], forging a completely new and highly innovative path towards the establishment of a biobased economy [Oswald *et al.* 2016].

2. Theoretical principles

2.1 Acetogenic microorganisms

2.1.1 Overview

Bacteria that are able to form acetate form C_1 units like CO_2 or CO are called acetogens. Those organisms are obligate anaerobes able to form acetic acid from either organic carbon and energy sources (hetertrophic growth) or hydrogen and carbon monoxide/carbon dioxide (autotrophic growth) [Diekert and Wohlfarth 1994]. The group of acetogenic microorganisms is quite heterogeneous and consists of many different genera of gram positive as well as gram negative bacteria [Drake 1994]. Although the majority of acetogens is mesophilic, there are also some thermophilic, like *Moorella thermoacetica*, and even psychrotrophic bacteria [Drake 1994], like *Acetobacterium tundrae* [Simankova *et al.* 2000] belonging in this group. Characteristic feature of this group is that they convert one mole of glucose or fructose to three moles of acetic acid by incorporating the CO_2 released by decarboxylation of pyruvate back into the methyl- and carbonyl group of acetic acid [Barker and Kamen 1945, Wood 1952].

2.1.2 Organoheterotrophic metabolism

In presence of hexoses or other organic carbon sources like pyruvate or lactate, acetogenic microorganisms grow organoheterotrophically while converting the substrates into acetyl-CoA. This is then used for cell growth or converted to acetic acid. Figure 2.1 gives an overview of the anaerob, organoheterotrophic metabolism. One mole of hexose or two moles of lactate are converted to two moles of pyruvate. This gains two moles of adenosine triphosphate (ATP) and four moles of reduction equivalents per mole hexose or four moles of reduction equivalents per two moles of lactate. A decarboxylation reaction splits off CO_2 from pyruvate and links the remaining acetaldehyde to CoA forming acetyl-CoA. With ethanol as a substrate, two moles ethanol are oxidized into two moles acetyl CoA and eight moles of reduction equivalents [Bertsch *et al.* 2016]. To recycle the reduction equivalents, two molecules CO_2 are reduced to an additional molecule acetyl-CoA. This also consumes one ATP. The carbon dioxide fixating pathway is called reductive Acetyl-CoA or Wood-Ljungdahl-Pathway (WLP) and is going to be described in detail in the next chapter. The WLP is a path of anaerobic respiration with CO_2 as the final electron acceptor and serves as
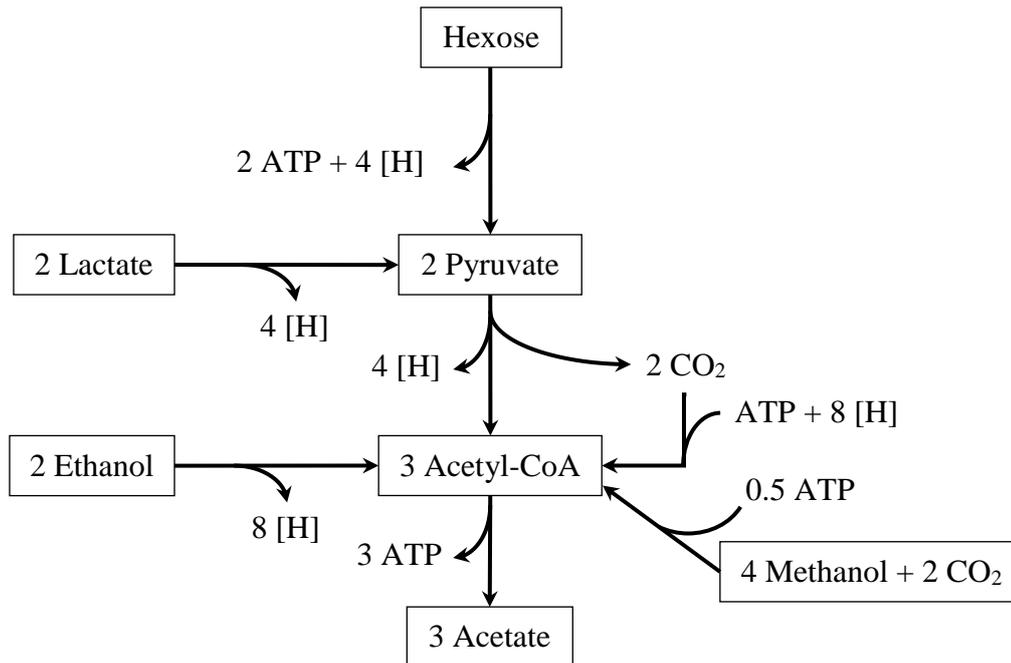
Figure 2.1 – Basic scheme of organoheterotrophic metabolism in acetogenic bacteria. One mol of hexose, two mol of lactate or two mol of ethanol are converted into two mol of acetate. Up to one additional mol of acetate is formed by fixation of CO_2 from pyruvate decarboxylation and recycling the reduction equivalents. In the case of ethanol, the reaction is only feasible if external CO_2 is present since the oxidation of ethanol does not result in CO_2 formation [Bertsch *et al.* 2016]. With methanol as an organic substrate four mol methanol are necessary to gain three mol acetyl-CoA [Kerby *et al.* 1983].

an electron sink to recycle ferredoxin, $NADP^+$ and NAD^+ under heterotrophic growth conditions [Drake 1994]. It is also the only known pathway of CO_2 fixation that does not link CO_2 to an organic compound produced during CO_2 fixation (e. g. Calvin-Cycle) but to another C_1-component [Wood 1991]. In contrast to hexoses, lactate or ethanol, the reactions for using methanol as a substrate are only located in the WLP. To form one mol of acetate, two mol of methanol are necessary. One mol is oxidized to CO_2 and fixed into the carboxyl group of acetyl-CoA while one mol serves as the methyl group of acetyl-CoA. [Kerby *et al.* 1983] Excess acetyl-CoA, which is not used for cell growth, gets converted to acetate, gaining one mole ATP per mole of acetate formed. End products of energetic metabolism are not limited to acetate alone. Other products are ethanol, acetone, propanol, butyrate, butanol and butandiol. Though, when growing on glucose, the formation of acetic acid yields more energy in the form of ATP per mole of glucose consumed than the formation of butyric acid [Gößner *et al.* 2008].

2.1.3 Chemolithoautotrophic metabolism

As mentioned above, the WLP enables acetogenic bacteria to use CO_2 as a carbon source. Figure 2.1 shows that for fixation of two molecules CO_2, energy in the form of one ATP and eight reduction equivalents is necessary. Without any organic substances to gain energy from, autotrophic growing acetogenes have to use anorganic energy sources such as carbon monoxide and/or hydrogen. Figure 2.2 gives a detailed view of the Wood-Ljungdahl-Pathway and the means of energy conservation in autotrophic growing acetogens. The WLP consist of two branches – the methyl branch and the carbonyl branch. The first step of the methyl branch is the reduction of CO_2 to formate. In *Clostridium autoethanogenum*, a close relative of *Clostridium ljungdahlii*, this reaction is catalyzed by the electron bifurcating [FeFe]-hydrogenase formate dehydrogenase complex HytA-E/FdhA [Wang et al. 2013]. Depending on the available substrates, either reduced ferredoxin (Fd^{2-}) and NADPH or H_2 is used as an electron donor [Wang *et al.* 2013, Mock *et al.* 2015]. Formate is then linked to tetrahydrofolate (THF) by formyl-THF synthase consuming one ATP per molecule formyl-THF formed. The following tree subsequent reactions reduce formyl-THF group via methenyl-THF and methylene-THF to methyl-THF. While the electron donor for the methylene-THF forming methylene-THF dehydrogenase in *C. autoethanogenum* is NADPH, the cofactor for the reduction of methenyl-THF to methyl-THF is unknown [Wang *et al.* 2013, Schuchmann and Müller 2014, Mock *et al.* 2015,]. The methyl group is then transferred to the iron-sulfur cluster of a corrinoid-protein (CoFeS).

In the carbonyl-branch, a carbon monoxide dehydrogenase acetyl-CoA synthase complex (CODH/Acs) reduces CO_2 to CO in the CODH part of the complex. CO is then transferred to the Acs side via channel-like structures inside the complex [Ragsdale and Wood 1985, Maynard and Lindahl 1999, Seravalli and Ragsdale 2000,]. The acetyl-CoA synthase then links the methyl group delivered by the corrinoid-protein, CoA and CO together to form acetyl-CoA [Ragsdale and Wood 1985]. Exchanging CoA by phosphate to form acetyl phosphate enables the generation of one ATP via substrate level phosphorylation (SLP) yielding acetic acid as the final product of WLP. Some Acetogenic bacteria can also form ethanol for witch two routes are possible. Direct conversion of acetyl-CoA to acetaldehyde and further to ethanol consumes two NADPH or NADH and will not yield ATP from SLP. The actual electron donor of aldehyde and alcohol dehydrogenase is not known. This route will result in an ATP yield of 0.5 per ethanol formed [Mock *et al*. 2015]. The other route is

Methyl Branch

CO

Fd

CODH

Fd²⁻

CO_2

H_2 ·····> 0,5 Fd²⁻ + 0,5 NADPH

HytA-E/
FdhA

0,5 Fd + 0,5 NADP⁺

HCO_2^-

THF — ATP

Fts

ADP + P_i

HCO−THF

Ftch

H_2O

HC≡THF

NADPH

Mtdh

NAD⁺

H_2C=THF

2 [H]

Mtr

H_3C−THF

CoFeS

Mt

THF CoA−SH CoFeS

H_3C−CoFeS

CODH/Acs

Carbonyl Branch

CO_2

Fd²⁻

CODH/Acs

Fd

[CO] ⇌ CO

2 H⁺

RnfA-G CM

Fd²⁻ Fd NAD⁺

Fd NADH

3.66 H⁺

F_0F_1

ATP ADP + P_i

2 NADPH 2 NADP⁺

4 H_2 **HytA-E**

8 H⁺ 2 Fd

2 Fd²⁻

2 NADPH 2 NADP⁺

NADH **Nfn**

NAD⁺ Fd

Fd²⁻

NAD(P)H NAD(P)⁺

CH_3CHO → CH_3CH_2OH

Adh Fd

Adh NAD(P)⁺ + CoA−SH

Afor Fd²⁻

NAD(P)H

CH_3CO−S−CoA →Pta→ CH_3CO−O−PO_3^{2-} →Ak→ CH_3COO^- + H⁺

P_i CoA−SH ADP ATP

Figure 2.2 – The Wood-Ljungdahl-Pathway and means of chemiosmotic energy conservation in *Clostridium autoethanogenum* **and** *Clostridium ljungdahlii*. Adh, aldehyde/alcohol dehydrogenase; AOR, aldehyde:ferredoxin oxidoreductase; Ak, acetate kinase; CM, cell membrane; CODH, carbon monoxide dehydrogenase; CODH/Acs, carbon monoxide dehydrogenase-acetyl-CoA-synthase complex; F_0F_1, ATP synthase; Fd, ferredoxin; THF, tetrahydrofolate; FdhA, formate dehydrogenase A; Ftch, formate-THF cyclohydrolase; Fts, formate-THF synthase; HytA-E, electron bifurcating [FeFe]-hydrogenase; HytA-E/FdhA, electron bifurcating [FeFe]-hydrogenase formate dehydrogenase complex; Mt, methyl transferase; Mtdh, methylene-THF dehydrogenase; Mtr, methylene-THF reductase; Nfn, ferredoxin depending electron bifurcating transhydrogenase; Pta, phosphotransacetylase; RnfA-G, membrane bound electron trasnfere chain. HytA-E/FdhA catalyzes the reduction of CO_2 to formate either with Fd²⁻ and NADPH (continuous line) or with H_2 (dotted line) [Wang *et al.* 2013].

the conversion of acetyl-CoA to acetic acid as described above and then, using an aldehyde:ferredoxin oxidoreductase (AOR) with Fd^{2-} as electron donor, form acetaldehyde [White et al. 1993, Huber et al. 1994, Huber et al. 1995] which is converted to ethanol. This yields 1.2 ATP per ethanol formed. [Mock et al. 2015] With an excess of reducing equivalents this second route to ethanol gives an energetic advantage because the WLP will stay ATP-neutral and ferredoxin can be recycled [Köpke et al. 2010]. Mock et al. [2015] showed that at an internal pH of 6 for $C.$ $autoethanogenum$ the reduction of acetate to acetaldehyde is exergonic at an acetate to acetaldehyde ratio of 1000. At extracellular pH-values near the pK_a-value of acetic acid undissociated acetic acid can diffuse freely through the cytoplasmic membrane resulting in an intracellular acetate concentration that is 10-fold higher than the extracellular concentration. Under these conditions an extracellular acetate concentration of 0.6 g L^{-1} is already enough to result in ethanol formation. [Mock et al. 2015]

Energy can be conserved in presence of carbon monoxide in the form of reduced ferredoxin through CODH catalyzed oxidation of CO or by oxidation of hydrogen. In $C.$ $autoethanogenum$ oxidation of hydrogen is catalyzed by a NADP and ferredoxin depending, electron bifurcating [FeFe]-hydrogenase (HytA-E) [Wang et $al.$ 2013]. Genes encoding for all subunits of HytA-E are present in $C.$ $ljungdahlii$ as well. [Köpke et $al.$ 2010, Wang et $al.$ 2013]. NADPH and Fd^{2-} can directly enter the WLP as electron donors. Fd^{2-} can also interact with the membrane bound Rnf-complex (RnfA-G) that transfers electrons from Fd^{2-} to NAD^+ translocating two protons for every two electrons transferred [Tremblay et $al.$ 2012]. This generates a transmembrane proton gradient that drives a membrane associated F_0F_1 ATP synthase [Köpke et $al.$ 2010] that generates one ATP per 3.66 H^+ [Mock et $al.$ 2015]. Although in C $autoethanogenum$ hydrogenase activity yields reduction equivalents in the form of equimolar amounts of NADPH and Fd^{2-} [Wang et $al.$ 2013], interaction of Fd^{2-} with the Rnf-complex gives NADH [Tremblay et $al.$ 2912]. If mainly acetic acid is the product of WLP there is not much need for NADH in the associated reactions. Hence the ferredoxin depending electron bifurcating transhydrogenase Nfn is a way of regenerating NADPH from NADH and Fd^{2-} [Wang et $al.$ 2010]. Simulations revealed that in this case Nfn is essential for the conversion of NADH to NADPH and with H_2 as electron donor, CO_2 as the electron acceptor and ethanol as WLP end-product 1.5 ATP can be gained through Rnf proton translocation per ethanol produced [Nagarajan et $al.$ 2013]. Nfn was first isolated form $Clostridium$ $kluyveri$ but the enzyme and encoding genes have also been found in $Moorella$ $thermoacetica$ (formerly known as $C.$ $thermoaceticum$), $C.$ $autoethanogenum$ and

C. ljungdahlii [Wang *et al.* 2010, Huang *et al.* 2012, Wang *et al.* 2013]. In the latter two the gene encoding for the two subunits of Nfn are fused together [Wang *et al.* 2013].

2.1.4   The acetogenic bacterium *Clostridium ljungdahlii*

C. ljungdahlii was first isolated by Barik *et al.* in 1988 using chicken yard waste as an inoculum for enrichment cultures. Cells are 0.6 by 2-3 µm in size, rod-shaped, gram-positive and motile [Tanner *et al.* 1993]. Tanner *et al.* [1993] also describe that the cells are covered by a thick coat of material, visible in their transmission electron micrograph. This can also be seen in Figure 2.3 where the same scanning electron microscope (SEM) picture was taken with two different detectors. With its size of 4.6 Mbp the genome of *C. ljungdahlii* is one of the largest known among clostridia [Köpke *et al.* 2010]. Although the genome contains genes involved in sporulation [Köpke *et al.* 2010] the formation of spores is rarely observed [Tanner *et al.* 1993].

Optimum conditions for growth of *C. ljungdahlii* are a pH-value of 6.0 and a temperature of 37 °C. The addition of vitamins and yeast extract to the media is necessary [Tanner *et al.* 1993]. The organism is not capable of synthesizing biotin on its own, making the presence of biotin in the media essential [Köpke *et al.* 2010]. *C. ljungdahlii* converts 1 mol of fructose to 2.44 mol of acetic acid which classifies this organism as an acetogen. It can also grow on H_2 and CO [Barik *et al.* 1988] or H_2 and CO_2 as sole energy- and carbon sources quantitatively converting 4 mol of hydrogen and 2 mol of carbon dioxide into 1 mol of acetic acid. Thus *C. ljungdahlii* uses the WLP of CO_2-fixation with acetic acid and ethanol as products. [Tanner *et al.* 1993] Organoheterotrophicaly *C. ljungdahlii* can grow on ethanol, 1-propanol, 1-butanol, α-ketoglutarate, pyruvate, citrate, fumarate, gluconic acid, erythrose, threose,
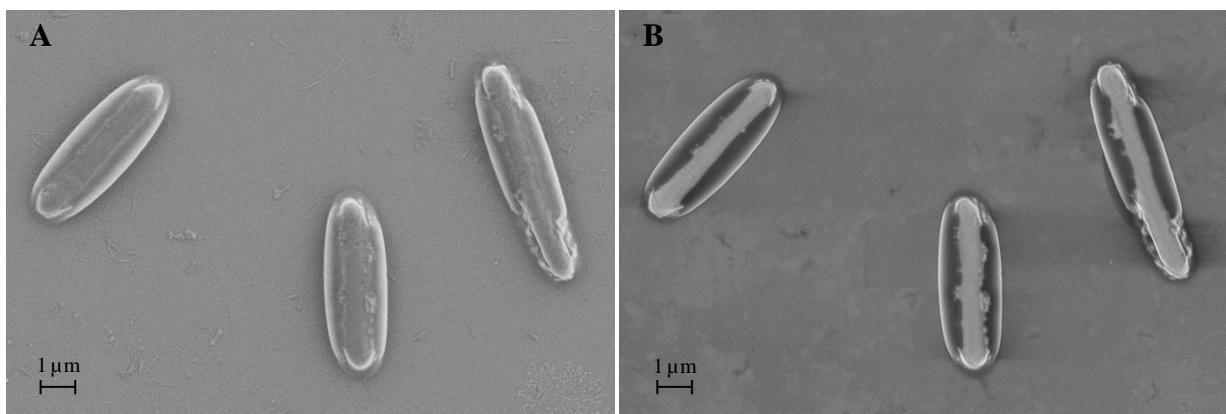
Figure 2.3 – Scanning electron micrographs of fructose grown cultures of *C. ljungdahlii*. Dehydrated cells of *C. ljungdahlii* encapsuled by an unknown material. Picture was taken with a secondary electron detector (A) and an InLens detector (B) for better distinction between the cell and its capsule.

arabinose, ribose, xylose, mannose, sucrose, glucose, rhamnose and fructose. It can also utilize various nitrogen sources such as alanine, arginine, glutamate, glutamine, histidine serine, choline, citrulline, guanine, hypoxantine. [Tanner and Laopaiboon 1997, Huhnke *et al*. 2010] Genetic information further revealed that *C. ljungdahlii* might be able to use nitrate as a source of nitrogen or even fix molecular nitrogen [Köpke *et al.* 2010].

2.2   Process characteristics and mass transfer

2.2.1   Cultivation of microorganisms

Processes for cultivation of microorganisms can be divided into three groups: batch, semi continuous and continuous processes. In batch processes, all nutrients necessary for microbial growth are present from the beginning. The reactor is inoculated and products are harvested after a specific process time. Semi continuous processes start like batch processes, but after a short batch phase nutrient solution is added to the reactor (fed-batch) or part of the culture broth is harvested and replaced with fresh media (repeated batch). Combinations of fed-batch and repeated batch are also possible. In continuous running cultivations a continuous harvest of the culture broth is balanced with a continuous feed stream of fresh media. For the purpose of this thesis only batch processes are relevant and will be described below. Without any initial inhibitions or limitations and all nutrients available in limited amounts, the growth of microbial cultures can be divided into six phases (see Figure 2.4). During the lag phase, the microorganisms adjust to the conditions of the freshly inoculated media and little to no growth happens. In the acceleration phase the number of cells increases slowly and leads to
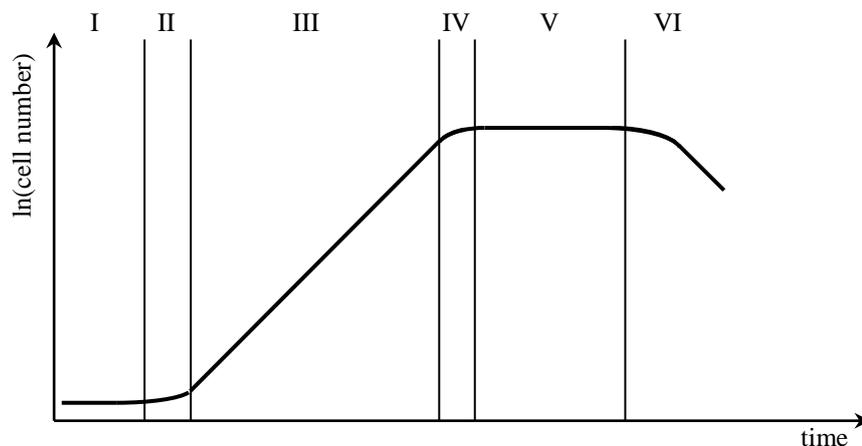
Figure 2.4 – Growth phases of a bacterial batch culture. I, lag phase; II, acceleration phase; III, exponential growth phase; IV, limitation phase; V, stationary phase; VI, death phase.

the exponential growth phase, in which the cell number increases with maximum growth rate. Once one or more substrates reach limiting concentrations or an inhibition due to a metabolite occurs, growth decreases (limitation phase) until growth rate and death rate are equal. This phase is called stationary phase. Death phase is reached when the death rate exceeds the growth rate and the cell number decreases.

2.2.2 Process parameters

To compare different experiments, certain parameters are necessary to describe the process. Some of those parameters can be derived from the mass balance which consists of a convective term and a reaction term as described in equation (2.1).

$$\frac{\mathrm{d}(\beta_i V)}{\mathrm{d}t} = \dot{V}_{in}\beta_i - \dot{V}_{off}\beta_i + r_i V \tag{2.1}$$

β_i	concentration of component i, $g\,L^{-1}$
V	reactor volume, L
$\dot{V}_{in}$	ingoing flux, $L\,min^{-1}$
$\dot{V}_{off}$	outgoing flux, $L\,min^{-1}$
r_i	reaction rate, $g\,L^{-1}\,h^{-1}$

For batch cultivation, all nutrients are available from the beginning. Besides pH-adjustment solutions and anti-foaming agent, no other liquids are added during the course of fermentation. Only the gaseous phase passes through the reactor continuously. Therefore, the bioreactor volume is approximately constant and the mass balance of a component i in the liquid phase for batch processes simplifies to

$$\frac{\mathrm{d}\beta_i}{\mathrm{d}t} = r_i. \tag{2.2}$$

The first process parameter is the grow rate μ of the biomass X. With $r_X = \mu\,\beta_X$ in (2.2) the solution of the differential equation is

$$\ln\left(\frac{\beta_{X,\,t}}{\beta_{X,\,t-1}}\right) = \mu\,\Delta t. \tag{2.3}$$

Substrate consumption rate and product formation rate are two other important process parameters:

$$r_S = Q_S = \frac{d\beta_S}{dt} \tag{2.4}$$

$$r_P = Q_P = \frac{d\beta_P}{dt} \tag{2.5}$$

Q_S substrate consumption rate, $g\,L^{-1}\,h^{-1}$

Q_P production rate, $g\,L^{-1}\,h^{-1}$

To evaluate the conversion efficiency of a bioprocess, it is useful to determine the yield of produced biomass per consumed substrate

$$Y_{X/S} = \frac{r_X}{r_S} = \frac{d\beta_X}{d\beta_S} \tag{2.6}$$

and analog determine the yield of produced product per consumed substrate:

$$Y_{P/S} = \frac{r_P}{r_S} = \frac{d\beta_P}{d\beta_S}. \tag{2.7}$$

The unit of Y is gram biomass or product per gram substrate, aka $g\,g^{-1}$.

2.2.3   Gas-liquid mass transfer

Gases such as carbon monoxide, hydrogen or oxygen have low solubility in water and aqueous solutions. Processes using gaseous substrates like carbon monoxide and hydrogen strongly depend on the mass transfer rate of these substrates from the gaseous- to the liquid phase because availability of substrates limits growth and product formation [Worden *et al.* 1997]. To describe mass transfer between gaseous- and liquid phase, three models regularly come up:

- The penetration model where mass transfer happens through nonsteady diffusion between laminar moving phases.
- The theory of surface renewal where volume elements on the gas-liquid interface are continuously replaced due to turbulent flow.
- The two-film theory where mass transfer happens through two thin layers on each side of the gas-liquid boundary surface by diffusion.
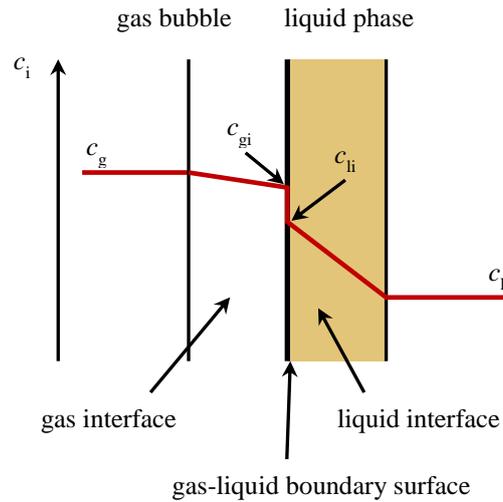
Figure 2.5 – Schematic drawing of concentration changes between a gas bubble and the surrounding liquid phase [Bailey and Ollis 1991].

Due to its simplicity of calculations the latter model is commonly used to describe mass transfer between gas bubbles and the culture broth in bioprocesses. Figure 2.5 gives a schematic view of mass transfer between a gas bubble and the surrounding liquid phase. According to two-film theory, thermodynamic balance at the boundary surface is established immediately. On both sides of the boundary surface, a laminar interface forms whereas the core of the gas bubbles and the surrounding liquid phase has turbulent flow. While concentration gradients are negligible for turbulent flow due to domination of convective mass transfer, driving force in the laminar interface is the concentration gradient between boundary surface concentration and the surrounding liquid- and gaseous phase. Diffusion in the laminar interface is defined by the diffusion coefficient D and the layer thickness. Since diffusion in gases is faster than in liquids and the gaseous interface is much smaller than the liquid interface, the main resistance for mass transfer from the gaseous to the liquid phase is on the liquid side. Therefore, the gas interface is negligible and mass transfer consists of the mass transfer coefficient k_l of the liquid phase, the gas-liquid boundary surface in relation to the reactor liquid volume $a = A/V_l$ and the concentration difference between gas-liquid boundary surface at equilibrium with the gaseous phase and surrounding liquid phase. In bubble sparged bioreactors k_l and a cannot be determined independently. Hence the volume-based mass transfer coefficient k_la in s^{-1} is introduced. It strongly depends on many parameters such as volumetric power input, coalescence properties of the liquid phase and flow pattern. k_la is defined via the gas transfer rate

$$\frac{\mathrm{d}c_i}{\mathrm{d}t} = k_l a \left(c_{i,\,l}^{*} - c_{i,\,l} \right).$$

(2.8)

c_i concentration of substance i, $\mathrm{mol\,L^{-1}}$

$c_{i,\,l}^{*}$ liquid phase concentration of substance i

        in equilibrium with the gaseous phase, $\mathrm{mol\,L^{-1}}$

$c_{i,\,l}$ liquid phase concentration of substance i, $\mathrm{mol\,L^{-1}}$

The $k_l a$ value indicates the efficiency of gas input into the liquid phase and therefore indicates how good the microorganisms are supplied with gaseous substrates. Equation (2.8) shows that the mass transfer rate depends on the gas-liquid boundary-surface, which is mainly defined by the bubble size, the saturation concentration and the actual concentration of the gas in the liquid phase. The mass transfer coefficient k_l could be increased by reducing the layer thickness of the liquid interface, but this is not possible with the conditions in a bioreactor.

Increasing the gas-liquid boundary surface actually means to decrease bubble size and increase the number of bubbles. The common approach for this in biotechnological applications is to increase the stirrer speed. With this, volumetric power input and shear forces at the tips of the stirrer blades are increased, resulting in smaller bubbles, thus increasing the $k_l a$-value. Also, smaller bubbles have lower rise velocities and stay longer in the aqueous phase and therefore have more time to solute [Bredwell and Worden 1998]. Increasing the gas sparging rate also leads to an increase in gas-liquid boundary surface due to a rise in bubble number, but the effect is smaller compared to increased stirrer speed.

Coalescence describes the process of small gas bubbles merging to bigger bubbles. The liquid layer between adjacent gas bubbles thins out until the layer bursts and the bubbles merge. This happens fast in pure liquids but with increasing concentration of soluble substances, the stable bubble diameters in the solution decrease. The more likely a liquid is to foam, the lower is the tendency of bubbles to coalescent. [Zlokarnik 1981] Due to the nutritional needs of bacteria, the possibilities of varying the coalescence of the culture broth are limited. But because of metabolic activity (e. g. secretion of proteins, surfactants or lysis of dead cells) bioreactor cultivations tend to foam. To prevent them from foaming over the addition of anti-foaming (AF) agents might be necessary. These AF-agents increase bubble coalescence which effectively destructs the foam. Increased bubble coalescence also means an increase in stable

bubble diameters, and therefore a decrease in total gas-liquid boundary surface and gas-liquid mass transfer [Zlokarnik 1979].

For certain gases like oxygen or carbon dioxide c and c^* can be measured with suitable methods, whereas the equilibrium concentration c^* can also be calculated for all gases from Henry's law to

$$c_{i,1}^* = H_i\, p_i = H_i x_i p. \tag{2.9}$$

H_i Henry's law solubility constant of substance i, mol m^{-3} Pa^{-1}

p_i partial pressure of substance i in the gaseous phase, Pa

x_i mol-fraction of substance i in the gaseous phase, -

p absolute pressure in the system, Pa

Hence, a third option of increasing the mass transfer rate is to increase the equilibrium or saturation concentration c^*. This can be achieved by either increasing the mol fraction/volume fraction of the desired substance in the gas stream or by increasing the total pressure of the system.

2.2.4 Scale-up

If experiments of the same kind are supposed to be compared in different scales, model theory demands that in each scale, the experiment has to be conducted in geometrical similar spaces and at least important dimensionless numbers describing the process have to be of the same value (partial similarity). For stirred tank reactors, geometric similarity means to keep the ratio of stirrer diameter to reactor diameter (d/D) constant. All other reactor lengths are scaled to this ratio. As for the dimensionless numbers, they have to be derived from dimensional analysis of the process. For gas sparged STRs important dimensionless numbers in addition to geometric similarity are Newton number, Reynolds number, Froude number and gas throughput number. The Reynolds number

$$\text{Re} = \frac{nd^2}{v} \tag{2.10}$$

n stirrer speed, min^{-1}

v kinematic viscosity, m^2 s^{-1}

d stirrer diameter, m

describes the flow condition inside STRs with homogenous media. For Re $\geq$ 50 (STR with baffles) or Re $\geq 10^4$ (STR without baffles) the flow condition is turbulent. Under those conditions the Newton number

$$\text{Ne} = \frac{P}{\rho n^3 d^5} \tag{2.11}$$

P impeller power, $\text{kg m}^2 \text{s}^{-3}$

ρ liquid density, kg m^{-3}

has a constant value depending on stirrer type and liquid density. For gas sparged STRs, the Froude number (Fr), surface tension coefficient (σ^*), coalescence number (S) and gas throughput number are added. However, Zlokarnik [1973] shows that in the area of technical relevant Newton numbers Fr, σ^* and S have no influence on Ne. Therefore, under turbulent conditions Ne only depends on the gas throughput number

$$Q = \frac{\dot{V}_g}{nd^3}. \tag{2.12}$$

$\dot{V}_g$ ingoing gas flow rate, L min^{-1}

The higher the gas flow into the STR, the lower gets the Ne number due to reduced power uptake of the stirrer.

2.3   Influence of gas impurities on *Clostridium ljungdahlii*

2.3.1   Composition of crude syngas

Hydrogen, carbon monoxide and carbon dioxide are main constituents of gas yielded by gasification of coal or biomass, also called syngas. Gasification is a thermal process that degrades carbon and hydrogen containing feedstocks in their molecular building blocks. The gas composition varies depending on gasifier type, feedstock and process mode but consists mainly of CO, CO_2, H_2 and, if air is used as gasifier media, N_2. In addition to this main constituents crude syngas also contains fluctuating amounts of: methane and volatile C_2-compounds (e. g. ethane, ethylene and acetylene), tar components (e. g. benzene, toluene, xylene and naphthalene), halogens (e. g. hydrogen chloride and hydrogen fluoride), sulfur compounds (e. g. hydrogen sulfide, carbonyl sulfide and carbonyl disulfide) and nitrogen species (e. g. nitrogen oxides, ammonia and hydrogen cyanide) as well as oxygen (O_2) and

reactive oxygen species (ROS). The amounts vary with feedstock and gasification method. Those minor constituents are known catalyst poisons for chemical applications of syngas and need to be removed. Compared to the chemical route, the above-mentioned microorganisms catalyze the conversion of syngas to acetic acid or ethanol at 37 °C and ambient pressures and some of the named minor constituents of syngas like NH_3 are usable substrates for microorganisms. If crude syngas is supposed to be used for syngas fermentations using organisms of the above-mentioned group, understanding of the effects of syngas impurities is necessary to avoid delays in reaching full scale production capacity and additional costs [Lane 2014].

2.3.2 Effects of gas impurities on carbon monoxide dehydrogenase

CODHs are found in various organisms; some inhibitory effects are well described in literature. Among the previously named impurities effects of cyanide on CODHs are well characterized. Thauer *et al.* [1974] show that carbon monoxide oxidation activity of cell-free extracts of *Clostridium pasteurianum* is inhibited by cyanide at concentrations of 10 µM. Ha *et al.* [2007] find that 75 µM cyanide completely inactivate purified CODH from *Carboxydothermus hydrogenoformans*. Inhibition is reversed by CO and is already a 100-fold lower in presence of the same concentration of CO and cyanide [Thauer *et al.* 1974]. Other researchers described the same competitive behavior of CODH inhibition by cyanide for *Methanosarcina thermophile* [Terlesky *et al.* 1986], *Methanosarcia barkeri* [Grahame and Stadtman 1987], *Moorella thermoaceticum* (formerly *Clostridium thermoaceticum*) [Ragsdale *et al.* 1983a, Diekert and Thauer 1978, Anderson *et al.* 1993], *Clostridium formicoaceticum* [Diekert and Thauer 1978], *Rhodospirillum rubrum* [Ensing *et al.* 1989, Smith *et al.* 1992], *Acetobacterium woodii* [Ragsdale *et al.* 1983b] and *C. hydrogenoformans* [Ha *et al.* 2007]. The competitive behavior and the protection against cyanide inhibition by CO indicate a common binding side of CN^- and CO [Terlesky *et al.* 1986, Grahame and Stadtman 1987, Ensing *et al.* 1989]. Anderson *et al.* [1993] discover that CN^- bind directly to the C-cluster of *M. thermoaceticum* and Ha *et al.* [2007] show that cyanide competes with CO at the [Ni-4Fe-5S]-cluster of CODH from *C. hydrogenoformans*. It is suggested that the C-cluster is part of the active side in all Ni-Fe CODHs [Anderson *et al.* 1993]. Cell-free extracts of *C. pasteurianum* regained CODH activity even without carbon monoxide treatment and Thauer *et al.* [1974] measure activity for rhodanese reaction that detoxifies cyanide and converts it to thiocyanate and sulphite.

Sulfur components are another class of CODH inhibitors. In this class, carbonyl sulfide (COS) and hydrogen sulfide (H_2S) are of special interest [Hyman *et al*. 1989, Vega *et al*. 1990]. The inhibition of CO oxidizing activity of purified CODH from *R. rubrum* by COS is completed in less than 5 s and hints toward a rapid-equilibrium inhibition. The inhibition kinetic seems to follow a ping-pong mechanism. CODH has to be in an oxidized state before COS can bind to the enzyme and the whole inhibition process is more complex than with cyanide. Nevertheless, the inhibition is fully reversible when COS is removed from the atmosphere and CODH is incubated in presence of CO. [Hyman *et al*. 1989] Experiments by Hyman *et al*. [1989] with purified CODH revealed that in presence of 11.5 µM COS in solution, the inhibitory effect of 100 µM cyanide is decreased 5-fold, thus indicating that COS, CN^- and CO share the same binding side. With increasing aqueous COS concentration, the protective effect against cyanide inhibition saturates at 70 % remaining activity (250 µM COS). Although COS, SO_2 and CS_2 can reverse cyanide inhibition, the latter two prove ineffective as inhibitors for CO oxidation. [Hyman *et al*. 1989] Vega *et al*. [1990] investigated four microorganisms on their tolerance against H_2S and COS components in syngas up to concentrations of 39.5 % of each compound. For *R. rubrum* and *Peptostreptococcus productus* the substrate gaseous phase consisted of CO and CO_2 in a ratio of 4:1 and for *Methanobacterium formicum* and *M. barkeri* it is H_2 and CO_2 in a ratio of 3:1. *R. rubrum* shows no changes in growth and substrate consumption in presence of up to 26.3 % H_2S in the gaseous phase, but is already inhibited at gaseous concentrations of 6.6 % COS. CO utilization by *P. productus* is inhibited at concentrations higher than 19.7 % of COS and H_2S respectively. *M. barkeri* is unaffected by H_2S and COS up to concentrations of 26.3 %, whereas *M. formicum* shows significant inhibition at 13.2 % H_2S and 6.6 % COS. [Vega *et al*. 1990] *C. ljungdahlii* cultures which are previously grown in Na_2S containing media showed no effects on growth or CO consumption at H_2S or COS concentrations in the gaseous phase of up to 5.2 % but at 9.9 % growth and CO consumption essentially stopped [Klasson *et al*. 1992].

2.3.3 Effects of gas impurities on hydrogenase activity

In 1988, Hyman and Arp published a review article about the inhibitory effects of acetylene on metaloenzymes and pointed out that studies on acetylene inhibition of purified hydrogenases has only focused on enzymes of aerobic, nitrogen-fixing microorganisms. Those organisms have dimeric, Ni-containing hydrogenases. Also, hydrogenase of the aerobic proteobacterium *Azotobacter vinelandii* proves to be unaffected by acetylene as soon as trace

amounts of hydrogen are present. Hydrogenases are insensitive to cyanide but are inhibited by carbon monoxide. [Hyman and Arp 1988] Isolated Ni-Fe hydrogenase from *Desulfovibrio gigas* remained less than 20 % of their activity in presence of 10 % acetylene in the gaseous phase without hydrogen. The same study states that acetylene has no inhibitory effect on Fe-only hydrogenase from *D. vulgaris* and Ni-Fe-Se hydrogenase from *D. baculatus* remains at 50 % activity when incubated with 100 % acetylene. Selenium (Se) containing Ni-Fe hydrogenases are less sensitive to acetylene than Ni-Fe hydrogenases without Se. The same tendency can be found for Ni-Fe and Ni-Fe-Se hydrogenases from *Methanococus voltae* and *Methanosarcina thermophila*. [He *et al.* 1989]. Experiments with whole cells of *R. rubrum* also revealed an insensitivity of hydrogen consumption in presence of acetylene [Maness and Weaver 2001].

Another inhibitor of hydrogenase activity is nitric oxide (NO). In cell-free extracts of *Proteus vulgaris* 87 % hydrogenase activity is lost when exposed to 20 ppm NO in the gas phase [Krasna and Rittenberg 1954]. Experimental data of Ahmed and Lewis [2006] showed that cells of *Clostridium carboxidivorans* are growth inhibited when exposed to 13 ppm NO after the inoculation, but but continued growth is observed when 130 ppm NO is applied after the cells reached the first stationary growth phase. 40 ppm nitric oxide showed no inhibitory effects – even when applied straight after inoculation. Studies on whole-cell hydrogenase activity of *C. carboxidivorans* show that activity decreases at NO concentrations higher than 40 ppm with 10-95 % inhibition between 60 and 130 ppm. Hydrogenase inhibition by NO is non-competitive. [Ahmed and Lewis 2006]

2.3.4   Effects of tar components

Tar components are lipophilic hydrocarbons. When exposed to microorganisms, those lipophilic molecules accumulate in the cell membrane, increasing the surface area. This changes structure and functionality and increases fluidity of the membrane as well as protein conformations. Those changes can lead to proton leakage, which negatively affects chemiosmotic energy conservation. [Sikkema *et al.* 1995] Exposure of continuous running *C. carboxidivorans* syngas fermentation to tar compounds resulted in cell dormancy and wash out of the cells [Ahmed *et al.* 2006].

3.   Materials & Methods

A complete list of all used chemicals and their respective suppliers can be found in the appendix of this thesis.

3.1   General procedures for cultivation and analytics

3.1.1   Cultivation of *Clostridium ljungdahlii*

Clostirium ljungdahlii DSM135228 belongs to the group of obligate anaerobic bacteria. Hence, all cultivations have to be carried out under oxygen-free conditions. Organisms used in the experiments of this thesis were kindly provided by the group of Peter Dürre at the University of Ulm. Cultivation medium for *C. ljungdahlii* is based on a modified medium from Tanner [2007] used by Bengelsdorf et al. [2016] and has been further optimized for low nitrogen content. All media, trace element solution (TES) and vitamin solution are prepared using ddH$_2$O. Table 3.1 displays the composition of the medium, TES and vitamin solution. The pH-value is adjusted to 5.9 using solid KOH before bottling. Culture bottles are anaerobized using a gas mixture containing 20 vol-% CO$_2$ in N$_2$. After autoclaving the bottles at 121 °C, 1 g Cystein-HCl · H$_2$O and 10 g fructose (for fructose-grown cultures) per liter are added. Bottle cultures are seeded with 10 % of their final volume using a 48 h grown culture or are seeded with 1 mL of a glycerol stock per 50 mL of culture medium. Cultures are cultivated for 48 h (72 h when seeding from a glycerol stock) at 37 °C. [Oswald *et al*. 2016]

3.1.2   Preparation of glycerol-stock cultures

The method for preparing glycerol-stock cultures is based on the one described in the PhD thesis of Melanie Straub [2012]. Glycerol-stock cultures are prepared in 10 mL Hungate vials as follows: 5 mL of a 48 h grown fructose culture of *C. ljungdahlii,* with an optical density (OD) not higher than 2.0, are filled in a sterile and anaerobic Hungate. The culture is then centrifuged at 3000 *g* and 4 °C for 5 min. The supernatant is carefully discarded with a syringe and the pellet is dissolved in 1 mL of a mixture consisting of one part anaerobic, 50 vol-% glycerol solution and one part fresh media as described above. The stock cultures are then stored at -80 °C.

Table 3.1 – Composition of cultivation medium, trace element solution (TES) and vitamin solution.

Component	Amount per liter
Cultivation medium	
2-(N-morpholino) ethansulfonic acid (MES)	20.0 g
Yeast extract	0.5 g
NaCl	2.0 g
NH_4Cl	0.33 g
KCl	0.25 g
KH_2PO_4	0.25 g
$MgSO_4 \cdot 7\ H_2O$	0.5 g
$CaCl_2 \cdot 2\ H_2O$	0.1 g
TES	10 mL
Vitamin solution	10 mL
Resazurin	0.001 g
TES	
Nitrilotriacetic acid	2.0 g
$MnSO_4 \cdot H_2O$	1.0 g
$FeSO_4 \cdot 7\ H_2O$	0.567 g
$CoCl_2 \cdot 6\ H_2O$	0.2 g
$ZnSO_4 \cdot 7\ H_2O$	0.2 g
$CuCl_2 \cdot 2\ H_2O$	0.02 g
$NiCl_2 \cdot 6\ H_2O$	0.02 g
$Na_2MoO_4 \cdot 2\ H_2O$	0.02 g
$Na_2SeO_3 \cdot 5\ H_2O$	0.02 g
$Na_2WO_4 \cdot 2\ H_2O$	0.022 g
Vitamin solution	
Biotin	0.002 g
Folic acid	0.002 g
Pyridoxine	0.01 g
Thiamine-HCl	0.005 g
Riboflavin	0.005 g
Niacin	0.005 g
Ca-pantothenate	0.005 g
Cobalamin	0.005 g
4-aminobenzoic acid	0.005 g
Lipoic acid	0.005 g

3.1.3 Determination of gaseous H_2, CO, CO_2 and N_2

A GC-2010 Plus AT gas chromatograph (GC) by Shimadzu (Japan) is used to analyze the off-gas composition of syngas cultivations for hydrogen, oxygen, nitrogen, carbon monoxide and carbon dioxide. The GC is equipped with a customized column setup using a ShinCarbon ST 80/100 Column (2 m×0.53 mm ID, Restek, Germany) and a Rtx-1 capillary column (1 µm, 30 m×0.25 mm ID, Restek, Germany). The installed detector is a thermal conductivity detector with helium used as carrier gas. Column flow rate is 3 mL min^{-1}. Oven temperature profile is 40 °C for 3 min followed by a ramp of 35 °C min^{-1}. Total analysis time is 7.5 min. For the automated measurement of off-gas data of different reactors, the off-gas lines of all bioreactors used are connected to the GC via a stream selector. [Oswald *et al*. 2016]

Gas samples of cyanide bottle experiments are analyzed with a 3000 micro-GC (Inficon, Switzerland) to determine the consumption of the individual syngas components. The micro-GC is equipped with a 10 m molecular sieve module for CO, H_2 and N_2 detection and a 10 m PoraPlot Q module for CO_2 detection. All modules are equipped with a thermal conductivity detector. Isothermal conditions at 80 °C are used for analysis.

3.1.4 Calculation of substance flow and substrate consumption during syngas fermentation

Syngas in this work contains N_2 and *C. ljungdahlii* does not consume noteworthy amounts of N_2 under the conditions used. Hence, the nitrogen mass flow in the off-gas equals the ingoing nitrogen mass flow. Therefore, the flow rate in the off-gas line ($\dot{V}_{\text{off}(t)}$) calculates to

$$\dot{V}_{\text{off}(t)} = \frac{x_{N_2,\,\text{in}}}{x_{N_2,\,\text{off}}}\;\dot{V}_{\text{in}(t)}. \tag{3.1}$$

$x_{N_2,\,\text{in}}$ nitrogen content of feed gas, -

$x_{N_2,\,\text{off}}$ nitrogen content of off-gas, -

$\dot{V}_{\text{in}(t)}$ gas feed rate, L min^{-1}

Using the result of equation (3.1) as well as the ideal gas law and calibration conditions of the mass-flow controller ($T = 273{,}15$ K; $p = 1{,}013$ bar) it is possible to calculate the amount of substance flow rate ($\dot{n}_i$) in mmol min^{-1} for each component i in the off-gas to

$$\dot{n}_{i(t)} = 0{,}0446 \; x_{i,\,off} \; \dot{V}_{off(t)}. \tag{3.2}$$

$x_{i,\,off}$ content of substance i in the off-gas,-

Equation (3.3) calculates the amount of substance balance ($\Delta \dot{n}_i$) between off-gas and gas inlet.

$$\Delta \dot{n}_{i(t)} = \dot{n}_{i,in(t)} - \dot{n}_{i,off(t)} \tag{3.3}$$

$\dot{n}_{i,in(t)}$ amount of substance flow rate of substance i in the feed gas, mmol min^{-1}

$\dot{n}_{i,off(t)}$ amount of substance flow rate of substance i in the off- gas, mmol min^{-1}

Since there is no other sink or source for H_2, CO and CO_2 other than the metabolism of *C. ljungdahlii*, $\Delta \dot{n}_i$ equates to the uptake- or release rate of those compounds by the bacteria. Equation (3.4) calculates the consumption in percent of the ingoing amount of substance flow rate.

$$e_i = 100 \frac{\Delta \dot{n}_{i(t)}}{\dot{n}_{i,in}} \tag{3.4}$$

For gaining the total consumed amount of substance ($n_{i,R(t)}$), linear interpolation of $\Delta \dot{n}_i$ between two points of measurement gives a better approximation. $n_{i,R(t)}$ is calculated by integration of the linear interpolation to

$$n_{i,\,R(t_j)} = n_{i,\,R(t_{j-1})} + \frac{\Delta \dot{n}_{i(t_j)} + \Delta \dot{n}_{i(t_{j-1})}}{2} \left(t_j - t_{j-1} \right). \tag{3.5}$$

Dividing $n_{i,\,R(t)}$ by the reactor volume gives a concentration equivalent for substance i ($c_{i,\,R} = n_{i,\,R(t)} \, V_R^{-1}$), while dividing by the total amount of substance i that has gone into the bioreactor gives the ratio of accumulation for each substance in percent as shown by equation (3.6).

$$E_{i(t)} = 100 \frac{n_{i,\,R(t)}}{t \, \dot{n}_{i,in}} \tag{3.6}$$

During experiments in this work, product yields are calculated based on consumed substrates

$$Y_{P/S}^* = \frac{\left(\Delta\beta_{\text{acetic acid}} + \Delta\beta_{\text{ethanol}}\right) V_R}{\Delta m_{\text{Sub}}} \tag{3.7}$$

$\Delta\beta_{\text{acetic acid}}$	concentration of formed acetic acid, $g\,L^{-1}$
$\Delta\beta_{\text{ethanol}}$	concentration of formed ethanol, $g\,L^{-1}$
Δm_{Sub}	mass of consumed substrates, g

and based on overall fed hydrogen and carbon monoxide

$$Y_{P/S}^{**} = \frac{\left(\Delta\beta_{\text{acetic acid}} + \Delta\beta_{\text{ethanol}}\right) V_R}{t_{\text{end}} \left(\dot{n}_{H_2,\text{ in}} \widetilde{M}_{H_2} + \dot{n}_{CO,\text{in}} \widetilde{M}_{CO}\right)} \, . \tag{3.8}$$

t_{end}	total process time, min
$\widetilde{M}_{H_2}$	molar mass of H_2, $g\,mol^{-1}$
$\widetilde{M}_{CO}$	molar mass of CO, $g\,mol^{-1}$

The mass of consumed substrates does include carbon dioxide if $n_{CO_2,R}$ is positive.

$$\Delta m_{\text{Sub}} = \begin{cases} n_{H_2,R} \widetilde{M}_{H_2} + n_{CO,R} \widetilde{M}_{CO} + n_{CO_2,R} \widetilde{M}_{CO_2} & \text{if } n_{CO_2,R} > 0 \\ n_{H_2,R} \widetilde{M}_{H_2} + n_{CO,R} \widetilde{M}_{CO} & \text{else} \end{cases}$$

The unit of $Y_{P/S}$ is gram product per gram substrate ($g\,g^{-1}$).

3.1.5   Determination of optical density and cell dry weight

OD of samples is measured at 600 nm wavelength using an Ultrospec1100pro spectrophotometer (Amersham Bioscience). The OD of a liquid sample is measured against air. Centrifugation for 10 min at 16100 g separates the cells from the broth and the OD of the supernatant is measured. The difference of both values gives the OD of the sample. This procedure is necessary because OD values of the supernatant change during fermentation. The linear range of the OD to cell dry weight (CDW) relation ends at measured OD values of 0.45 and samples exceeding this value must be diluted using a $9\,g\,L^{-1}$ NaCl solution. 30 mL samples for CDW determination are taken once the OD reaches a stationary value. Samples are centrifuged in dry, pre-weight sample tubes at 4816 g and 4 °C for 15 min. Supernatant is discarded and cells are washed two times with $9\,g\,L^{-1}$ NaCl solution. Washed pellets are dried at 60 °C for 72 h before weighting. [Oswald *et al.* 2016]

3.1.6   Fructose, acetic acid, formic acid and ethanol

Contents of formic acid of all samples and fructose, acetic acid, and ethanol of fructose containing samples are measured by using enzymatic assays for D-fructose/D-glucose, acetic

acid and ethanol by Roche Yellow Line (Hoffman-La Roche, Switzerland) following their respective instructions. Gas chromatographic measurement of acetic acid and ethanol is used for fructose free samples and is conducted with a 6890N GC (Agilent), equipped with auto-sampler, FFAP capillary column (0.5 µm, 30 m×0.32 mm ID, Macherey-Nagel) and flame ionization detector. Carrier gas is helium with a pressure of 1 bar and split ratio is 7.5:1. Analytical standard mixture consists of 10 mM ethanol, 10 mM sodium acetate and 9.09 mM isobutanol in 0.18 M HCl. Samples are prepared by acidifying 500 µL with 50 µL internal standard solution, consisting of 100 mM isobutanol in 2 M HCl. Analysis is conducted by injecting 1 µL of sample or standard. The temperature profile of the column oven starts with initial 60 °C for 2 min, followed by a temperature ramp of 10 °C/min up to an end temperature of 180 °C. Total analysis time is 20 min. [Oswald *et al.* 2016]

3.2 Characterization of stirred tank reactor system

3.2.1 Stirrer configurations

Two stirrer configurations are tested for mass transfer properties and substrate consumption. Figure 3.1 shows both stirrer configurations used in this thesis. The first stirrer configuration is a set-up of two Rushton impellers arranged on the bottom and middle part of the stirrer shaft and three additional baffles at the walls of the reactor. This configuration will be referred to as Rushton-Rushton-Baffles (RRB) configuration throughout this thesis. Rushton impellers are radial flow impellers which cause high shear forces at the outer edges of the blades and therefore are good for dispersing gas bubbles. Both impellers dissipate the gas bubbles from the microsparger and the high shear forces in this arrangement result in finely dispersed bubbles through the whole liquid phase.
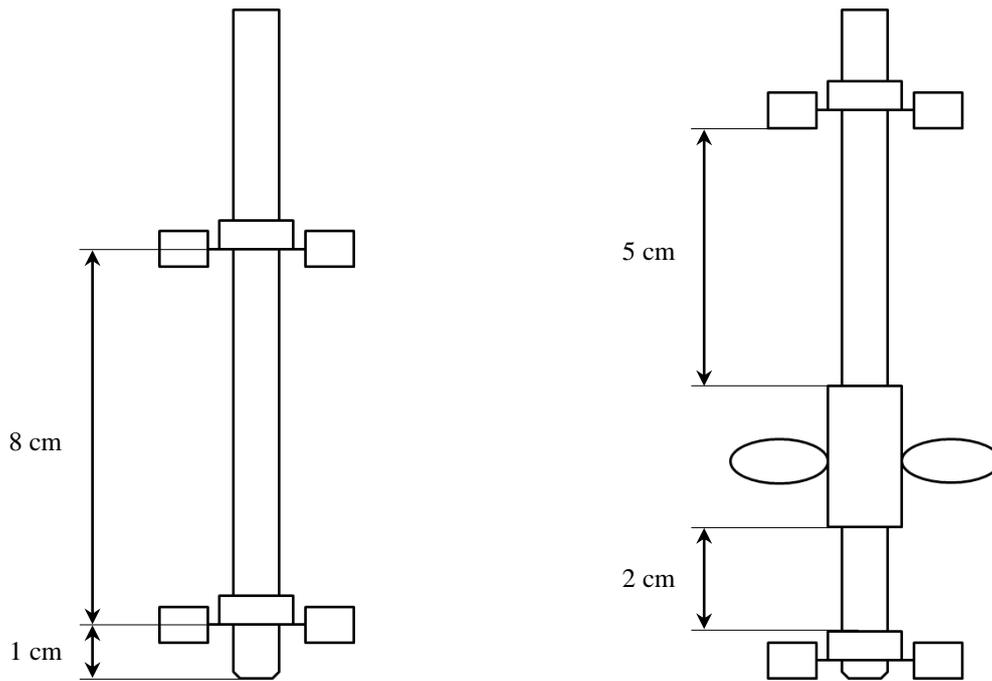
Figure 3.1 – Stirrer configurations used for syngas fermentation in this work. Rushton-Rushton-Baffles (RRB, left) consist of two Rushton impeller arranged on the stirrer shaft and additional baffles in the reactor. The Rushton-Marine-Rushton (RMR) approach (right) consist of a marine impeller between two Rushton impellers and no additional baffles.

The second configuration is consisting of a marine impeller between two Rushton impellers, with no baffles in the reactor. This will be referred to as Rushton-Marine-Rushton (RMR) configuration throughout this thesis. The marine impeller causes a vortex which enables the upper Rushton impeller to intensely mix the liquid with the gaseous phase from the headspace of the reactor. The Rushton impeller at the bottom of the stirrer shaft disperses the gas bubbles from the microsparger in the liquid phase. In this configuration, no additional baffles inside the reactor are used other than the installed probes, sparger and sample line.

3.2.2 Determination of k_La-values

There are different methods on how to determine mass transfer coefficients in stirred tank reactors. The most reliable and accurate one is the steady state sulphite method [Linek and Vacek 1981, Lara Márguez *et al.* 1994] which uses a model system consisting of about $0.8\,\text{M}$ $NaSO_3$ solution at pH 8 with Co^+ or Cu^+ as catalyst. The disadvantage of this method lies in the fact that determined k_La-values do not reflect the values of the biological system. Salt concentrations and kinds of salt strongly influence the properties of the gaseous-liquid boundary layer and coalescence properties of the liquid [Zlokarnik 1999]. Hence, those properties are different in the biological and chemical system.

Dynamical methods are suitable for measurements in the actual culture medium but require sterile procedures. The most common dynamic method is the desorption of nitrogen by air or pure oxygen. Detailed descriptions of this method can be found e. g. in Zlokarnik [1999] and Gaddis [1999]. However, this method has one major drawback. Due to nonideal mixing in noncolascent dispersions, the composition of the gaseous phase will be inhomogeneous after a step change of the inlet gas composition (e. g. from nitrogen to air). This leads to lower measured $k_l a$-values [Linek *et al.* 1989]. An alternative option, which avoids this drawback and gives back accurate values for $k_l a$, is proposed by Linek *et al.* [1989] and uses a sudden pressure step instead of a change in the ingoing gas composition. With our bioreactor set-up, this method is not usable and the method of nitrogen desorption by air is used to determine $k_l a$-values for the RRB and RMR stirrer configuration. Therefore, bioreactors are filled with 1.5 L freshly prepared media (see Table 3.1 for composition) without fructose and equipped with Pt-100 temperature probe (Infors-HT), microsparger (Infors-HT), pH-probe (Mettler Toledo) and an optical dissolved oxygen probe (Hamilton). The total volume of each bioreactor is 2.5 L. Hence, the headspace of each reactor has a volume of 1 L. Red-y smart series MFCs by Vögltin Instruments (Switzerland) calibrated for air are used to maintain constant air and nitrogen flow rates. $k_l a$-vaules are determined at 37 °C for each stirrer configuration with gas feed rates of 18 mL min^{-1}, 25 mL min^{-1} and 50 mL min^{-1} each at stirrer speeds of 600 min^{-1}, 800 min^{-1} and 1000 min^{-1}. In a first step, all oxygen in the bioreactor is displaced with nitrogen. Once the pO$_2$-signal is close to zero, the aeration is switched to air. Upon reaching oxygen saturation, the aeration is switched back to nitrogen. To determine the $k_l a$-vaules equation (2.8) is integrated to

$$
\ln\left(\frac{c^*_{O_2} - c_{O_2,\, t_0}}{c^*_{O_2} - c_{O_2,\, t_i}}\right) = k_l a \, (t_i - t_0).
\tag{3.9}
$$

The $k_l a$-value is gained as the slope of the linear regression of $\ln\left(\frac{c^*_{O_2} - c_{O_2,\, t_0}}{c^*_{O_2} - c_{O_2,\, t_i}}\right)$ over Δt. For determining the $k_l a$-vaule with the nonsteady dynamic method, the response characteristic of the pO$_2$-probe is of utter importance. Unadulterated values are gained only if the time constant τ_p of the oxygen probe is much smaller than $k_l a^{-1}$. [Gaddis 1999] This is true for the optical oxygen probe used in this work and therefore τ_p of the oxygen probe is not taken into further consideration.

If the $k_l a$-value for one gas is known for a given system and process parameters, then $k_l a$-values of other gases can be calculated according to

$$\frac{k_l a_i}{k_l a_j} = \frac{D_i}{D_j}.$$ (3.10)

D Diffusion coefficient of substance i or j in water, $m^2\,s^{-1}$

Equation (3.10) is based on the 1st Fick's law of diffusion and the assumption that the gas composition does not affect the specific interfacial area a and $k_l a$-values of different gases differ only in their diffusion coefficients. [Kodama $et\ al.$ 1976, Löser $et\ al.$ 2005] This is in accordance with the two-film theory, but Kodama $et\ al.$ [1976] showed that experimentally measured $k_l a$-values are better resembled by

$$\frac{k_l a_i}{k_l a_j} = \sqrt{\frac{D_i}{D_j}}.$$ (3.11)

Differences between results calculated by equation (3.10) and (3.11) are rather small [Chisti 2010], so that for the purpose of this thesis, $k_l a$-values are calculated with equation (3.11).

The diffusion coefficients necessary to calculate $k_l a$-values for other gases are estimated with the equation by Wilke and Chang [1955]

$$D_{i,\,H_2O} = 7.4 \cdot 10^{-8}\ \frac{T\ \sqrt{\phi_{H_2O}\ \widetilde{M}_{H_2O}}}{\eta_{H_2O}\ \widetilde{V}_M{}^{0.6}}$$ (3.12)

T temperature, K

ϕ_{H_2O} association parameter for i in water, -

$\widetilde{M}_{H_2O}$ molar weight of water, $g\,mol^{-1}$

$\widetilde{V}_M$ molal Volume of dissolved gas at normal boiling point, $mL\,g^{-1}\,mol^{-1}$

as suggested by Kodama $et\ al.$ [1976]. The association parameter ϕ for water is 2.6 [Wilke and Chang, 1955] and molal volumes of H_2, O_2, CO and CO_2 are $14.3\,mL\,g^{-1}\,mol^{-1}$, $25.6\,mL\,g^{-1}\,mol^{-1}$, $30.7\,mL\,g^{-1}\,mol^{-1}$ and $34.0\,mL\,g^{-1}\,mol^{-1}$ respectively [Arnold 1930, Wilke and Chang 1955].

For comparison of k_la-values with values from literature, it is necessary to calculate the k_la-value at 20 °C. Zlokarnik [1999] suggests the following equation:

$$k_la_{(20\,°C)} = \frac{100\,k_la_{(\vartheta)}}{100 + 2{,}665\,(\vartheta\text{-}20)}.$$

(3.13)

ϑ relative temperature, °C

3.2.3 Evaluation of substrate consumption

Both stirrer configurations are investigated for their substrate consumption performance. Therefore, for each combination of stirrer configuration and gas feed rate from section 3.2.2, cultivations with *C. ljungdahlii* using artificial syngas are conducted. Syngas is composed of 32.5 vol-% H_2, 32.5 vol-% CO and 16.0 vol-% CO_2 in nitrogen. Bioreactor cultivations are conducted in triplicates, using a Minifors stirred tank reactor (STR) by Infors-HT (Switzerland) equipped as described above with an ORP-probe (Hamilton, Switzerland) instead of the optical dissolved oxygen probe and the stirrer configurations from Figure 3.1. Temperature of the cultivation broth is maintained at 37 °C using the heating block of the bioreactor housing. The pH-value is regulated to 5.9 using 4 M KOH which is kept under a nitrogen atmosphere. In case of intense foam formation, all bioreactors of a triplicate are supplemented with one drop of the anti-foaming agent Contraspum A 4050 HAC (Zschimer und Schwarz, Germany). Substrate consumption is evaluated at atmospheric pressure for the following gas feed rates: 10 mL min^{-1} (0.007 vvm), 18 mL min^{-1} (0.012 vvm) and 44 mL min^{-1} (0.029 vvm). The installed microsparger generates fine microbubbles, which enhance mass transfer between the gaseous and liquid phase [Bredwell 1998]. Stirrer speed for these fermentations is set to 800 min^{-1}. For bioreactor cultivations, the media is prepared under aerobic conditions with the composition described in chapter 3.1.1. Only exceptions are that fructose is omitted and cysteine-HCl is reduced to 0.53 g L^{-1}. After autoclaving at 121 °C for 20 min, the redox potential of the media was lowered to about -200 mV by sparging with syngas and adding the amount of cysteine-HCl stated above. Bioreactors are seeded with 150 mL of a 48 h grown bottle culture. Off-gas data is evaluated as described in section 3.1.4 and off-line samples are analyzed for OD, CDW, ethanol and acetic acid as described above. Total cultivation time for all conducted experiments is 96 h.

3.3 Elevated pressure for increased mass transfer

3.3.1 Influence of pressure on the gas-liquid mass transfer

One possibility to overcome potential mass transfer is increasing the mass transfer coefficient. According to Equation (2.8), increasing the driving force Δc also leads to an increase in mass transfer. As outlined in the theory section, this can be done by either increasing the mole fraction of a gas component in the gas stream or by increasing the total pressure of the system. Both will lead to an increased partial pressure of the component. But increasing the mole fraction of one component requires the mole fraction of another component in the gas stream to be reduced. It also offers only limited range of increased partial pressure due to the stoichiometry of the acetogenic metabolism. Therefore, this part of the thesis focuses on increasing mass transfer by increasing the total pressure of the system. For these experiments, *C. ljungdahlii* is grown in medium of section 3.1.1 with a mixture of 53,3 vol-% H_2 and 26.7 vol-% CO_2 in nitrogen as energy and carbon source.

3.3.2 Experiments in 1.5 L-scale

Experiments in 1.5 L scale are conducted at atmospheric pressure using the same bioreactor set-up, fermentation procedure and medium as described in section 3.2.3 with the RRB stirrer configuration from Figure 3.1. The fructose content of the preculture media is reduced to $5\,g\,L^{-1}$ and the gas feed rate for the bioreactor cultivation is $43\,mL\,min^{-1}$ (0.029 vvm). If necessary, AF-agent is added manually to all bioreactors one drop at a time.

3.3.3 Scale-up to 2.5 L and elevated pressure

Cultivations at elevated pressure are carried out together with the group of Dr. Nikolaos Boukis in the course of the PhD thesis of Katharina Stoll at the Institute of Catalysis Research and Technology (IKFT) at the Karlsruhe Institute of Technology. To ensure the comparability of results obtained in 1.5 L-scale and 2.5 L-scale, the geometric similarity between both scales needs to be given and important dimensionless numbers describing the process must be kept constant.

Figure 3.2 shows a schematic drawing of both reactor scales. The bioreactor for experiments in 2.5 L-scale is a stainless steel, double jacket vessel (VEB CLG – Chemieanlagenkombinat Leibzig-Grima, Germany) with an inner diameter $D_{2.5}$ of 126 mm and a total volume of 4 L.
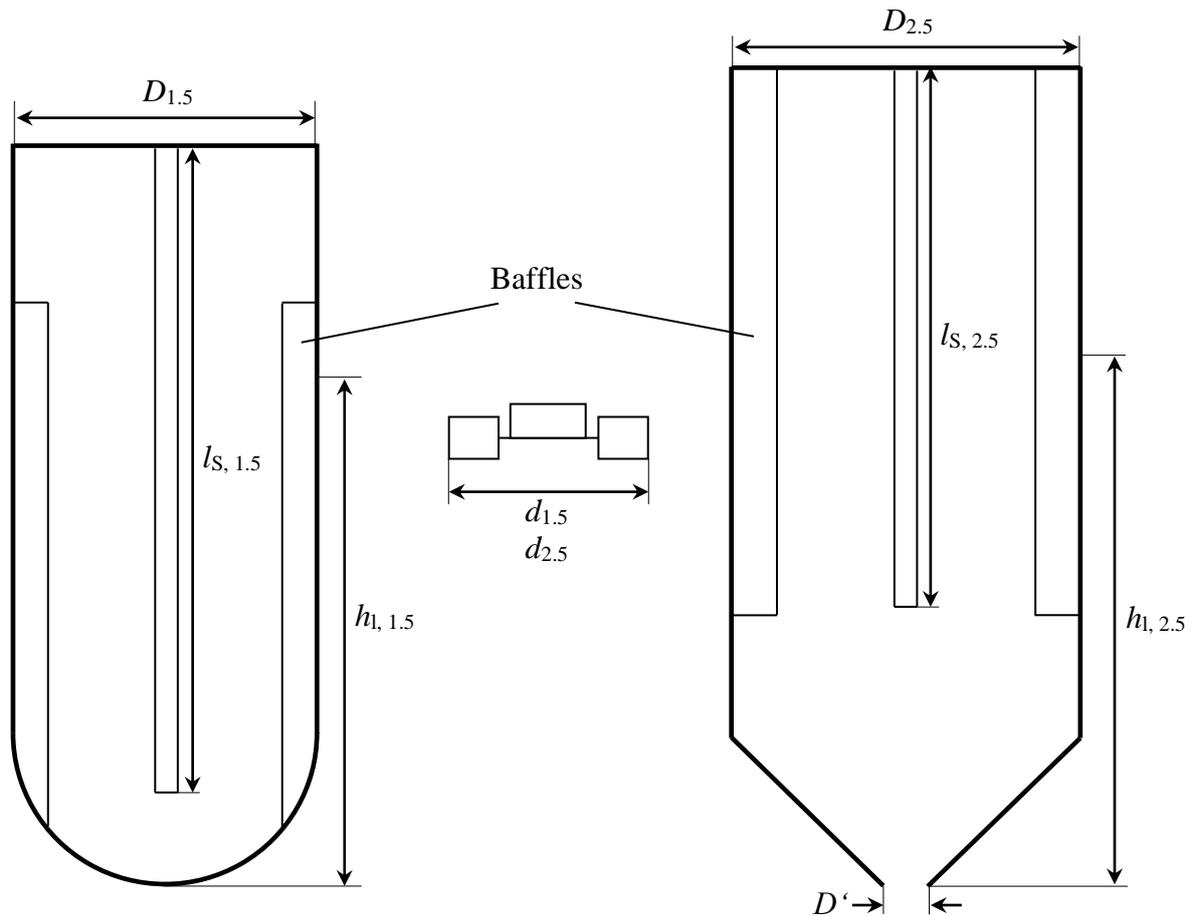
Figure 3.2 – Schematic drawing of the STRs used for 1.5 L scale (left) and 2.5 L scale (right). Between both is one of the two Rushton-Turbines used in each of the reactors. $D_{1.5} = 110$ mm, $d_{1.5} = 46$ mm, $l_{S, 1.5} = 235$ mm, $h_{l, 1.5} = 176$ mm, $D_{2.5} = 126$ mm, $d_{2.5} = 52.7$ mm, $l_{S, 2.5} = 240$ mm, $h_{l, 2.5} = 234.6$ mm. Filling level h_l is without installed equipment (stirrer shaft, baffles, probes, sparger). [Oswald *et al.* 2018a]

The total height of the internal space is 349 mm with a conical bottom of 54 mm height. For 1.5 L-scale experiments, a glass vessel by Infors (see also section 3.5.1) with an inner diameter $D_{1.5}$ of 110 mm, a total height of 270 mm and a hemispherical bottom (r = 55 mm) is used. With the fixed dimensions of the stainless-steel vessel, the only possibility to keep d/D constant is by adjusting the stirrer diameter $d_{2.5}$. Using the stirrer diameter from 1.5 L-scale $d_{1.5} = 46$ mm and the inner diameter of the glass vessel $d_{1.5}/D_{1.5}$ calculates to 0.418. Transferring this to the measures of 2.5 L-scale results in $d_{2.5}$ of 57.5 mm. The stirrer of the 2.5 L-scale is a proportional magnification of the stirrer in 1.5 L-scale. [Oswald *et al.*2018a]

The geometric similarity representing stirrer positions would be 51.5 mm and 157 mm above the deepest part of the stainless-steel vessel. As Figure 3.2 shows, the stirrer shaft (Büchi, Switzerland) of the bigger scale does not reach into the conical part of the vessel. With that, a position of 51.5 mm above the deepest part of the reactor is not possible. Hence, the

compromise is to calculate the stirrer positions, filling volume and filing level from the cylindrical part of the vessel and neglecting the conical bottom. Resulting stirrer positions are 105.5 mm and 211 mm above the deepest part of the vessel (including the conical part) and total filling level $h_{l,2.5}$ is 234.6 mm. This also affects the filling volume of the reactor (without installed equipment) which is the volume of the 1.5 L-scale multiplied with $(D_{2.5}/D_{1.5})^3$ plus the volume of the conical part yielding a volume of 2.51 L. [Oswald *et al.* 2018a]

To ensure comparability of both scales, it is necessary to keep the important process characteristics constant. Ju and Chase [1992] summarize different scale-up strategies from literature. The strategies used in this thesis are geometric similarity as well as constant $k_l a$-value, stirrer speed and Ne number. Schlüter *et al.* [1992] state that if volumetric power input P/V_l and volumetric gas feed rate $\dot{V}_g/V_l$ are of the same value in both scales, then the volumetric mass transfer coefficient has the same value as well. Other authors conclude that a reliable scale-up with constant $k_l a$-value depends on keeping the superficial gas velocity (v) constant [Van't Riet 1979; Henzel 1982; Zlokarnik 1999]. Schlüter *et al.* [1992] also state that for small changes in scale, the $k_l a$ correlation with $\dot{V}_g/V_l$ instead of v leads only to insignificant deviations. Therefore, power input for 1.5 L-scale is measured as the difference in power uptake of stirring in air and stirring in 1.5 L of water and a gas feed rate of 0.029 vvm. Keeping Ne constant allows calculating the necessary stirrer speed at P/V_l = constant to 757 min^{-1}. The gas feed rate of the larger scale calculates to 72 mL min^{-1}. [Oswald *et al.* 2018a]

3.3.4 Experiments in 2.5 L-scale

The following pressure steps are investigated (in absolute pressure): 1 bar, 4 bar and 7 bar. The medium composition is explained in section 3.1.1, cultivation volume is 2.5 L. the volumetric amount of substance flow rate $\dot{n}\,V_l^{-1}$ is kept constant for all experiments.

Gas is dispersed inside the reactor by a sintered metal plate at the end of a ¼"-tube and pressurization of the bioreactor starts immediately after inoculation. Each experiment is seeded with 10 % of the final volume of a 48 h, fructose grown culture. Cultivation temperature and pH-value are set to 37 °C and 5.9 respectively and the stirrer speed and gas feed rate as calculated above are applied. Maximum cultivation time is 90 h. Figure 3.3 shows the flow chart of the high-pressure reactor and its installed periphery. Mass flow of feed gas is

controlled and regulated by a Coriolis force MFC (Bronkhorst, Netherlands) and mass-flow-meter (MFM, Bronkhorst, Netherlands). Pressures higher than 1 bar absolute are regulated by a pressure regulator and sensory valve (Bronkhorst, Netherlands) positioned in the off-gas line behind the MFM. Off-gas composition is measured by a GC (Shimadzu, Japan). Cultivation temperature is maintained via the double jacket and a thermostat (Haake, Germany) and the off-gas is cooled to minimize water loss through evaporation. A HPLC-pump (Bischoff, Germany) controls the addition of pH adjustment solutions through capillary tubes. If necessary, a six-port valve allows switching between $4\,M\ H_3PO_4$ and $4\,M\ KOH$. Both pH adjustment solutions are kept under a nitrogen atmosphere. A second HPLC-pump (Bischoff, Germany) adds AF-agent (Zschimer und Schwarz, Germany) in case the AF-electrode gives a signal. Gas streams are sterile filtered by a $0.2\,\mu m$ sinter metal filter (Swagelock, USA) before the feed gas enters the reactor and before the off-gas enters the pressure senor. A check valve between the reactor and feed gas filter prevents liquid from the reactor to block the filter. ORP-probe (Corr Instruments, USA) and pH-probe (Corr Instruments, USA) are mounted horizontally at half height through the sides of the reactor. The pH-probe is disinfected with
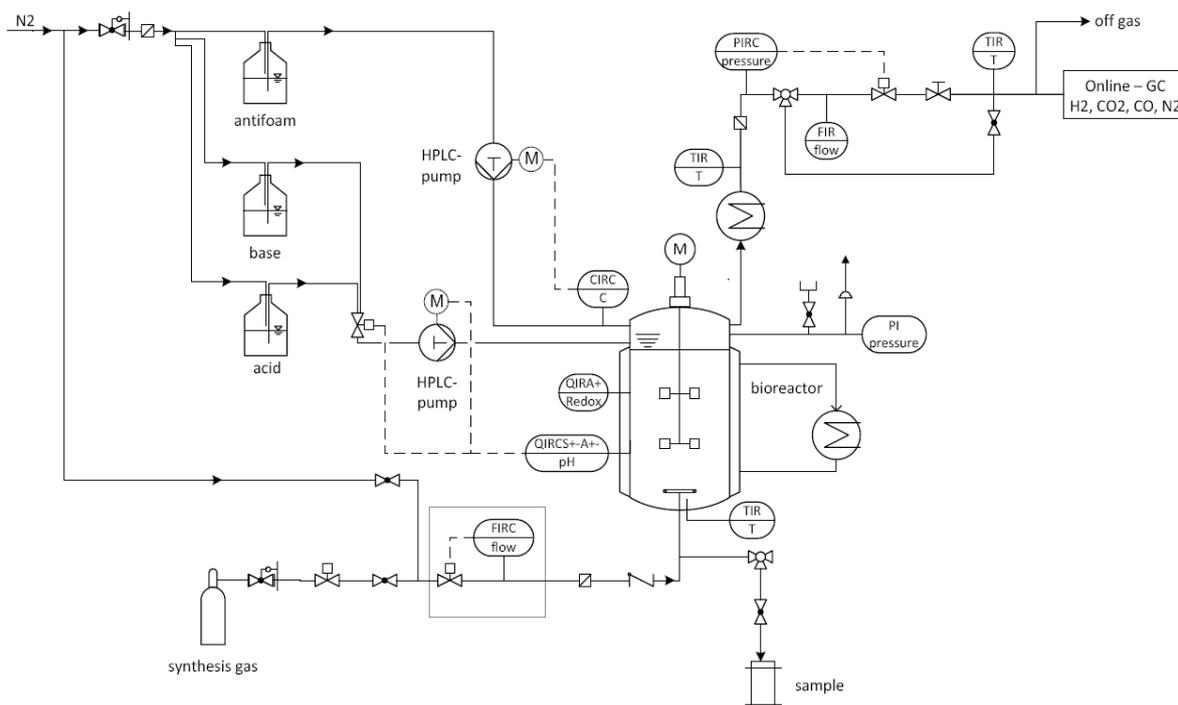
Figure 3.3 – Flow chart of STR used for elevated pressure cultivations with installed periphery. FIRC, flow indication, recording and control; QIRCS+-A+-, pH indication, recording and control (pH probe); QIRA+, redox potential indication and recording (redox probe); CIRC, courent indication, recording and control (AF-electrode); TIR, temperature indication and recording; PIRC, pressure indication, recording and control; FIR, flow indication and recording; PI, pressure indicator. [Oswald *et al.* 2018]

isopropanol. It is installed after steam sterilizing at 121 °C and before medium is filled into the reactor, due to a maximum temperature tolerance of the pH-probe of 80 °C. [Oswald *et al.* 2018a]

3.4 Influence of cyanide on growth and product formation of *Clostridium ljungdahlii*

CODH is an important enzyme in the WLP, since it not only catalyzes the oxidation of CO to CO_2, but also forms a functional complex with acetyl-CoA synthase which links the methyl-branch and the carbonyl-branch of WLP to form the central metabolite acetyl-CoA. As outlined in chapter 2.3.2, a well-known inhibitor of CODH is cyanide, which is also a minor constituent of crude synthesis gas. Data on how cyanide affects *C. ljungdahlii* is scarce. Therefore, the experiments in this thesis are conducted to show the influence of cyanide on growth and product formation of this organism. Cyanide is prepared as potassium cyanide solution in 100 mM potassium phosphate buffer at pH 11 to prevent hydrogenation of CN^- and degassing of HCN during anaerobisation, sterilization and storage. All buffers are prepared in sealed serum bottles. *C. ljungdahlii* DSM135228 is grown in 50 mL complex media with either $10 \, g \, L^{-1}$ fructose or 2.02 bar absolute pressure of synthesis gas as carbon and energy source. Fructose experiments are conducted in 125 mL serum bottles and syngas experiments

50 mL Culture media
+
1 mL H_2O, potassium phosphate buffer or potassium phosphate buffer with KCN

2.02 bar
Synthesis gas

$10 \, g \, L^{-1}$
Fructose
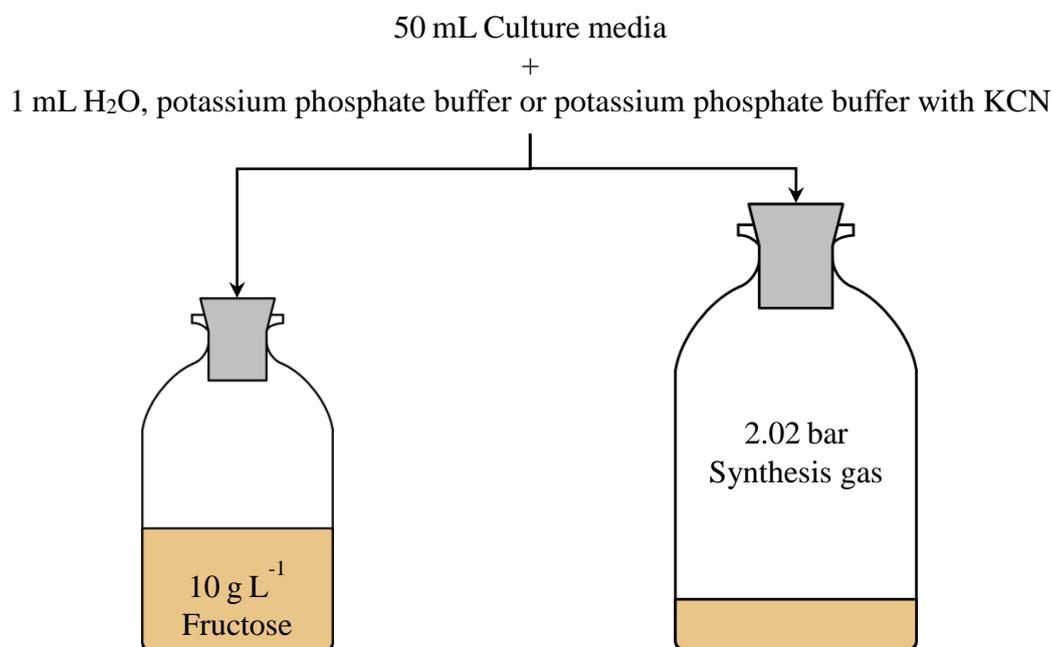
Figure 3.4 – Overview of cyanide experiments with *C. ljungdahlii*. Effects of cyanide are investigated in both fructose and syngas growing cultures with cyanide concentrations of $0 \, mmol \, L^{-1}$, $0.025 \, mmol \, L^{-1}$, $0.05 \, mmol \, L^{-1}$, $0.1 \, mmol \, L^{-1}$ and $1.0 \, mmol \, L^{-1}$. [Oswald *et al.* 2018b]

in 250 mL serum bottles. Culture media and bottles are prepared as described in section 3.1.1. Figure 3.4 gives an overview of the experiments. The following final cyanide concentrations are investigated (all numbers are in mM): 0.025, 0.05, 0.1 and 1.0. To achieve the desired KCN concentrations for every flask, 1 mL of potassium phosphate buffer with cyanide is added per 50 mL of culture media. Cultures with 1 mL sterile anaerobic water or 1 mL of sterile anaerobic phosphate buffer per 50 mL of culture media are used as controls for growth and product formation. Headspace pressure in cultures growing with syngas is used as an indicator of substrate consumption and is measured before and after collection of liquid and gas samples. Gas samples are analyzed with a micro-GC (see section 3.1.3) to determine the consumption of the individual components of the syngas. [Oswald *et al.* 2018b]

3.5 Process link-up: From syngas to malic acid

3.5.1 Nitrogen reduction in culture media for *Clostridium ljungdahlii*

This experiment aims to show that acetic acid, as the main product of the acetogenic metabolism, can be used as a substrate for further aerobic cultivations. For this, acetic acid containing broth of a *C. liungdahlii* syngas fermentation is fed to *Aspergillus oryzae*, a filamentous fungus, for the production of malic acid. This is a cooperation experiment with Stefan Dörsam from the "BLT section II: Technical Biology" who does the fungal fermentation part of the experiment. Due to that, the following chapters show the syngas part and the final link-up experiment. Methods and results of preliminary experiments for the fungal part can be found in Oswald *et al.* [2016].

The original medium used by Benglesdorf *et al.* [2016] contains $2.5 \, \text{g L}^{-1}$ ammonia chloride, but *A. oryzae* produces malic acid only under nitrogen limited conditions [Knuf *et al.* 2013]. To use the syngas fermentation broth as culture media for *A. oryzae*, it is necessary to check how much ammonia is left in the broth after 96 h of syngas fermentation and reduce the initial amount if necessary. Therefore, bioreactor cultivations are conducted in triplicates using the set-up and procedures described in section 3.2.3. The stirrer set-up for this experiment is the RMR configuration from section 3.2.1. Figure 3.5 shows the stirrer configuration for the nitrogen reduction experiments. [Oswald *et al.* 2016]

The total volume of each bioreactor is 2.5 L, the filling volume is 1.5 L; thus leaving a headspace of 1 L. Carbon- and energy source is a synthesis gas consisting of 32.5 vol-% H_2, 32.5 vol-% CO and 16.0 vol-% CO_2 in Nitrogen. This mixture resembles the composition of
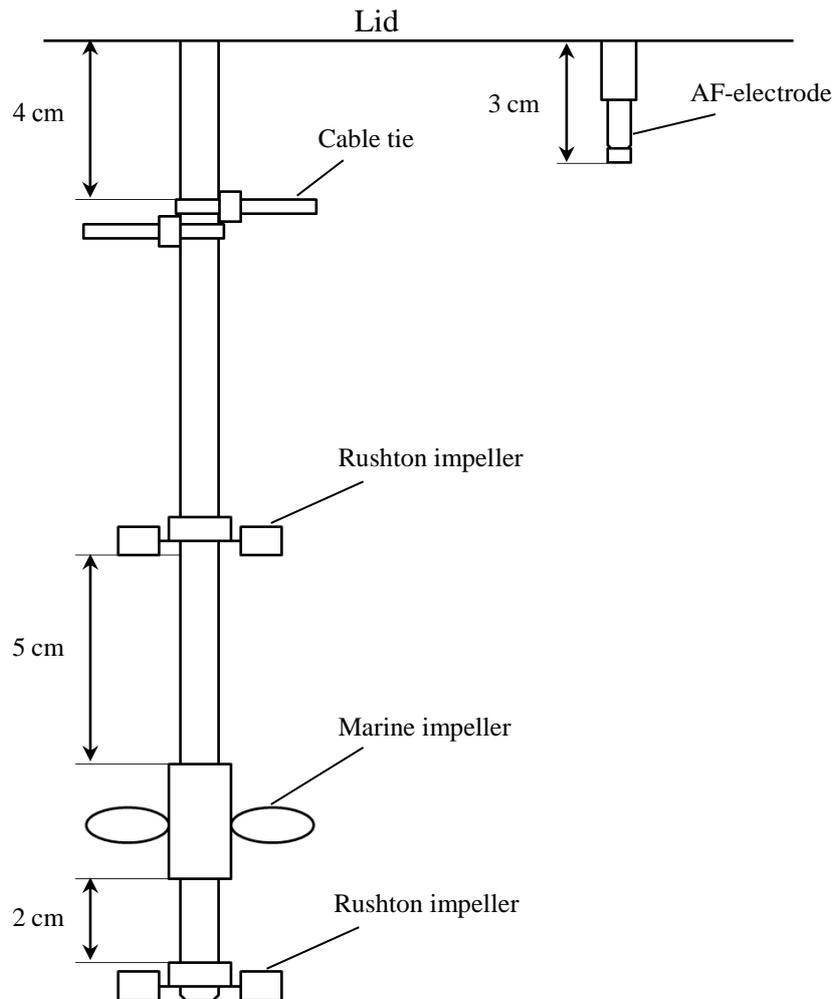
Figure 3.5 – Rushton-Marine-Rushton stirrer configuration for syngas fermentation. The cable ties on the upper part of the stirrer shaft are in total 7.5 cm long and serve as foam disrupter.

syngas from entrained flow gasification of straw. In case of intense foam formation, each bioreactor is fitted with an anti-foam probe as seen in Figure 3.5 using Contraspum A 4050 HAC (Zschimer und Schwarz, Germany) as an anti-foaming agent. Red-y smart series MFC by Vögtlin Instruments (Switzerland) keep the gas flow rate in the bioreactor at 10.4 mL min^{-1} and stirrer speed is set to 800 min^{-1}. The ammonia content for the nitrogen limited media is reduced according to the results of the first triplicate. Concentrations of ammonia at the beginning and the end of each cultivation are measured with an ion chromatograph. Measurements are kindly conducted by the group of Prof. Clemens Posten (BLT Section III: Bioprocess engineering). Cultivation time on syngas is 96 h and the broth is harvested and handed to Stefan Dörsam for preliminary experiments with *A. oryzae*. [Oswald *et al.* 2016]

3.5.2 Process link-up via sequential mixed culture

Bioreactor set-up and cultivation procedure for the syngas fermentation part of the sequential mixed culture is the same as stated in chapter 3.5.1. The syngas flow rate is set to $12.6\,mL\,min^{-1}$ and is increased to $18\,mL\,min^{-1}$ between $41.5\,h$ and $71.5\,h$. Instead of harvesting the culture broth after $96\,h$, the conditions are changed to aerobic. Therefore, the reactor is flushed with air for approx. 30 min to replace all remaining syngas and temperature is reduced to $35\,°C$. After that, to avoid clogging of the microsparger by the fungus, the anti-foam probe is exchanged for a standard issue sparger of the Minifors reactors and the microsparger is turned sideways to make space for the new sparger. The ORP-probe is removed so that $90\,g\,L^{-1}$ $CaCO_3$ can be added to get the pH-value to 5.5 and to reseed the broth with washed precultures of *A. oryzae*. Figure 3.6 shows the process set-up for both parts of the sequential mixed culture. The aerobic fungal fermentation part of the sequential mixed culture takes $100\,h$, an aeration rate of $600\,mL\,min^{-1}$ and a stirrer speed of $300\,min^{-1}$. The added amount of $CaCO_3$ is enough to keep the pH-value at 5.5 for the whole course of the fungal fermentation. [Oswald *et al.* 2016]
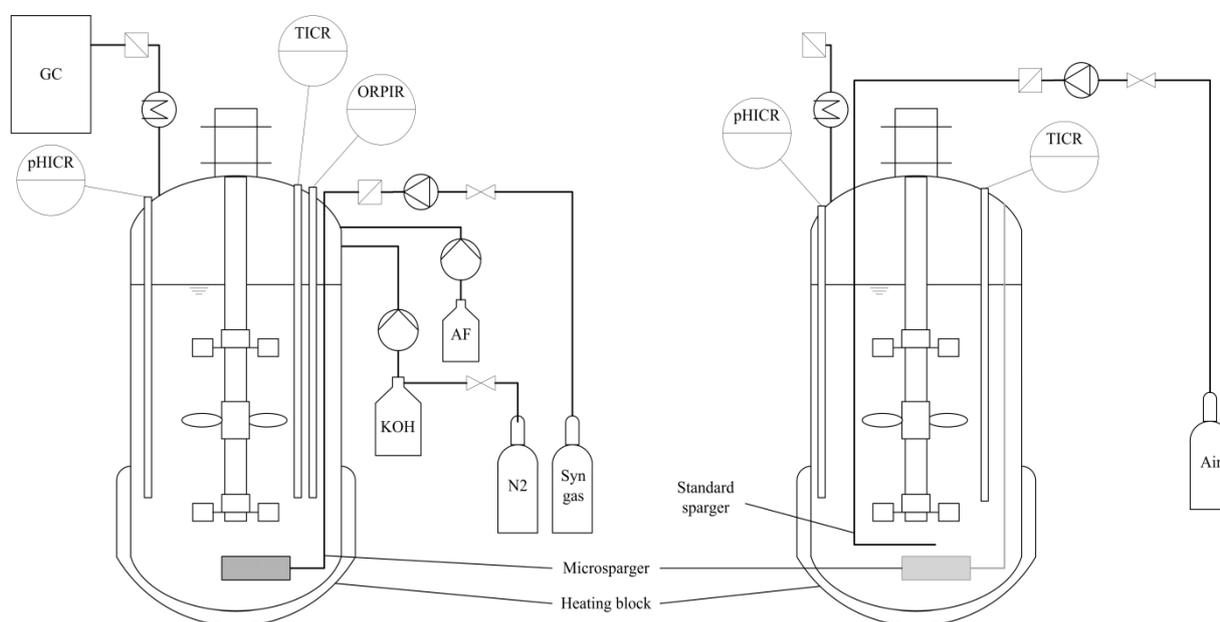
Figure 3.6 – Process scheme for anaerobic syngas fermentation (left) and aerobic fungal fermentation (right). pHICR: pH indicate, control and record, TICR: temperature indicate, control and record, ORPIR: ORP indicate and record, AF: anti foam, GC: gas chromatograph. For aerobic fungal fermentation the microsparger had to be turned sideways to make room for the standard sparger. No pH adjustment was conducted during fungal fermentation. [Oswald *et al.* 2016]

4. Results

4.1 Characterization of stirred tank reactor system

4.1.1 Determination of $k_l a$-values

The stirrer set-ups RRB and RMR are tested for their mass transfer properties and effect on substrate consumption. The RRB set-up shows high shear forces at the tips of the turbine blades and ensures formation of fine bubbles while the additional marine impeller and missing baffles in the RMR set-up allows for vortex formation and partial recirculation of gas from the headspace. Values for the volumetric mass transfer coefficient are determined at stirrer speeds of 600 min^{-1}, 800 min^{-1} and 1000 min^{-1} using air at flow rates of 18 mL min^{-1}, 25 mL min^{-1} and 50 mL min^{-1} each. Figure 4.1 and Figure 4.2 show the measured $k_l a$-values for both stirrer set-ups with air and ammonia reduced medium.

Values in Figure 4.1 are determined with the given flow rates, while simultaneously aerating the headspace of the bioreactor with 0.2 L min^{-1}. This is to quickly replace the nitrogen in the headspace. Thus, reflecting a situation where headspace and feed gas have the same composition. For 18 mL min^{-1} average $k_l a$-values at 800 min^{-1} and 1000 min^{-1} are of the same
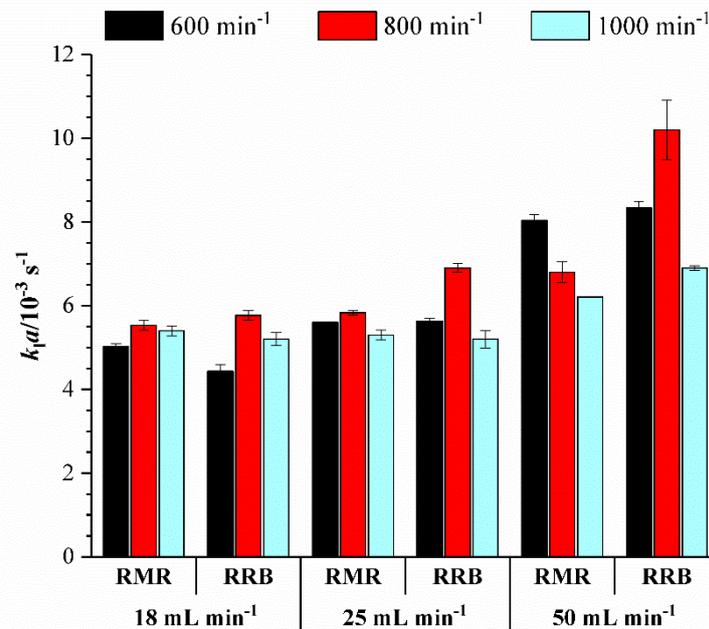
Figure 4.1 – $k_l a$-values for 600 min^{-1}, 800 min^{-1} and 1000 min^{-1} with simultaneous aeration of the headspace, sorted by stirrer configuration and air flow rate.

order of magnitude for both stirrer set-ups with a maximum average of $5.5 \, 10^{-3} \, s^{-1}$ for the RMR and $5.7 \, 10^{-3} \, s^{-1}$ for the RRB. At $25 \, mL \, min^{-1}$ average values of the RMR set-up for all three stirrer speeds are between $5.3 \, 10^{-3} \, s^{-1}$ and $5.8 \, 10^{-3} \, s^{-1}$ whereas for the RRB set-up maximum average k_la is $6.9 \, 10^{-3} \, s^{-1}$. At $50 \, mL \, min^{-1}$, the RMR stirrer arrangement has a maximum k_la-value of $8.0 \, 10^{-3} \, s^{-1}$ at a stirrer speed of $600 \, min^{-1}$ and the RRB set-up at $800 \, min^{-1}$ with a value of $10.2 \, 10^{-3} \, s^{-1}$.

Resulting values for gas-liquid mass transfer rate without additional aeration of the headspace are summarized in Figure 4.2. Without flushing the headspace of the bioreactor with air, nitrogen is not removed from the headspace. Therefore, these values represent k_la-vaules of a process feed gas and headspace are not similar (e. g. when all fed substrates are immediately consumed). Similar to the results in Figure 4.1, maximum k_la-vaules for each stirrer set-up and -speed are achieved at a gas feed rate of $50 \, mL \, min^{-1}$ with $5.9 \, 10^{-3} \, s^{-1}$ for the RMR set-up at $600 \, min^{-1}$ and $8.3 \, 10^{-3} \, s^{-1}$ for the RRB set-up at $800 \, min^{-1}$.

The main reason behind the RMR stirrer configuration is the recirculation of gas from the headspace in the vortex zone of the fluid flow. Significant vortex formation is achieved at minimum stirrer speed of $800 \, min^{-1}$ which therefore is chosen for both configurations in the following substrate consumption cultivations. After conducting the experiments for the evaluation of substrate consumption, it has been found that the calibration of the syngas mass
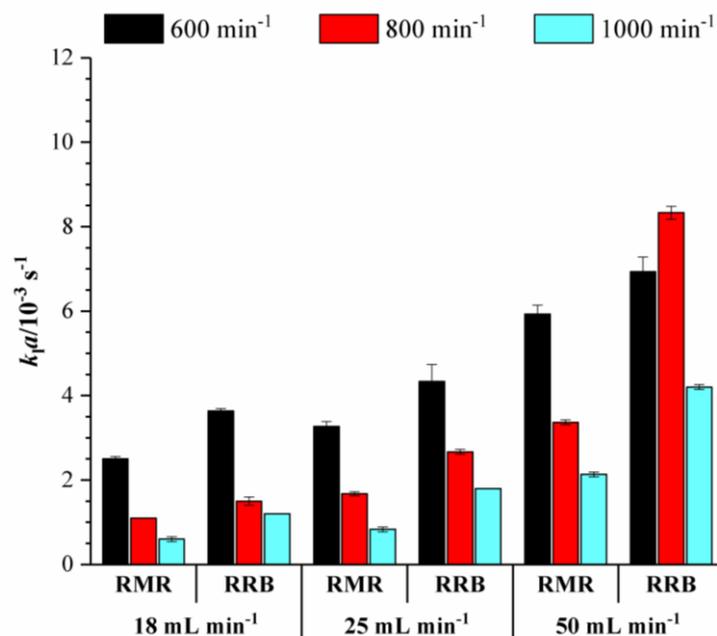
Figure 4.2 - k_la-values for $600 \, min^{-1}$, $800 \, min^{-1}$ and $1000 \, min^{-1}$ sorted by stirrer configuration and air flow rate.

flow controllers delivered by the manufacturer is wrong. For settings of $18\,\text{mL min}^{-1}$, $25\,\text{mL min}^{-1}$ and $50\,\text{mL min}^{-1}$ the resulting gas flow rates are $10.3\,\text{mL min}^{-1}$, $17.8\,\text{mL min}^{-1}$ and $44.4\,\text{mL min}^{-1}$ respectively. Figure 4.3 A shows results of $k_l a$ measurements at $800\,\text{min}^{-1}$ and afore mentioned resulting flow rates while simultaneously aerating the headspace. It also contains values for headspace aeration alone. Those are $3.7\,10^{-3}\,\text{s}^{-1}$ for the RMR and
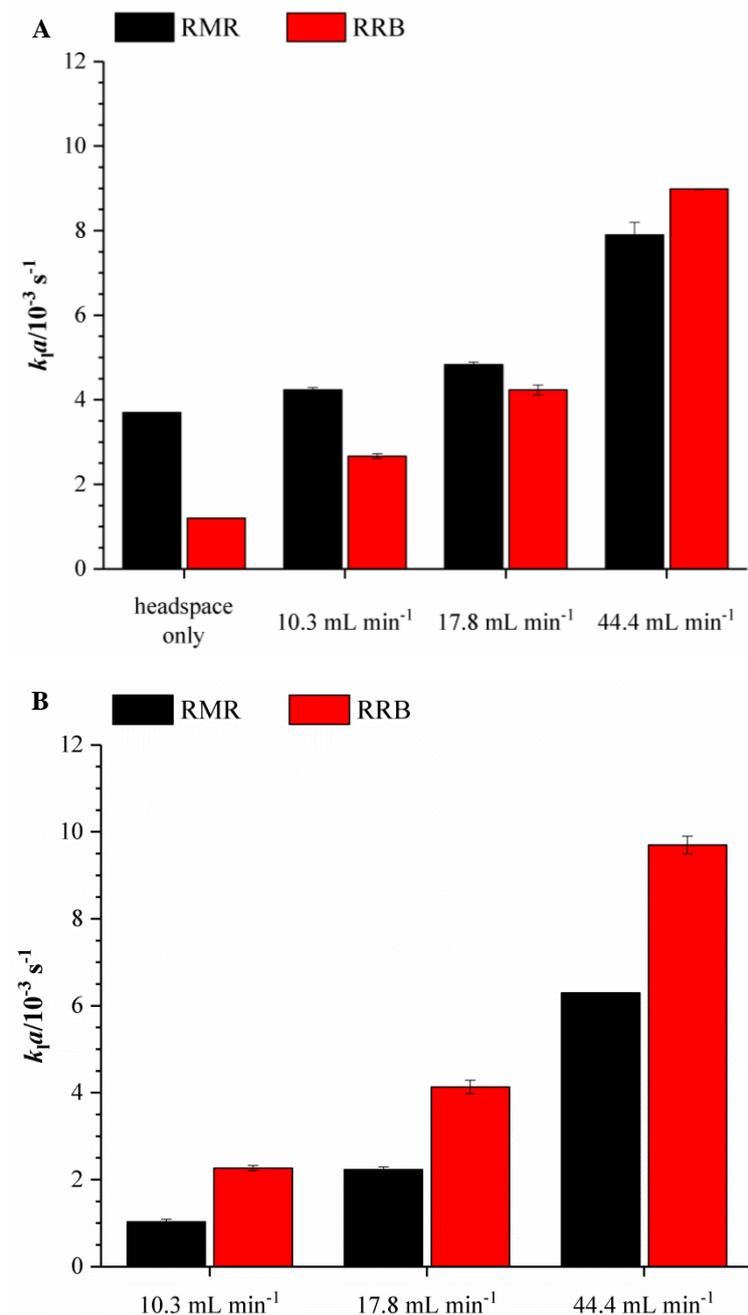
Figure 4.3 – $k_l a$-values for gas feed rates of $10.3\,\text{mL min}^{-1}$, $17.8\,\text{mL min}^{-1}$ and $44.4\,\text{mL min}^{-1}$ at $800\,\text{min}^{-1}$. A with simultaneous aeration of the headspace. Also included are gas-liquid mass transfere coeficients for headspace areation only. **B** without headspace aeration.

$1.2\,10^{-3}\,s^{-1}$ for the RRB set-up. Maximum mass transfer coefficients for both set ups are achieved with a gas feed rate of $44\,mL\,min^{-1}$ with $7.9\,10^{-3}\,s^{-1}$ (RMR) and $9.0\,10^{-3}\,s^{-1}$ (RRB). Like Figure 4.2, Figure 4.3 B shows mass transfer coefficients for the resulting flow rates of the wrong calibrated MFCs without additional headspace aeration. Values increase from $1.0\,10^{-3}\,s^{-1}$ (RMR) and $2.3\,10^{-3}\,mL\,min^{-1}$ (RRB) at $10.3\,mL\,min^{-1}$ to $6.3\,10^{-3}\,s^{-1}$ and $9.7\,10^{-3}\,s^{-1}$ (RRB) at $44.4\,mL\,min^{-1}$.

4.1.2 Evaluation of substrate consumption

Experiments for the determination of substrate consumption are carried out with the MFCs as described in section 3.2.3 for gas feed rate set points of $18\,mL\,min^{-1}$, $25\,mL\,min^{-1}$ and $50\,mL\,min^{-1}$. As explained previously, the manufacturer calibration of those MFCs is incorrect and resting gas flowrates are: $10.33 \pm 0.21\,mL\,min^{-1}$ ($18\,mL\,min^{-1}$ setting), $17.78 \pm 0.22\,mL\,min^{-1}$ ($25\,mL\,min^{-1}$ setting) and $44.38 \pm 0.26\,mL\,min^{-1}$ ($50\,mL\,min^{-1}$ setting). This directly impacts the total volume of syngas and amount of substance for H_2, CO and CO_2 used for each experiment. Although experiments are conducted in triplicates, one and always the same, bioreactor of each experimental set-up behaves differently than the other two. Since these bioreactors show little deviation between each other, the following results show the average of these two bioreactors. The data of the third bioreactor can be found in the appendix for comparison. Table 4.1 summarizes the results of product and fructose analytics and online off-gas analytics as well as the total gas volume and amount of substance for H_2, CO and CO_2 that have been fed during each experimental set-up. For gas feed rates of $10.3\,mL\,min^{-1}$ and $17.8\,mL\,min^{-1}$ final concentrations of acetic acid increase from $15\,g\,L^{-1}$ to $21\,g\,L^{-1}$. At $44.4\,mL\,min^{-1}$, the final acetic acid concentration goes down to $10.49 \pm 0.13\,g\,L^{-1}$ for the RMR approach while the RRB approach yields with $8.82 \pm 0.46\,g\,L^{-1}$ the lowest acetic acid concentration. On the other hand, ethanol concentrations increase from $0.5\,g\,L^{-1}$ to $2.7\,g\,L^{-1}$ with increasing gas feed rates.

While the amount of consumed carbon monoxide increases with increasing gas feed rates, the consumed amount of hydrogen shows a maximum at $17.8\,mL\,min^{-1}$ and is close to zero at $44.4\,mL\,min^{-1}$. This is also reflected in the overall consumption ratio for hydrogen, which decreases from $72.5\,\%$ to $3.3\,\%$ for the RMR set-up and from $77.3\,\%$ to zero for RRB. The overall amount of consumed carbon monoxide might increase with increasing gas feed rates, but when compared to the ingoing amount of carbon monoxide, the consumption ratio

Table 4.1 – Results of substrate consumption experiments with *C. ljungdahlii* growing with syngas as sole carbon and energy source.

Set-up	RMR-10	RRB-10	RMR-18	RRB-18	RMR-44	RRB-44
β_{CDW}/g L^{-1}	0.73 ± 0.04	0.71 ± 0.01	0.82 ± 0.02	0.77 ± 0.05	0.53 ± 0.03	0.28 ± 0.05
$\beta_{acetic\ acid}$/g L^{-1}	14.95 ± 0.22	15.27 ± 1.91	21.48 ± 0.05	20.72 ± 0.78	10.49 ± 0.13	8.82 ± 0.46
β_{EtOH}/g L^{-1}	0.47 ± 0.07	0.55 ± 0.21	2.15 ± 0.18	2.42 ± 0.72	2.68 ± 0.29	1.91 ± 0.38
$\beta_{fructose}$/g L^{-1}	0.57 ± 0.00	0.45 ± 0.02	0.59 ± 0.02	0.53 ± 0.00	0.73 ± 0.02	0.79 ± 0.02
$c_{H2,R}$/mol L^{-1}	0.42 ± 0.00	0.45 ± 0.01	0.57 ± 0.02	0.62 ± 0.01	0.08 ± 0.01	0.00 ± 0.01
$c_{CO,R}$/mol L^{-1}	0.45 ± 0.00	0.46 ± 0.00	0.68 ± 0.19	0.78 ± 0.01	1.15 ± 0.02	0.91 ± 0.03
$c_{CO2,R}$/mol L^{-1}	0.00 ± 0.00	0.00 ± 0.02	-0.15 ± 0.02	-0.07 ± 0.01	-0.62 ± 0.00	-0.56 ± 0.02
$V_{gas,\ total}$/L	60.40 ± 0.39	60.01 ± 0.02	103.50 ± 0.01	102.42 ± 0.03	257.05 ± 0.78	256.39 ± 0.91
t/h	97.73 ± 0.63	97.10 ± 0.03	96.91 ± 0.01	95.90 ± 0.03	96.49 ± 0.29	96.24 ± 0.34
E_{H2}/%	72.49 ± 0.09	77.32 ± 1.09	57.43 ± 1.86	65.63 ± 1.06	3.26 ± 0.40	0.00 ± 0.28
E_{CO}/%	81.38 ± 0.05	83.91 ± 0.37	83.60 ± 0.21	81.50 ± 0.66	47.46 ± 1.00	37.87 ± 1.17
E_{CO2}/%	-1.76 ± 1.94	0.93 ± 9.21	-36.51 ± 4.26	-16.45 ± 2.96	-55.25 ± 0.05	-50.88 ± 2.44

Average values of two bioreactors per experimental set-up. The numbers behind RMR and RRB in the table header stand for the gas feed rate with $10 = 10.3\ mL\ min^{-1}$, $18 = 17.8\ mL\ min^{-1}$, $44 = 44.4\ mL\ min^{-1}$. β_{CDW}, maximum concentration of CDW; $\beta_{Fructose}$, concentration of fructose at beginning of fermentation; $\beta_{acetic\ acid}$, final concentration of acetic acid; β_{EtOH}, final concentration of ethanol; $c_{H_2,R}$, consumed amount of hydrogen per liter reactor volume; $c_{CO,R}$, consumed amount of carbon monoxide per liter reactor volume; $c_{CO_2,R}$, consumed amount of carbon dioxide per liter reactor volume; $V_{gas,\ total}$, total volume of used syngas over the course of fermentation; t, total process time; E_{H_2}, consumption ratio of hydrogen as consumed amount of hydrogen in per cent of total amount of ingoing hydrogen; E_{CO}, consumption ratio of carbon monoxide as consumed amount of carbon monoxide in per cent of total amount of ingoing carbon monoxide; E_{CO_2}, consumption ratio of carbon dioxide as consumed amount of carbon dioxide in per cent of total amount of ingoing carbon dioxide. Negative Values in the columns $c_{CO_2,R}$ and E_{CO_2} mean that more CO_2 has left the reactor than has gone in.

between $10.3\ mL\ min^{-1}$ and $17.8\ mL\ min^{-1}$ increases for the RMR set-up and decreases for the RRB set-up. At $44.4\ mL\ min^{-1}$, the consumption ratio decreases to 47.5% (RMR) and 37.9 % (RRB) at.

Yields based on either consumed substrate ($Y_{P/S}{}^{*}$) or total fed substrate ($Y_{P/S}{}^{**}$) can be found in Table 4.2 together with average durations of complete substrate consumption ($t_{e_i \geq 97\,\%}$). In this thesis, complete substrate consumption is defined as the time in which the actual consumption rate (e_i) is more than 97 % of the ingoing substrate feed rate (see equation 3.4). The yields based on consumed substrates and used substrates show the same tendency. $Y_{P/S}{}^{*}$ gives

Table 4.2 – Product yields based on consumed and used substrate as well as average durations of complete substrate consumption.

Set-up	RMR-10	RRB-10	RMR-18	RRB-18	RMR-44	RRB-44
$Y_{P/S}{}^{*}$/g g^{-1}	1.05 ± 0.04	0.99 ± 0.02	0.95 ± 0.00	0.97 ± 0.03	0.41 ± 0.01	0.41 ± 0.03
$Y_{P/S}{}^{**}$/g g^{-1}	0.85 ± 0.03	0.85 ± 0.05	0.78 ± 0.00	0.78 ± 0.03	0.19 ± 0.01	0.15 ± 0.02
$t_{eH2 \geq 97\%}$/h	53.95 ± 0.78	69.47 ± 1.0	9.51 ± 0.07	18.25 ± 1.80	0.00 ± 0.00	0.00 ± 0.00
$t_{eCO \geq 97\%}$/h	71.31 ± 0.16	74.60 ± 0.28	37.84 ± 12.05	61.46 ± 13.97	0.00 ± 0.00	0.00 ± 0.00

*, based on consumed H_2 and CO; **, based on totally fed H_2 and CO; $t_{eH2 \geq 97\%}$, duration of complete hydrogen consumption; $t_{eCO \geq 97\%}$, duration of complete carbon monoxide consumption. Average values of two bioreactors per experimental set-up.

information about the ratio in which consumed substrates are converted into products (acetic acid and ethanol) while $Y_{P/S}{}^{**}$ gives information about the overall substrate-to-product conversion ratio of the process. Both yields decrease with increasing gas feed rate. At 10 mL min^{-1}, all consumed substrates end up in products. Both stirrer set-ups give here the same yield for totally used substrates of 0.85 g g^{-1} with only slight difference in the standard deviation. With increasing gas feed rate yields decrease to $Y_{P/S}{}^{*}$ of 0.41 g g^{-1} (both set-ups) and $Y_{P/S}{}^{**}$ of 0.19 g g^{-1} (RMR) and 0.15 g g^{-1} (RRB). The value for $Y_{X/S}$ decreases with increasing gas feed rate to 0.02 g g^{-1} at 17.8 mL min^{-1} and 0.005 g g^{-1} at 44.4 mL min^{-1} for both stirrer configurations.

Times of complete substrate consumption shown in Table 4.2 indicate that the duration of complete hydrogen consumption is always shorter than the duration of complete carbon monoxide consumption. The difference between the two durations is 5.1 h for the RRB set-up at 10 mL min^{-1} gas feed rate. At the lowest gas feed rate, once complete consumption of hydrogen and carbon monoxide is established it is kept up until the end of the fermentation. For 18 mL min^{-1} durations of complete substrate consumption are shorter, being 22.35 ± 0.49 h (RMR) and 10.65 ± 3.61 h (RRB) for hydrogen and 30.45 ± 3.18 h (RMR) and 43.15 ± 3.61 h (RRB) for carbon monoxide. At 44 mL min^{-1}, complete hydrogen consumption is achieved in none of the two stirrer configurations. This is also visualized in Figure 4.4 which shows the amount of substance flow rates per liter reactor medium for H_2, CO, and CO_2 in the off-gas of substrate consumption experiments. In addition to the information from Table 4.2, the figure
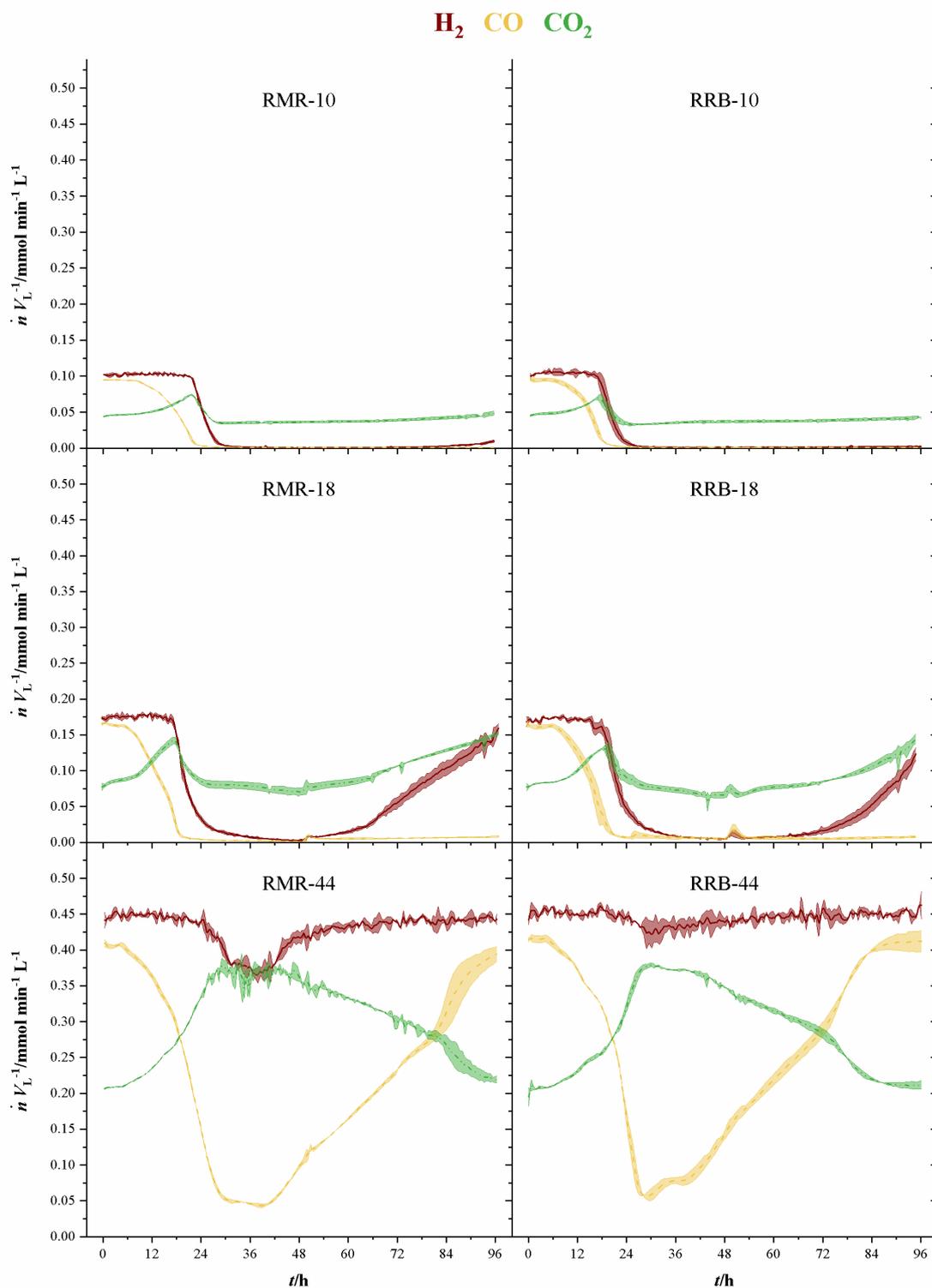
Figure 4.4 – Average amount of substance flow rates per liter medium in the off-gas of substrate consumption experiments. Graphs show average values of two bioreactors per experimental set-up. Results of experiments with RMR (left) and RRB stirrer set-up (right) at average gas flow rates of 10.33 ± 0.21 mL min^{-1}, 17.78 ± 0.22 mL min^{-1} and 44.38 ± 0.26 mL min^{-1} (top to bottom). Hydrogen (red line), carbon monoxide (yellow line) and carbon dioxide (green line). The areas around the lines indicate the standard deviation.

shows that for each gas feed rate the development of off-gas data shows the same tendency. While at a gas feed rate of $10\,mL\,min^{-1}$ hydrogen consumption only starts to decline at the end of RMR-10, it starts to decline at 48 h in RMR-18 and 56 h in RRB-18. At $44\,mL\,min^{-1}$, there is only significant hydrogen consumption in RMR-44. Carbon monoxide stays at complete consumption in all experiments with $10\,mL\,min^{-1}$ and $18\,mL\,min^{-1}$ gas feed rate with an increase in off-gas carbon monoxide at 48 h (RMR-18) and 50 h (RRB-18) due to manual addition of AF agent. At $44\,mL\,min^{-1}$ carbon monoxide goes down to $0.03\,mmol\,min^{-1}$ (RMR-44) and $0.05\,mmol\,min^{-1}$ (RRB-44) but starts to increase again between 36 h and 40 h.

4.2 Elevated pressure for increased mass-transfer

According to Henry's law of solubility, increasing the total system pressure while keeping the gas composition constant will result in higher solubility of the gas components. Therefore, the driving force for mass transfer, Δc, will be increased, too. To avoid any possible inhibitory effects by increased carbon monoxide partial pressures, the following experiments are conducted only with hydrogen, carbon dioxide and nitrogen. Figure 4.5 shows the volumetric amount of substance flow rates $\dot{n}\,V_L^{-1}$ in the off-gas of three fermentations in 1.5 L-scale. Initial carbon dioxide and hydrogen flow rates of $0.3\,mmol\,min^{-1}\,L^{-1}$ (CO_2) and
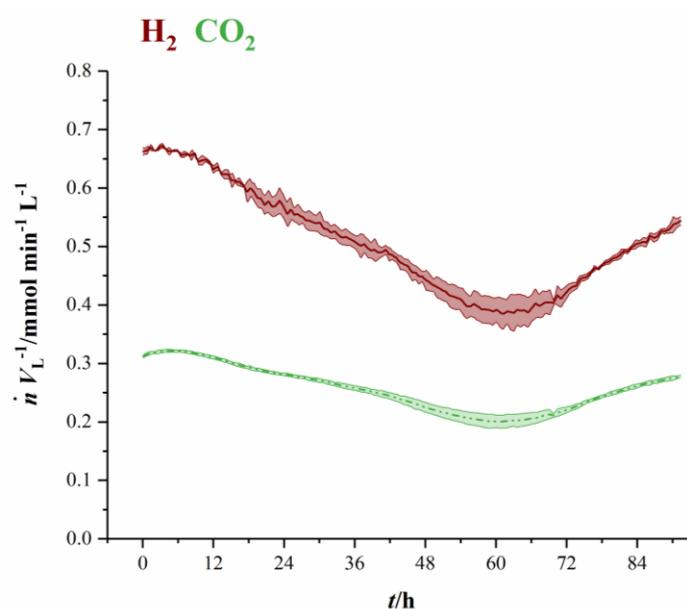
Figure 4.5 – Amount of substance flow rates per liter medium for hydrogen (red, solid) and carbon dioxide (green, dashed) in the off-gas of 1.5 L-scale. Results are average values of three experiments. Standard deviation is indicated by the light-colored area around the average lines. [Oswald *et al.* 2018a]

$0.63\,\mathrm{mmol\,min^{-1}\,L^{-1}}$ (H_2) continuously decrease until $60\,\mathrm{h}$ (CO_2) and $63\,\mathrm{h}$ (H_2), where they reach their local minimum of $0.18\,\mathrm{mmol\,min^{-1}\,L^{-1}}$ (CO_2) and $0.35\,\mathrm{mmol\,min^{-1}\,L^{-1}}$ (H_2), respectively. Here, *C. ljungdahlii* consumes $45\,\%$ of the ingoing hydrogen and $38\,\%$ of the ingoing carbon dioxide. From that point on, uptake rate of both gases decreases and reaches off-gas flow rates of $0.25\,\mathrm{mmol\,min^{-1}\,L^{-1}}$ for carbon dioxide and $0.49\,\mathrm{mmol\,min^{-1}\,L^{-1}}$ for hydrogen at the end of fermentation. Transferring the $1.5\,\mathrm{L}$-scale to $2.5\,\mathrm{L}$ for pressurized experiments while keeping $\dot{n}\,V_L^{-1}$ constant resulted in decreasing volumetric flow rates with increasing pressure. Development of $\dot{n}\,V_L^{-1}$ in off-gases from $2.5\,\mathrm{L}$-scale are shown in Figure 4.6. Off-gas data from high pressure fermentation at $1\,\mathrm{bar}$ of absolute pressure (HPF-1) shows a development comparable to the data of $1.5\,\mathrm{L}$-scale in Figure 4.5. The three experiments summarized in HPF-1 (Figure 4.6) show some degree of variation in the development of hydrogen and carbon dioxide in the off-gas and thus have a higher standard deviation than the data from $1.5\,\mathrm{L}$-scale. Off-gas data from both, high pressure fermentation with $4\,\mathrm{bar}$ of absolute pressure (HPF-4) and $7\,\mathrm{bar}$ of absolute pressure (HPF-7) show a similar development. Hydrogen and carbon dioxide have a sharp decrease and while in HPF-4 hydrogen jumps back to about $1.4\,\mathrm{mmol\,min^{-1}}$, the amount of substance flow rate of carbon dioxide asymptotically increases to the initial flow rate in both. In HPF-7 hydrogen asymptotically goes back to the initial value. Pressure build up takes $30\,\mathrm{min}$ for HPF-4 and $75\,\mathrm{min}$ for HPF-7. Complete consumption of substrates could not be achieved in any of the
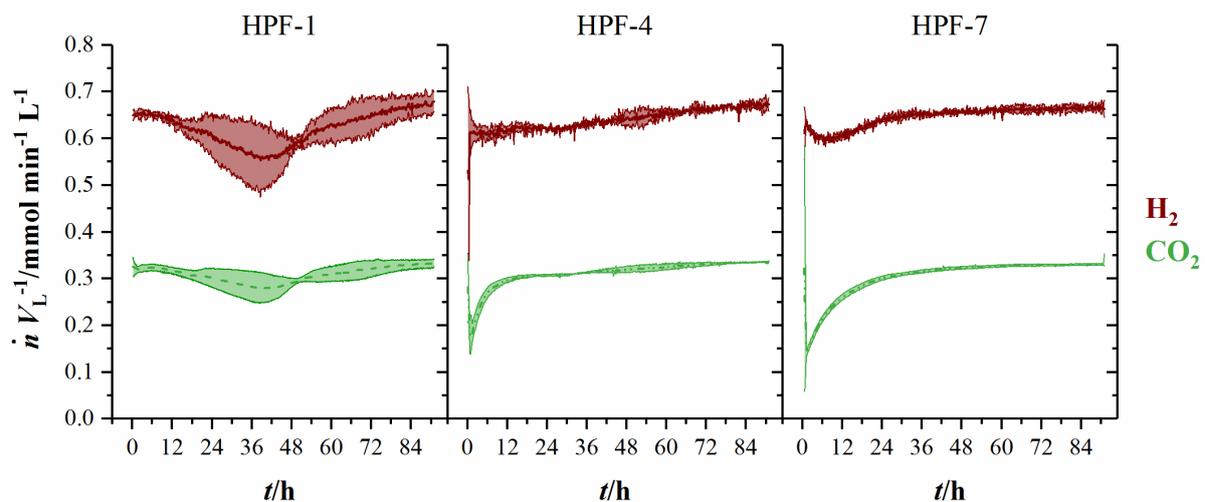
Figure 4.6 – Amount of substance flow rates per liter medium for hydrogen (red, solid) and carbon dioxide (green, dashed) in the off-gas of 2.5 L-scale experiments. Results are average values of three experiments for HPF-1 and HPF-7 and two experiments for HPF-4. Numbers behind HPF indicate the absolute pressure of the fermentation in 2.5 L-scale. Standard deviation is indicated by the light-colored area around the average lines. [Oswald *et al.* 2018]
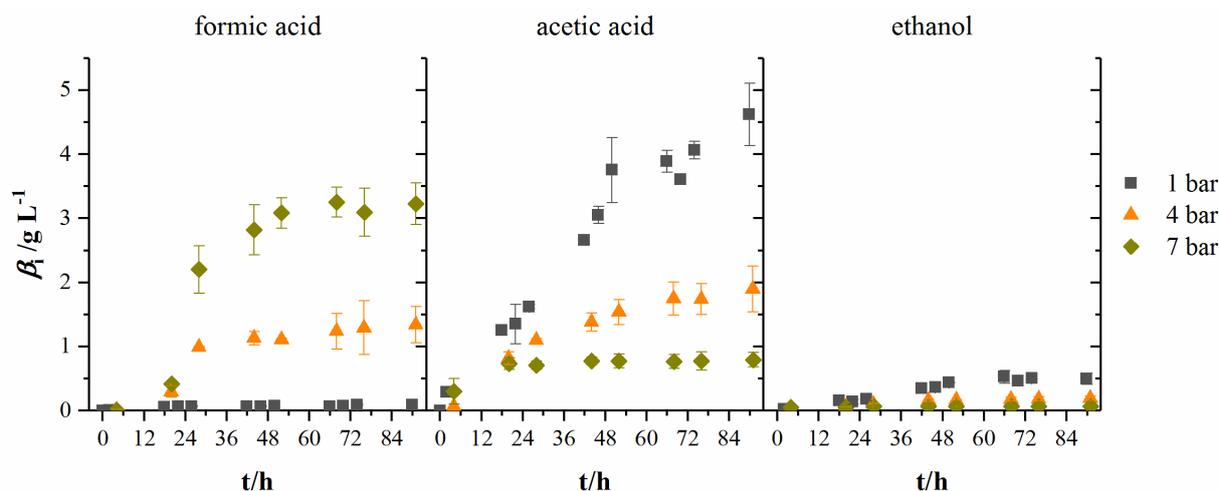
Figure 4.7 – Development of product concentrations for formic acid, acetic acid and ethanol at different headspace pressures. Results are average values of three experiments for HPF-1 (dark grey squares) and HPF-7 (dark yellow diamonds) and two experiments for HPF-4 (orange triangles). Numbers behind HPF indicate the absolute pressure of the fermentation in 2.5 L-scale. [Oswald *et al.* 2018]

conducted fermentations. [Oswald *et al.* 2018]

Figure 4.7 shows the development of product concentrations over the course of the fermentations in 2.5 L-scale while Table 4.3 shows resulting product concentrations and consumed amount of substrates per liter reactor volume of experiments in 1.5 L-scale together with the results form HPF-1, HPF-4 and HPF-7. In difference to the experiments from 4.4 and 4.1.2 the fructose content of the pre-culture is reduced from $10 \, g \, L^{-1}$ to $5 \, g \, L^{-1}$ to have as little fructose left as possible when inoculating the bioreactor. At atmospheric pressure, ethanol and acetic acid are the main products, their concentrations decrease with increasing pressure whereas formic acid concentration increases from final concentrations of $0.09 \, g \, L^{-1}$ to $1.34 \, g \, L^{-1}$ at 4 bar and $3.23 \, g \, L^{-1}$ at 7 bar absolute pressure. Acetic acid production starts in all experiments immediately after inoculation while formic acid formation has its strongest increase between 12 h and 28 h. [Oswald *et al.* 2018]

Table 4.3 gives the average values for product concentrations and consumed substrates at the end of the fermentation for all conducted cultivations in this project. The consumed amounts of substrates per liter reactor volume at atmospheric pressure in 2.5 L-scale are a third of the amounts in 1.5 L-scale. Whereas the overall consumption ratio E (consumed amount of substance divided by the total fed amount of substance in per cent) is about half the value from 1.5 L-scale. Comparing the biomass specific uptake rates for hydrogen (q_{H_2}) and carbon dioxide (q_{CO_2}) shows only differences in the uptake of hydrogen. Experiments in HPF-1 show

Table 4.3 – Average values for products and consumed substrates from cultivations of *C. ljungdahlii* with hydrogen and carbon dioxide as sole energy- and carbon source at different pressures after 90 h of cultivation.

Set-up	1.5 L	HPF-1	HPF-4	HPF-7
$\beta_{formic\ acid}$/g L^{-1}	0.03 ± 0.00	0.09 ± 0.09	1.34 ± 0.28	3.23 ± 0.32
$\beta_{acetic\ acid}$/g L^{-1}	9.30 ± 2.30	4.29 ± 0.67	1.90 ± 0.36	0.79 ± 0.11
β_{EtOH}/g L^{-1}	2.81 ± 0.13	0.42 ± 0.15	0.20 ± 0.03	0.07 ± 0.01
$c_{H2,R}$/mol L^{-1}	$1,00 \pm 0.06$	0.32 ± 0.08	N/A	N/A
$c_{CO2,R}$/mol L^{-1}	$0,40 \pm 0.02$	0.14 ± 0.03	NA	N/A
E_{H2}/%	25.63 ± 1.32	12.17 ± 3.07	N/A	N/A
E_{CO2}/%	21.52 ± 0.90	11.17 ± 2.79	N/A	N/A
$q_{H2,\ max}$/mmol min^{-1} g^{-1}	2.40 ± 0.10	4.56 ± 4.69	N/A	N/A
$q_{CO2,\ max}$/mmol min^{-1} g^{-1}	1.00 ± 0.05	1.05 ± 0.61	N/A	N/A

Numbers behind HPF indicate the absolute pressure of the fermentation in 2.5 L-scale. In 1.5 L-scale, the absolute pressure is 1 bar. Average values of three bioreactors per experimental set-up except for HPF-4. For this, values are averages of two bioreactors. $c_{H_2,R}$, consumed amount of hydrogen per liter reactor volume; $c_{CO_2,R}$, consumed amount of carbon dioxide per liter reactor volume; E_{H_2}, consumption ratio of hydrogen as consumed amount of hydrogen in per cent of total amount of ingoing hydrogen; E_{CO_2}, consumption ratio of carbon dioxide as consumed amount of carbon dioxide in per cent of total amount of ingoing carbon dioxide; $q_{H_2,\ max}$, maximum biomass specific uptake rate of hydrogen; $q_{CO_2,\ max}$, maximum biomass specific uptake rate of carbon dioxide; N/A, data not available.

about twice the maximum uptake rates for hydrogen than the ones found for 1.5 L-scale. However, the replicates in HPF-1 divert significantly from each other as can be seen in the off-gas data in Figure 4.6. This results in rather high standard deviations. Despite the differences in overall consumption, the product yields based on consumed substrates (H_2 and CO_2) are quite similar with 0.67 g g^{-1} in 1.5 L-scale and 0.64 g g^{-1} in HPF-1. For experiments at 4 bar and 7 bar, no consumption data is available. As can be seen from the off-gas data in Figure 4.6, under pressurized conditions no reasonable values for consumed substrates can be determined since the data resembles saturation curves for carbon dioxide at elevated pressures. Therefore, yields are only calculated based on totally fed substrates ($Y_{P/S}^{**}$). In 1.5 L-scale, an $Y_{P/S}^{**}$ of 0.15 g g^{-1} is achieved whereas in 2.5 L-scale for HPF-1, HPF-4 and HPF-7 $Y_{P/S}^{**}$ values of 0.05 g g^{-1}, 0.04 g g^{-1} and 0.04 g g^{-1} are achieved, respectively. No significant increase in OD is observed at elevated pressures (data not shown). [Oswald *et al.* 2018]

Because in 2.5 L-scale the pH-probe is installed after the reactor is sterilized, contamination with *Bacillus cereus* spores can be found in all HPF cultivations. Blank cultivations without *C. ljungdahlii* inoculum but with the 0.1 g L^{-1} of fructose carried over from the pre-culture, yield the same degree of contamination as the samples from experiments with *C. ljundahlii* cells. Neither growth nor products can be found in these blank cultivations. [Oswald *et al*. 2018]

4.3 Influence of cyanide on growth and product formation of *Clostridium ljungdahlii*

4.3.1 Experiments with fructose as substrate

Cyanide is a potent inhibitor of CODH, the central enzyme of the WLP. At heterotrophic conditions, the WLP is the only way for acetogens to recycle reduction equivalents while simultaneously fixating carbon into acetic acid. Heterotrophic growth in presence of cyanide can give an indication as to what the critical cyanide concentration might be. All experiments are conducted in sealed serum bottles. First experiments on the influence of cyanide use concentrations of 0 mM, 0.025 mM, 0.05 mM, 0.1 mM and 1.0 mM potassium cyanide in cultures with either fructose or synthesis gas as a substrate. The effects of cyanide on growth and product formation are shown in Figure 4.8. With increasing cyanide concentration, lag-phase increases, and maximum growth rate decreases from 0.1 h^{-1} without cyanide to 0.08 h^{-1} (0.025 mM cyanide), 0.05 h^{-1} (0.05 mM cyanide), 0.02 h^{-1} (0.1 mM cyanide) and 0.05 h^{-1} (1.0 mM cyanide). Substrate consumption and product formation show this tendency as well. While cultures without cyanide reach a maximum CDW of 0.73 ± 0.03 g L^{-1}, all cyanide containing cultures reach, within the margin of standard deviation, the same maximum CDW of approximately 0.49 g L^{-1}. The exception is the culture with 1.0 mM cyanide where the cells do not start to grow until 168 h and the maximum CDW is the same as at cyanide free conditions. After the 1.0 mM cyanide culture starts to grow, they consume the same amount of fructose as the other cultivations within the following 96 h. Another effect of increasing cyanide concentrations can be found with the formed products. *C. ljungdahlii* converts consumed fructose into acetic acid and ethanol. The yields for those two are 0.76 g g^{-1} (acetic acid) and 0.03 g g^{-1} (ethanol) when growing without cyanide. Those yields shift with increasing cyanide concentrations. For acetic acid values of 0.61 g g^{-1} (0.025 mM cyanide),
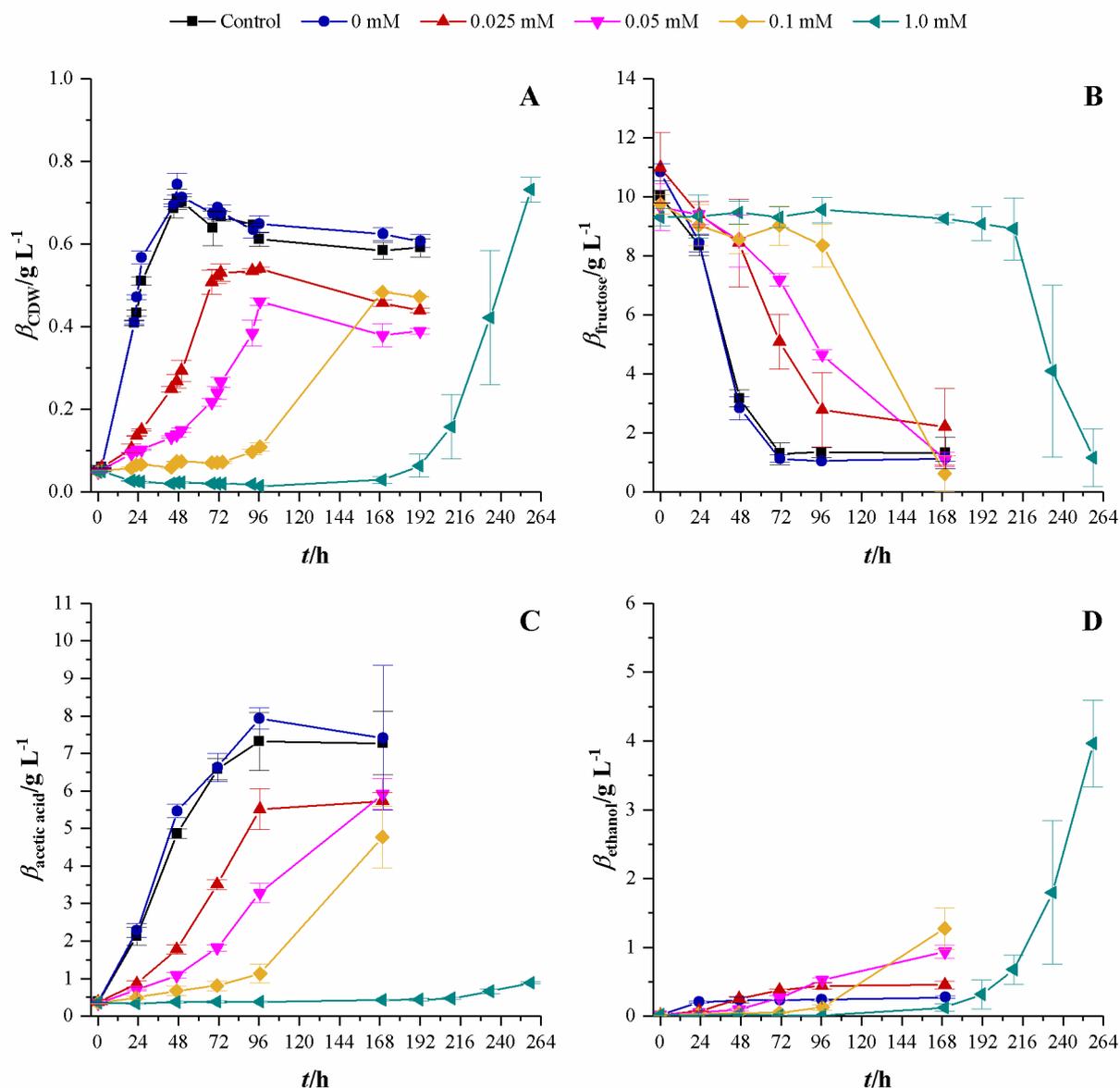
Figure 4.8 – Response of fructose growing *C. ljungdahlii* to increasing concentrations of cyanide. Control cultures (black squares) do not contain any phosphate buffer or cyanide while cultures with 0 mM cyanide (blue dots) contain 1 mL 100 mM potassium phosphate buffer at pH 11. Other cyanide concentrations are 0.025 mM (red triangles), 0.05 mM (magenta upturned triangles), 0.1 mM (yellow diamonds) and 1.0 mM (petrol tilted triangles). **A**, CDW; **B**, mass concentration of fructose; **C**, mass concentration of acetic acid; **D**, mass concentration of ethanol. Average values of three independent cultivations. [Oswald *et al.* 2018b]

$0.65 \, \text{g g}^{-1}$ (0.05 mM cyanide), $0.48 \, \text{g g}^{-1}$ (0.1 mM cyanide) and $0.06 \, \text{g g}^{-1}$ (1.0 mM cyanide) are obtained while the yields for ethanol are $0.05 \, \text{g g}^{-1}$ (0.025 mM cyanide), $0.11 \, \text{g g}^{-1}$ (0.05 mM cyanide), $0.14 \, \text{g g}^{-1}$ (0.1 mM cyanide) and $0.48 \, \text{g g}^{-1}$ (1.0 mM cyanide). [Oswald *et al.* 2018b]

Since *C. ljungdahlii*, once it starts growing at 1.0 mM cyanide, reaches CDW concentrations of the same value as without cyanide, the next step is to use the grown culture from 1.0 mM cyanide containing medium (aka adapted strain) to inoculate fresh, cyanide containing media. Experiments with 0 mM, 0.1 mM and 1.0 mM cyanide are conducted, using not-adapted *C. ljungdahlii* and the adapted strain. Figure 4.9 shows the results of that comparison. Without cyanide present the strains reach comparable maximum CDW of 0.72 ± 0.03 g L^{-1} (not-adapted strain) and 0.78 ± 0.11 g L^{-1} (adapted strain). However, with increasing cyanide
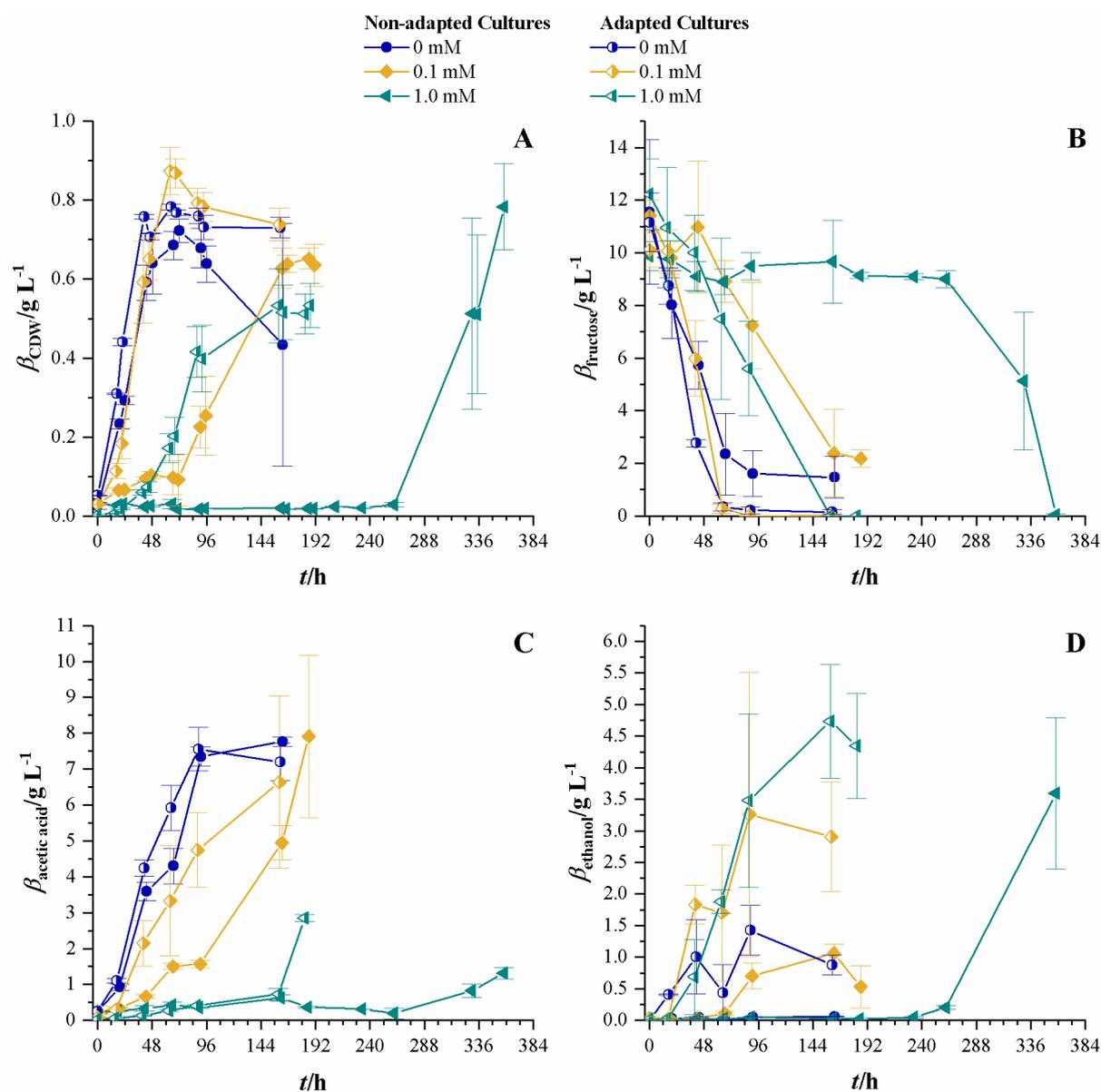
Figure 4.9 – Not-adapted *C. ljungdahlii* (full symbols) vs. the adapted strain (half filled symbols) at different cyanide concentrations with fructose as carbon source. Cyanide concentrations are 0 mM (blue dots), 0.1 mM (yellow diamonds) and 1.0 mM (petrol tilted triangles). **A**, CDW; **B**, mass concentration of fructose; **C**, mass concentration of acetic acid; **D**, mass concentration of ethanol. Average values of three independent cultivations. [Oswald *et al*. 2018b]

concentrations the adapted strain shows no significant delay in growth at 0.1 mM cyanide and a lag-phase of about 24 h at 1.0 mM cyanide. The not-adapted strain on the other side has a lag-phase of about 24 h at 0.1 mM cyanide and of about 260 h at 1.0 mM. Notably the adapted strain reaches a maximum CDW of 0.83 g L^{-1} at 0.1 mM cyanide, which is above the values found in cultures of both strains without cyanide. As for the maximum growth rates, the not-adapted strain reaches values of 0.11 h^{-1} (0 mM cyanide), 0.05 h^{-1} (0.1 mM cyanide) and 0.04 h^{-1} (1.0 mM cyanide) while the adapted strain reaches 0.10 h^{-1} (0 mM and 0.1 mM cyanide) and 0.06 h^{-1} (1.0 mM cyanide). [Oswald *et al*. 2018b]

Substrate consumption of the adapted strain is unaffected by 0.1 mM cyanide and only slightly affected by 1.0 mM cyanide. At 0.1 mM cyanide, the not-adapted strain shows a consumption comparable to the adapted strain at highest cyanide concentration and at 1.0 mM cyanide, fructose uptake is not observable before 260 h. When looking at product formation the adapted strain and not-adapted strain yield the same concentration of acetic acid at 0 mM cyanide and while the not adapted strain only produces 0.06 g L^{-1} ethanol at this cyanide concentration, the adapted strain produces a maximum of 1.43 g L^{-1}. For cyanide concentrations of 0.1 mM the adapted strain produces more ethanol than the not-adapted strain, too. Maximum acetic acid concentrations in not-adapted and adapted strain culture are comparable to the values found in cultures without cyanide. At highest cyanide concentrations not-adapted and adapted strain produce equal amounts of ethanol with the difference that the adapted strain reaches the maximum concentration after 159 h while the not-adapted strain takes 358 h. At 1.0 mM cyanide the not-adapted strain produces a maximum of 1.3 ± 0.16 g L^{-1} acetic acid while the adapted strain produces 2.85 ± 0.10 g L^{-1}. [Oswald *et al*. 2018b]

4.3.2 Cultivations with syngas as carbon and energy source

To investigate whether the cyanide present in crude syngas affects autotrophic metabolism of *C. ljungdahlii*, sealed serum bottle cultures are studied for the same concentrations of cyanide as for heterotrophic growth. Figure 4.10 shows the development of CDW and headspace pressure for cultures growing in presence of 0 mM, 0.025 mM, 0.05 mM, 0.1 mM and 1.0 mM potassium cyanide with a gas atmosphere of 21.1 ± 3.13 vol-% H_2, 23.1 ± 3.74 vol-% CO, 10.4 ± 1.70 vol-% CO_2 and 39.5 ± 6.85 vol-% N_2. Cultures are seeded from 5 % inoculated cultures grown for 7 d with syngas as carbon and energy source. The control culture without additional phosphate buffer added and the culture with 0 mM cyanide show the same growth behavior. For cyanide concentrations of 0.025 mM, 0.05 mM and 0.1 mM the lag-phase

increases with increasing cyanide concentration. However, despite that cultures at 0.05 mM and 0.1 mM cyanide reach the same maximum CDW of about $0.20\,\mathrm{g\,L^{-1}}$, the 0.025 mM culture reaches with $0.16\pm0.01\,\mathrm{g\,L^{-1}}$ a slightly lower value. Maximum growth rates are $0.08\,\mathrm{h^{-1}}$ (control), $0.08\,\mathrm{h^{-1}}$ (0 mM cyanide), $0.03\,\mathrm{h}$ (0.025 mM cyanide), $0.04\,\mathrm{h^{-1}}$ (0.05 mM cyanide), $0.04\,\mathrm{h^{-1}}$ (0.1 mM cyanide). No growth can be observed within 497 h in presence of 1.0 mM cyanide. Due to lack of samples between 96 h and 150 h it might be possible that the maximum growth rate in the 0.025 mM cyanide cultures is higher than 0.03 h. [Oswald *et al.* 2018b]

The development of headspace pressure, representing the available substrate, shows a similar trend as the CDW development. Final pressure in cyanide free cultures is 0.86 ± 0.01 bar. At this pressure the gas atmosphere consists only of carbon dioxide and nitrogen (data not shown). With their lag-phase reflecting time delay, cultures with 0.025 mM and 0.05 mM cyanide reach the same pressure as cyanide free cultures. At 432 h (18 d) the 0.1 mM cyanide containing culture reaches a pressure of 0.90 ± 0.04 bar but has only completely consumed carbon monoxide. Hydrogen partial pressure in that culture after 18 d is 34.42 ± 3.31 mbar. The pressure drop in 1.0 mM cultures is due to liquid and gaseous samples taken from the
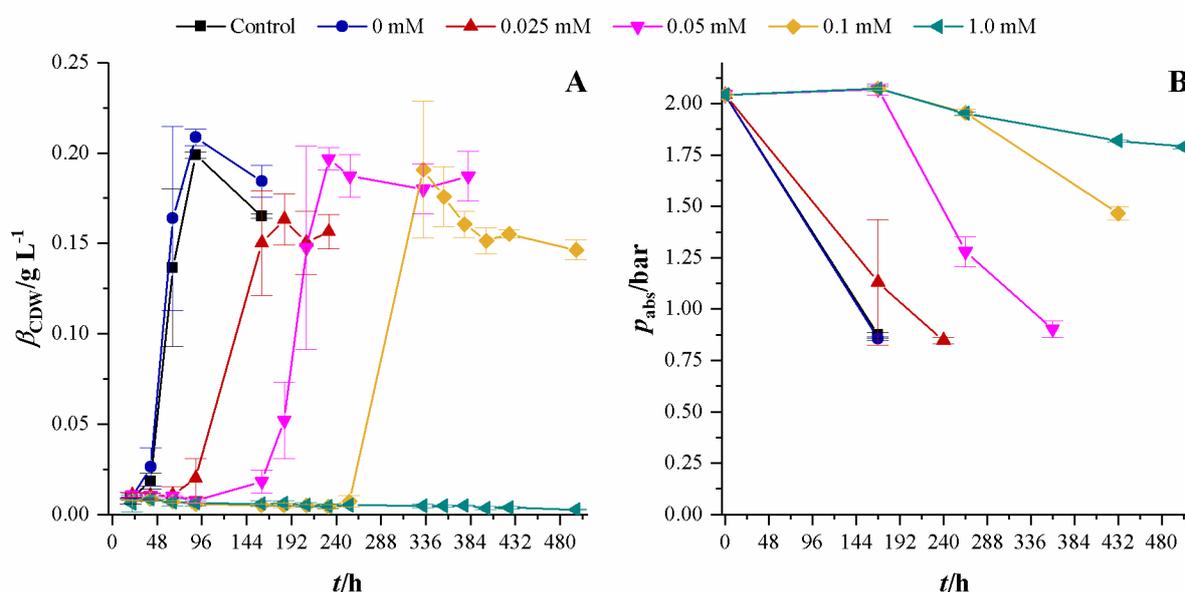
Figure 4.10 – Development of CDW and headspace pressure of cultivations of *C. ljungdahlii* in prescence of different cyanide concentrations. Control cultures (black suqares) do not contain any phosphate buffer or cyanide while cultures with 0 mM cyanide (blue dots) contain 1 mL 100 mM potassium phosphate buffer at pH 11. Other cyanide concentrations are 0.025 mM (red triangles), 0.05 mM (magenta upturned triangles), 0.1 mM (yellow diamonds) and 1.0 mM (petrol tilted triangles). **A**, CDW; **B**, headspace pressure. Average values of three independent cultivations. [Oswald *et al.* 2018b]
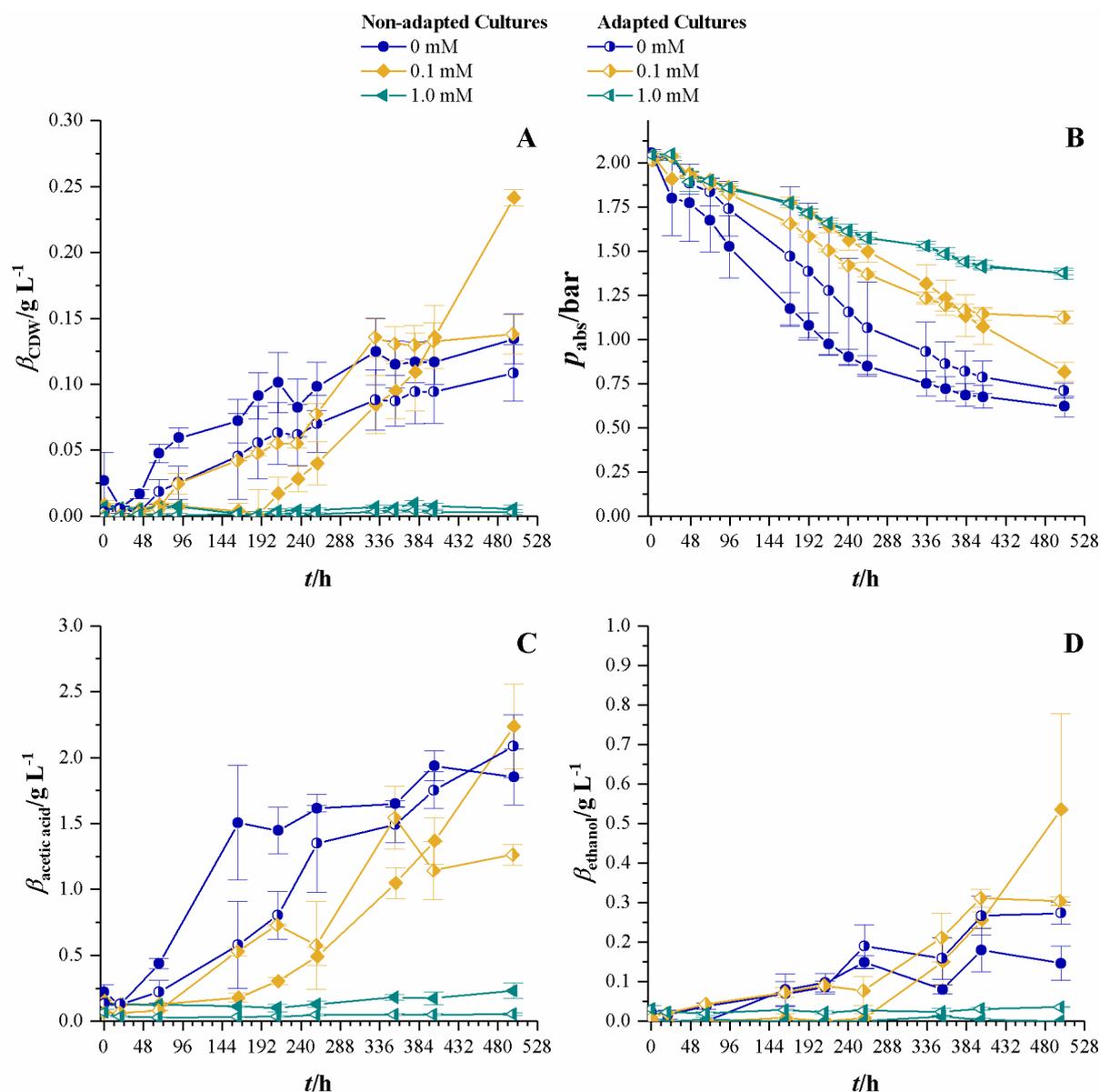
Figure 4.11 – Not-adapted *C. ljungdahlii* (full symbols) vs. the adapted strain (half filled symbols) at different cyanide concentrations with syngas as carbon and energy source. Cyanide concentrations are 0 mM (blue dots), 0.1 mM (yellow diamonds) and 1.0 mM (petrol tilted triangles). **A**, CDW; **B**, mass concentration of fructose; **C**, mass concentration of acetic acid; **D**, mass concentration of ethanol. Average values of three independent cultivations. [Oswald *et al.* 2018b]

bottles since no growth or product formation occurred (data not shown).

Similar to the approach with fructose growing cultures, bottles with 0 mM, 0.1 mM and 1.0 mM are seeded with not-adapted *C. ljungdahlii* and a strain adapted on fructose in 1.0 mM cyanide containing medium. Pre-cultures for this experiment are grown for 48 h with syngas as carbon and energy source. Syngas composition is 27.1 ± 0.6 vol-% H_2, 29.0 ± 0.5 vol-% CO, 13.5 ± 0.2 vol-% CO_2 and 28.3 ± 0.4 vol-% N_2. Figure 4.11 shows the results for CDW,

headspace pressure and concentrations of acetic acid and ethanol. Cultures of the not-adapted strain without cyanide show the shortest lag-phase and reach maximum CDW of $0.12 \pm 0.02\,\mathrm{g\,L^{-1}}$. Not-adapted cultures at $0.1\,\mathrm{mM}$ cyanide do not start to grow before $188\,\mathrm{h}$ and reach a maximum CDW of $0.24 \pm 0.01\,\mathrm{g\,L^{-1}}$. As for the adapted cultures, the ones with $0\,\mathrm{mM}$ and $0.1\,\mathrm{mM}$ cyanide show the same growth behavior in the first $259\,\mathrm{h}$. The cyanide free cultures of adapted *C. ljungdahlii* reach a maximum CDW of $0.11 \pm 0.02\,\mathrm{g\,L^{-1}}$ while the ones at $0.1\,\mathrm{mM}$ cyanide reach $0.13 \pm 0.01\,\mathrm{g\,L^{-1}}$. No increase in CDW is measured for $1.0\,\mathrm{mM}$ cyanide for both not-adapted and adapted strain. Maximum growth rates for not-adapted cultures are $0.04\,\mathrm{h^{-1}}$ ($0\,\mathrm{mM}$ cyanide) and $0.03\,\mathrm{h^{-1}}$ ($0.1\,\mathrm{mM}$) and for the adapted strain $0.03\,\mathrm{h^{-1}}$ ($0\,\mathrm{mM}$ cyanide) and $0.06\,\mathrm{h^{-1}}$ ($0.1\,\mathrm{mM}$ cyanide). Initial headspace pressure is $2.03 \pm 0.01\,\mathrm{bar}$. For each cyanide concentration, the not-adapted cultures reach the lowest final pressure except for $1.0\,\mathrm{mM}$ where no growth occurred. [Oswald *et al.* 2018b]

Final acetic acid concentrations are within the same margin of standard deviation for not-adapted and adapted strain at $0\,\mathrm{mM}$ cyanide and the not-adapted at $0.1\,\mathrm{mM}$ cyanide. On average they reach $2.06\,\mathrm{g\,L^{-1}}$. At $353\,\mathrm{h}$ maximum concentration of acetic acid in $0.1\,\mathrm{mM}$ cultures of the adapted strain are measured with $1.54 \pm 0.24\,\mathrm{g\,L^{-1}}$. Final ethanol concentrations are below $0.3\,\mathrm{g\,L^{-1}}$ for all cultures except the not-adapted cultures in $0.1\,\mathrm{mM}$ cyanide containing medium which have $0.53 \pm 0.24\,\mathrm{g\,L^{-1}}$ ethanol. [Oswald *et al.* 2018b]

4.4 Process link-up: From syngas to malic acid

4.4.1 Nitrogen reduction in culture media for *Clostridium ljungdahlii*

As Knuf *et al.* [2013] outlined, *A. oryzae* only produces malic acid under nitrogen limited conditions. Hence, if acetic acid from syngas fermentation is to be converted to malic acid by *A. oryzae* it is necessary to adjust the ammonia contend of the syngas fermentation medium so that no ammonia is left at the end of syngas fermentation. Table 4.4 summarizes the results of initial cultivations on syngas using culture medium from section 3.1.1 with a starting concentration of ammonia chloride of $2.5\,\mathrm{g\,L^{-1}}$ and medium were the ammonia contend is reduced to $0.33\,\mathrm{g\,L^{-1}}$. The concentration of ammonia chloride for the NH_4-reduced medium (NH_4-red) calculates from the consumed amount of ammonia during syngas fermentation using the original medium composition. This is reflected by $\Delta\beta_{NH_4Cl}$ of $0.3\,\mathrm{g\,L^{-1}}$ and $0.41\,\mathrm{g\,L^{-1}}$ for the original medium. Due to a huge potassium peak in the ion chromatograph

chromatogram of the ammonia reduced medium it is not possible to determine the exact amount of ammonia left after 96 h of syngas fermentation. [Oswald *et al.* 2016]

The first cultivation using the original medium composition from section 3.1.1 consists of a single fermentation experiment. The initial gas flow rate of 10.4 mL min^{-1} is increased to 18 mL min^{-1} after reaching 98 % consumption of CO and H$_2$. In difference to the first, the second cultivation with unaltered ammonia contend consists of two independent fermentation experiments in which the gas flow rate is kept at 10.4 mL min^{-1} over the course of the cultivation. The same conditions apply for the first set of three experiments with medium featuring a reduced ammonia contend whereas in the second triplicate of fermentations with

Table 4.4 – Results of preliminary experiments with *C. ljungdahlii* growing with syngas as sole carbon and energy source.

Medium	Original[1]	Original[2]	NH$_4$-red[3]	NH$_4$-red[3]
β_{NH4Cl}/g L^{-1}	2.5	2.5	0.33	0.33
β_{CDW}/g L^{-1}	0.62	0.83 ± 0.37	0.59 ± 0.02	0.59 ± 0.03
$\beta_{acetic\ acid}$/g L^{-1}	16.34	14.74 ± 2.00	15.38 ± 1.83	18.78 ± 0.98
β_{EtOH}/g L^{-1}	1.24	0.23 ± 0.08	0.47 ± 0.29	1.80 ± 0.22
$\Delta\beta_{NH4Cl}$/g L^{-1}	0.30	0.41 ± 0.05	N/A	N/A
$c_{H2,R}$/mol L^{-1}	0.59	0.46 ± 0.01	0.42 ± 0.01	0.47 ± 0.06
$c_{CO,R}$/mol L^{-1}	0.67	0.48 ± 0.00	0.46 ± 0.02	0.76 ± 0.04
$c_{CO2,R}$/mol L^{-1}	-0.02	0.02 ± 0.00	0.02 ± 0.00	-0.18 ± 0.04
$Y_{P/S}^{*}$/g g^{-1}	0.85	0.92 ± 0.15	1.00 ± 0.03	0,89 ± 0.01
$V_{gas,\ total}$/L	79.5	59.46 ± 1.13	59.84 ± 1.13	97.01 ± 1.37
$n_{H2,in}$/mol	1.21	0.85 ± 0.00	0.80 ± 0.03	1.37 ± 0.04
$n_{CO,in}$/mol	1.21	0.84 ± 0.01	0.82 ± 0.03	1.36 ± 0.02
$n_{CO2,in}$/mol	0.55	0.37 ± 0.00	0.37 ± 0.02	0.59 ± 0.01
$Y_{P/S}^{**}$/g g^{-1}	0.69	0.84 ± 0.11	0.90 ± 0.04	0.73 ± 0.02

$c_{H_2,R}$, consumed amount of hydrogen per liter reactor volume; $c_{CO,R}$, consumed amount of carbon monoxide per liter reactor volume; $c_{CO_2,R}$, consumed amount of carbon dioxide per liter reactor volume; $V_{gas,total}$, total volume of used syngas over the course of 96 h; $n_{H_2,in}$, total amount of fed hydrogen; $n_{CO,in}$, total amount of fed carbon monoxide; $n_{CO_2,in}$, total amount of fed carbon dioxide

* based on consumed substrates

** based on totally fed H$_2$ and CO

[1] single experiment

[2] two replicas

[3] three replicas

reduced ammonia contend the gas feed rate is varied in different stages of cultivation. Similar to the first cultivation with the original ammonia contend the first increase in gas flow rate from $10.4\,\mathrm{mL\,min^{-1}}$ to $12.6\,\mathrm{mL\,min^{-1}}$ happens after reaching $98\,\%$ consumption of carbon monoxide and hydrogen. $8.6\,\mathrm{h}$ later the gas flow rate is increased to $18\,\mathrm{mL\,min^{-1}}$ and again after additional $13\,\mathrm{h}$ to $28.2\,\mathrm{mL\,min^{-1}}$. At both points consumption of hydrogen and carbon monoxide is $98\,\%$. After the last increase in gas feed rate the hydrogen consumption continuously decreased and, in an attempt to stabilize the cultivation, the gas feed rate is reduced first to $23.3\,\mathrm{mL\,min^{-1}}$ and $12.6\,\mathrm{mL\,min^{-1}}$ at $11.2\,\mathrm{h}$ and $33.4\,\mathrm{h}$ after the last increase in gas feed rate respectively. Despite the reduction in gas feed rate the hydrogen consumption continues to decrease until the end of the cultivation.

Among final values for CDW and product concentrations Table 4.4 states consumed amounts of substance per liter reactor volume for hydrogen ($c_{H_2,R}$), carbon monoxide ($c_{CO,R}$) and carbon dioxide ($c_{CO_2,R}$) as well as the overall amount of substance of those three ($n_{H_2,in}$, $n_{CO,in}$, $n_{CO_2,in}$) in the total syngas volume used during fermentation. It also gives two values for substrate-based product yields ($Y_{P/S}$), the first one ($Y_{P/S}^{*}$) is based on consumed substrates only. In this case substrates include CO_2 if $c_{CO_2,R}$ is positive. $Y_{P/S}^{**}$ is based on the overall fed mass of hydrogen and carbon monoxide during cultivation.

Since preliminary aerobic experiments with *A. oryzae* were conducted by Stefan Dörsam, those results are only summarized briefly here and can be found in Oswald *et al*. [2016]. Using the established malic acid production medium and acetic acid as carbon source $Y_{P/S}$ values of $0.28\,\mathrm{g\,g^{-1}}$ and L-malic acid concentrations of $8.62 \pm 1.15\,\mathrm{g\,L^{-1}}$ are achieved. Cultivations of *A. oryzae* on acetic acid in presence of ethanol result in maximum yields of $0.55\,\mathrm{g\,g^{-1}}$ but ethanol is not used as a carbon source. When syngas fermentation broth is harvested from the reactor and used for *A. oryzae* cultivation yields of $0.27\,\mathrm{g\,g^{-1}}$ are achieved only if *C. ljungdahlii* cells are not removed. Otherwise no malic acid is produce. [Oswald *et al*. 2016]

4.4.2 Process link-up via sequential mixed culture

Based on the above shown preliminary results the main link-up experiment is using NH$_4$-red medium to ensure ammonia limited conditions after $96\,\mathrm{h}$. This is necessary to enable malic acid production. Starting gas feed rate is $12.6\,\mathrm{mL\,min^{-1}}$ and is increased to $18\,\mathrm{mL\,min^{-1}}$ at $41.5\,\mathrm{h}$ after inoculation. $71.5\,\mathrm{h}$ after inoculation the gas feed rate is reduced back to the initial

12.6 mL min^{-1} due to decreasing hydrogen consumption. Figure 4.12 shows average online and offline values (A), overall concentration of consumed substrates and consumption rates for hydrogen, carbon monoxide and carbon dioxide (B).

Between 0 h and 20 h, fructose concentration and amount of carbon monoxide in the off-gas decrease constantly until fructose is not detectable anymore. Biomass concentration continuously increases until 49 h and stays at 0.3 g L^{-1} for the rest of the fermentation. Acetate and Ethanol concentrations increase to maximum mean values at the end of the syngas fermentation of 15.9 g L^{-1} and 2.0 g L^{-1}, respectively. Similar to the decrease of carbon
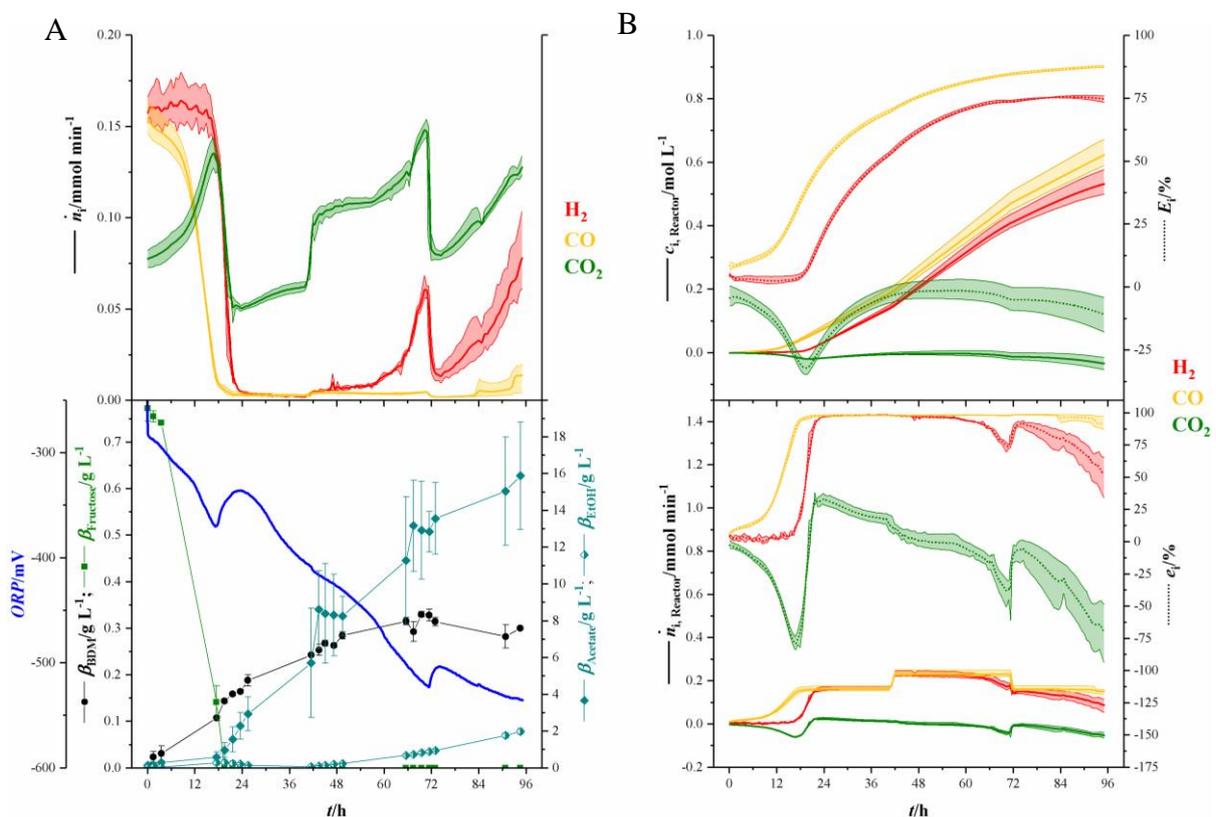
Figure 4.12 – Mean online and offline values for syngas fermentation part of sequential mixed culture as well as overall concentration and consumption rate of consumed substrates. A Upper part: Average amount of substance flow rates for hydrogen (red), carbon monoxide (yellow), and carbon dioxide (green) in the off-gas. The lightly colored areas around the average lines show minimum and maximum variance between bioreactors. Bottom part: Average values for ORP (blue line), β_{CDW} (black dots), $\beta_{fructose}$ (light green squares), $\beta_{acetate}$ (blue-green diamonds), and $\beta_{ethanol}$ (orange half-filled diamonds). **B** Overall concentration of consumed substrates and consumption rates. Values are given as absolute values $c_{i,\,Reactor}$ and $\dot{n}_{i,\,Reactor}$ (solid lines) and in percent of the fed syngas at each specific time E_i and in percent of the amount of substance fed rates e_i (dotted lines). Hydrogen (H_2, red), carbon monoxide (CO, yellow), and carbon dioxide (CO_2, green). The lightly colored areas around the average lines show minimum and maximum variance between three bioreactors. [Oswald *et al.* 2016]

monoxide in the off-gas, carbon dioxide increases up to a local maximum of $0.13\,\text{mmol min}^{-1}$ after 17 h of cultivation. With starting hydrogen consumption, carbon dioxide flow rate in the off-gas drops to an average of $0.05\,\text{mmol min}^{-1}$. Hydrogen off-gas flow rates stayed as low as $0.002\,\text{mmol min}^{-1}$ and slightly increased when the rate of ingoing syngas was increased. After about 47 h the hydrogen content in the off-gas started to increase. In contrast to hydrogen and carbon dioxide, carbon monoxide values in the off-gas stayed low until 83.0 h when they started to increase until the end of the fermentation. The decreasing gas flow rates at 71.0 h are due to reduction of the gas feed rate to $12.6\,\text{mL min}^{-1}$. [Oswald *et al.* 2016]

The amount of consumed carbon monoxide per liter medium increases continuously and reaches an average maximum of $0.62\,\text{mol L}^{-1}$. This equals to 87.4 % of the total CO that went into the bioreactor (dotted yellow line). The amount of consumed hydrogen per liter medium started to increase considerably after 19 h and went up to $0.53\,\text{mol L}^{-1}$ or 74.9 % of total hydrogen (dotted red line). Similar to the increase of carbon dioxide in the off-gas in Figure 4.12 A, the amount of consumed carbon dioxide decreased down to $-0.02\,\text{mol L}^{-1}$ or -32.4 % of the amount of carbon dioxide at 20 h. From that point, the amount of consumed carbon dioxide increased to $0\,\text{mol L}^{-1}$ and started to decrease down to $-0.03\,\text{mol L}^{-1}$ (-10.5 %) when hydrogen consumption faded. Uptake rate of carbon monoxide increased continuously during the first 20 h, where it reached its maximum average of $0.16\,\text{mmol min}^{-1}$ equaling 98.3 % of
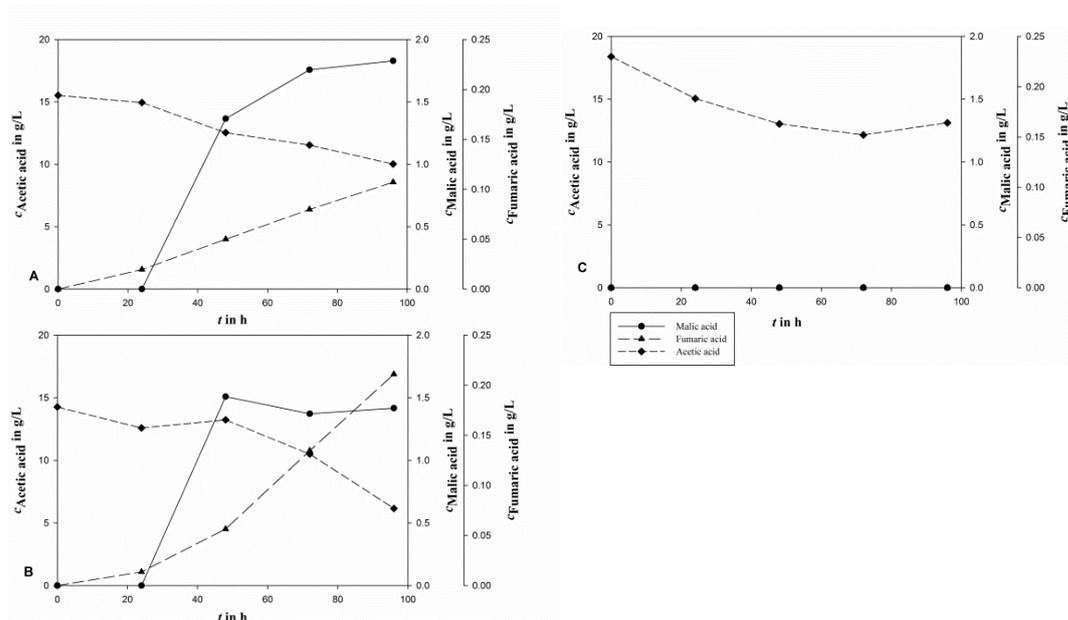
Figure 4.13 - Malic acid production ($c_{\text{Malic acid}}$), and acetic acid ($c_{\text{Aetic acid}}$) consumption in three bioreactors A, B, C from syngas fermentation after 96 h of fermentation. Fumaric acid is the main side product during *A. oryzae* fermentation. [Oswald *et al.* 2016]

the ingoing carbon monoxide stream at that time. Hydrogen uptake rate started to increase at 16 h and reached a maximum average of 0.16 mmol min^{-1} or 98.5 %. At 41.5 h the uptake rate of carbonmonoxide and hydrogen increased to 0.23 mmol min^{-1}, due to the elevated gas feed rate. After 48 h the hydrogen uptake rate started to decrease and went down to 0.10 mmol min^{-1} at the end of the fermentation. Following the syngas fermentation, the reactor is changed to fungal fermentation as stated in section 3.2.2 without removing of microbial biomass. [Oswald *et al.* 2016]

As with the preliminary results of experiments with *A. oryzae* and conversion of acetic acid to malic acid, the experiments of the fungal part of the process link-up are conducted by Stefan Dörsam. The results are taken from Oswald *et al.* [2016], the resulting publication of that project. Figure 4.13 shows the results of the three replicates approach of direct fungal fermentation of fermentation broth from syngas fermentation (see directly above).

Malic acid production can only be detected in two of the three bioreactor runs (A and B). In reactor C however, acetic acid is partly metabolized, but no product is formed. Acetic acid concentration of reactor A decreases from 15.53 g L^{-1} to 10.02 g L^{-1} and results in 1.83 g L^{-1} malic acid. This corresponds to a yield of 0.33 g g^{-1}. The initial acetic acid concentration of 14.26 g L^{-1} in reactor B decreases to 6.15 g L^{-1} during the fermentation and, with a yield of 0.18 g g^{-1}, gains 1.42 g L^{-1} malic acid. A total of 5.39 g L^{-1} of the initial 18.39 g L^{-1} acetic acid is consumed in reactor C but no malic acid formation occurred. [Oswald *et al.* 2016]

5.   Discussion

5.1   Characterization of stirred tank reactor system

5.1.1   Determination of $k_l a$-values

Two phases of operation with two different stirrer set-ups (RMR and RRB) are investigated. In the first phase the gas composition in the off-gas and the headspace of the bioreactor is close to the composition of the inlet gas stream. In the second phase, the off-gas and gas in the headspace consists only of non-usable gases like nitrogen and carbon dioxide. Values for the volumetric mass transfer coefficient in the first phase increase with increasing gas feed rate for each of the two stirrer set-ups. If gas from the headspace is entrained back into the liquid in a well-mixed STR both, sparged gas and entrained gas together determine the $k_l a$-value [Van't Riet 1979]. The results with headspace aeration alone show that. For the RMR stirrer set-up the influence of the headspace gas is 87 % (10.3 mL min^{-1}), 78 % (17.8 mL min^{-1}) and 48 % (44.4 mL min^{-1}). While for the RRB set-up the influence is 47 % (10.3 mL min^{-1}), 29 % (17.8 mL min^{-1}) and 14 % (44.4 mL min^{-1}). Looking at the values for each gas feed rate reveals highest $k_l a$-values at 800 min^{-1} except for the RMR set-up at 50 mL min^{-1} where the maximum can be found at 600 min^{-1}. However, at 1000 min^{-1} the RRB and RMR set-up only show an increase in $k_l a$-values at a gas feed rate of 50 mL min^{-1} while there is no difference at 18 mL min^{-1} and 25 mL min^{-1}.

The higher volumetric power input at 1000 min^{-1} results in smaller gas bubbles which have a higher residence time. If air or any other mixture of oxygen and an inert gas is used, they also reach diffusion equilibrium faster due to their increased ratio of surface to volume [Linek *et al.* 1987]. At diffusion equilibrium no net mass transfer across the gas-liquid boundary surface is possible and gas bubbles in this state are considered dead volume. Hence, small gas bubbles in the state of diffusion equilibrium combined with increased gas residence times reduce the observed $k_l a$-value. [Linek *et al.* 1987] Working with a gas atmosphere consisting only of oxygen (or the desired substrate gases) would omit this problem [Linek e*t al.* 1989] but typical sources for gases for syngas fermentation usually contain still other gases as well [Abubackar *et al.* 2011, Liew *et al.* 2013, Neumann *et al.* 2016] so that this is a problem that cannot be easily avoided at process conditions.

For the other phase, where the headspace consists mainly of inert gases (e. g. nitrogen), the $k_l a$-values decrease with increasing stirrer speed for both stirrer set-ups at all investigated gas feed rates. Except for the RRB set-up at a gas feed rate of $50\,\mathrm{mL\,min^{-1}}$. Here, the highest volumetric mass transfer coefficient is obtained at $800\,\mathrm{min^{-1}}$. Since the headspace in this scenario is not replaced with air at the beginning of each measurement, one explanation is that with increasing stirrer speed more gas from the headspace is brought back into the liquid phase. For the RMR set-up this is the prime intention, but this also means for this situation, that the mean oxygen content of the dispersed gas bubbles is lower than $21\,\%$ due to the nitrogen atmosphere in the headspace. In consequence, the mean concentration difference in RMR set-up is lower than in the RRB set up. [Gaddis 1999] As described above also in the second phase part of the gas bubbles can be considered dead volume which do not contribute to mass transfer [Linek *at al.* 1987]. Of course, this only holds true as long as the gas composition above the surface is different from the composition of the feed gas. Values for $k_l a$ at each stirrer speed are always lower for the RMR set-up than the corresponding values with the RRB set-up while the values in phase one are quite similar for $18\,\mathrm{ml\,min^{-1}}$ and $25\,\mathrm{mL\,min^{-1}}$. Due to the above-mentioned problems with the mean concentration difference for the RMR set-up the measured values are not reflecting the $k_l a$-values at process conditions properly. Using the dynamic pressure method for determination of $k_l a$-values as described by Linek *et al.* [1989] would avoid such problems but is not applicable in the used glass vessel.

For proper comparison with $k_l a$-values from other syngas converting processes available in literature, it is necessary to find a suitable correlation that takes all influencing parameters into account. Schlüter *et al.* [1992] describe the influencing parameters on the mass transfer coefficient as power input by the stirrer per volume of liquid (P/V_l, $\mathrm{W\,m^{-3}}$) and the gas feed rate per volume of liquid ($\dot{V}_g/V_l$, vvm). However, Van't Riet [1979] Henzler [1982] and Zlokarnik [1999] write that the superficial gas velocity (v, $\mathrm{m\,s^{-1}}$) is more suitable for comparison of different scales. The correlation

$$k_l a \left(\frac{v}{g^2}\right)^{\frac{1}{3}} = A \left(\frac{P}{V_l\,\rho\,(g^4\,v)^{\frac{1}{3}}}\right)^a \left(\frac{v}{(g\,v)^{\frac{1}{3}}}\right)^b \tag{5.1}$$

was introduced by Henzler [1982] and connects the $k_l a$ with volume-based power input by the stirrer, superficial gas velocity (v, $\mathrm{m\,s^{-1}}$) earth gravitational force (g, $\mathrm{m\,s^{-2}}$) and the liquid

parameters density (ρ, kg m^{-3}) and dynamic viscosity (v, m^2 s^{-1}). With A, a and b being constants. Furthermore, Henzler [1982] simplifies this correlation to

$$\frac{k_l a}{v} \left(\frac{v^2}{g}\right)^{\frac{1}{3}} = A \left(\frac{P}{V} \frac{1}{v \rho g}\right)^a \tag{5.2}$$

because $b \approx 1 - a$ for all investigated systems. Unfortunately, literature data on mass transfer coefficients for syngas fermentation processes does not generally state values for P/V_l. But under turbulent conditions ($\mathrm{Re} > 10^4$) and $\mathrm{Fr} \geq 0.65$ as well as $D/d \geq 2.2$, the equation

$$\mathrm{Ne} = 1.5 + \left(0.5 \left(\mathrm{Q} \left(1 + 38 \left(\frac{D}{d}\right)^{-5}\right)\right)^{0.075} + 1600 \left(\mathrm{Q} \left(1 + 38 \left(\frac{D}{d}\right)^{-5}\right)\right)^{2.6}\right)^{-1} \tag{5.3}$$

by Zlokarnik [1973] is used to calculate P/V_l for reactor systems with one Rushton turbine. Where D is the inner diameter of the reactor, d is the stirrer diameter and the gas-throughput number $\mathrm{Q} = \dot{V}_g \, n^{-1} \, d^{-3}$. For stirrer set-ups with more than one Rusthon turbine on the same stirrer shaft the equation

$$\mathrm{Ne} = z \, \frac{\mathrm{Ne}_0 + 187 \, \mathrm{Q} \, \mathrm{Fr}^{-0.32} \left(\frac{d}{D}\right)^{1.53} - 4.6 \, \mathrm{Q}^{1.25}}{1 + 136 \, \mathrm{Q} \left(\frac{d}{D}\right)^{1.14}} \tag{5.4}$$

from Judat [1976] was modified by Henzler [1982] for different amounts of stirrer (z) with Ne_0 being the Newton number of the stirrer without aeration. Using equations (5.3) and (5.4) as well as the relation in (5.2), literature data from Kapic *et al.* [2006] and Orgill *et al.* [2013] for stirred tank reactors is plotted together with own measurements at 800 min^{-1} and the RRB set-up without additional headspace aeration in Figure 5.1.

The data presented in Figure 5.1 shows that for $\dot{V}_g/V_l < 0.029$ vvm at 800 min^{-1} changes in gas feed rate are proportional to the resulting changes in $k_l a$ since $k_l a \, v^1$ results in the same value for all three investigated gas feed rates. Note that $(v^2 \, g^{-1})^{1/3}$ is constant for all datapoints. For $\dot{V}_g/V_l > 0.029$ vvm values for $k_l a \, v^1$ decrease, indicating an only small effect of the gas feed rate on $k_l a$. This as has also been stated by Schlüter *et al.* [1992] and is commonly found for all STR systems [Zlokarnik 1999]. Increasing $\dot{V}_g$ also reduces the power necessary for stirring
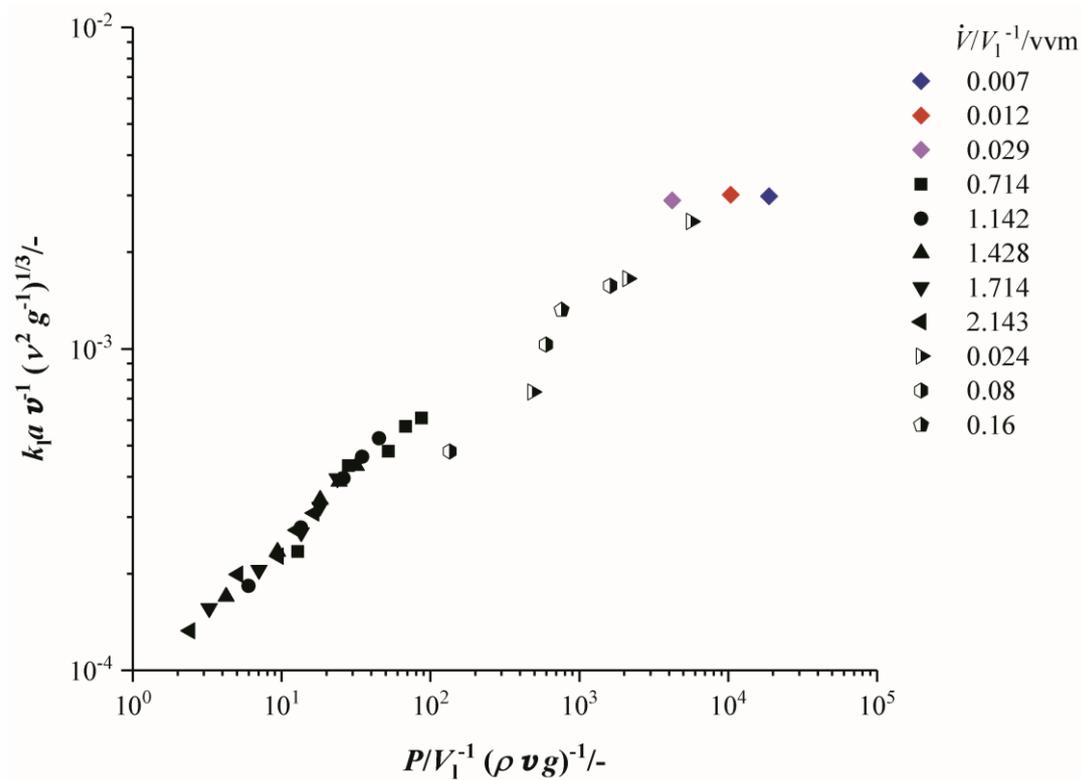
Figure 5.1 – Sorption characteristic for CO in STRs with one and two Rushton turbines.
Black, filled symbols are calculated from data in Kapic *et al.* [2006] and half-filled symbols from data in Orgill *et al.* [2013] with two stirrers. Colored diamonds are calculated data from own measurements at 800 min^{-1} and the RRB stirrer set-up. k_la-values are all calculated to 20 °C using equation (3.13).

[Zlokarnik 1973; Henzler 1982]. Over all, the k_la-values found in this work are in agreement with literature data for STRs.

Vega *et al.* [1989a] investigated the conversion of carbon monoxide to acetic acid in continuous running STR cultivations with hydrogen and carbon monoxide containing syngas. They find that the most economical optimum of such processes can be achieved only at mass transfer limited conditions, when every substrate that goes into solution is immediately taken up by the cells. Here, risks of inhibition from substrates, like inhibition of hydrogenase activity by CO [Gray and Gest 1965; Kim *et al.* 1984; Devarapalli *et al.* 2016], is eliminated [Vega *et al.* 1989a] and complete usage of fed substrates can be achieved. Because partial recirculation of gas atmosphere from the headspace is intended with the RMR set-up, the stirrer speed of 800 min^{-1} is chosen for all cultivations.

5.1.2 Evaluation of substrate consumption

Increasing the mass-transfer coefficient in syngas cultivation processes is only reasonable within certain boundaries. It has been shown that the economic ideal mode of operation is under mass-transfer limited conditions [Vega *et al.* 1989a] so that the liquid concentration of limiting gaseous substrates is always zero. As long as this criterion is met, the productivity will increase with increasing $k_l a$. However, Bredwell *et al.* [1999] pointed out that increasing $k_l a$ by means of increasing $\dot{V}_g$ can lead to decreasing overall conversion efficiency of syngas into products. The reason for this is that the bubble residence time becomes too short to allow for complete diffusion of CO and H_2 of a gas bubble from the gaseous into the liquid phase [Bredwell *et al.* 1999]. In the experiments conducted in this thesis, $k_l a$ is increased by means of increased gas feed rate. The results show that at a volume-based gas-feed rate of as low as 0.029 vvm (44.4 mL min^{-1} experiments) complete substrate consumption cannot be achieved in both of the investigated stirrer set-ups under batch cultivation conditions. Even though, the mass transfer coefficient is at 0.029 vvm six-fold (RMR) and four-fold (RRB) increased compared to the value at 0.007 vvm. Figure 5.2 shows the consumption rates for all six investigated set-ups in per cent of the amount of substance feed rate. The data of those experiments shows that hydrogenase activity is inhibited during the first 18 h of cultivation at 0.007 vvm and 0.012 vvm due to high CO contend [Gray and Gest 1965; Kim *et al.* 1984; Devarapalli *et al.* 2016]. Hydrogen continues to be co-consumed with CO for the rest of the cultivation at 0.007 vvm with the RRB stirrer set-up and up until 78 h with the RMR set-up. At 0.012 vvm duration of co-consumption of H_2 and CO is also longer with the RRB set-up but starts to decrease in the last third of the cultivation, too. At 0.029 vvm H_2 consumption could only be observed for the RMR stirrer set up. It is likely that the liquid CO concentration is no low enough in 0.029 vvm experiments to allow hydrogenase activity [Vega *et al.* 1989a]. The phenomenon of decreasing hydrogen consumption with liquid batch cultures of *C. ljungdahlii* can also be found in Cotter *et al.* [2009] and Maddipati *et al.* [2011] but both publications do not state an explanation on that topic. However, Liu *et al.* [2014] compared corn steep liquor (CSL) and yeast extract as sources of nitrogen and vitamins in CSTR cultivations with *Alkalibaculum bacchi* strain CP15 and fond that with CSL the consumption of hydrogen is 1/3 lower than with yeast extract. Comparing this findings from continuous running culture with the data in Figure 5.2 indicates that a component of yeast extract negatively influences hydrogenase activity when it becomes limiting.
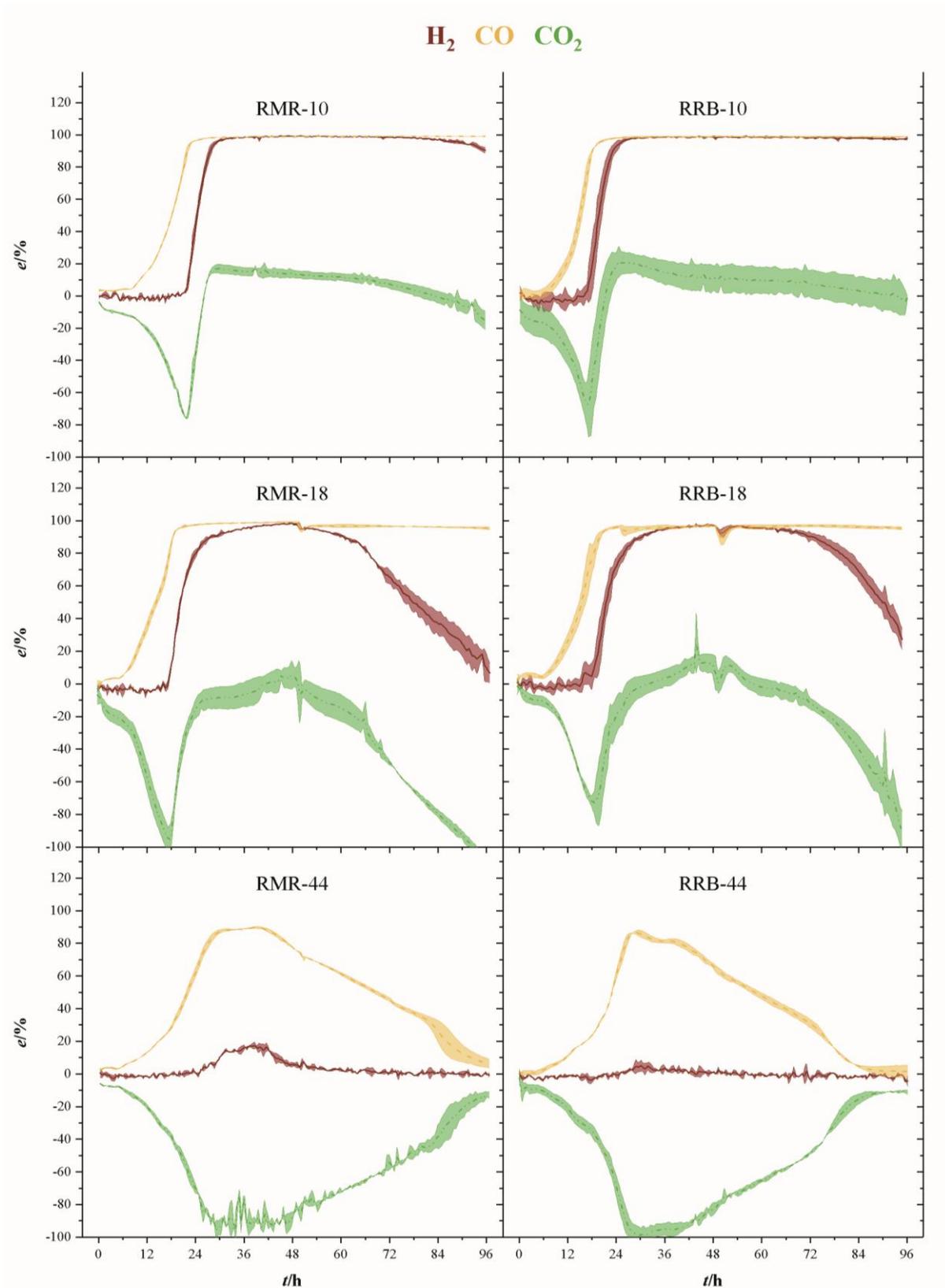
Figure 5.2 – Consumption rates for syngas fermentation with *C. ljungdahlii* in per cent of the amount of substance feed rate. Results of experiments with RMR (left) and RRB stirrer set-up (right) at average volume based gas flow rates of 0.007 vvm, 0.012 vvm and 0.029 vvm (top to bottom). Hydrogen (red line), carbon monoxide (yellow line) and carbon dioxide (green line). The areas around the lines indicate the standard deviation. Graphs show average values of two bioreactors per experimental set-up.

The incorporation of an axial flow impeller between two radial flow impellers and the abandonment of baffles in the RMR set-up resulted in vortex formation and dissipation of gas from the vortex zone by the upper Rushton impeller. The lower Rushton impeller dissipated the gas from the sparger. Zlokarnik [1999] describes that an intensively stirred vessel without baffles becomes a centrifuge, causing most of the dissipated gas to exit the liquid near the stirrer. Gas within the vortex zone experiences high recirculation rates but vortex aeration alone is no alternative to gas sparging by a hollow shaft stirrer or submerged sparger. [Zlokarnik 1999] The recirculation in the vortex zone could explain the observed hydrogen consumption at 0.029 vvm in the RMR set-up while the RRB set-up shows less entrainment of headspace gas.

Between RMR and RRB stirrer set-up the difference in substrate consumption is the duration and amount of hydrogen consumption. Table 5.1 summarizes the ratio of consumed substrates, product yields based on consumed ($Y_{P/S}{}^{*}$) and fed ($Y_{P/S}{}^{**}$) substrates and the molar ratio of acetic acid to ethanol at the end of each fermentation. For 0.007 and 0.012 vvm the total consumption of carbon monoxide is in the range of 81 % to 84 % for both stirrer set-ups while hydrogen consumption decreases. At 0.029 vvm the RMR set-up consumes 3.26 % and

Table 5.1 – Per cent consumption of substrates, yield based on consumed and fed substrates and molar acetic acid to ethanol ratio of substrate consumptions experiments.

Set-up	E_{H2} %	E_{CO} %	E_{CO2} %	$Y_{P/S}{}^{*}$ g g^{-1}	$Y_{P/S}{}^{**}$ g g^{-1}	HAc:EtOH -
RMR-10	72.49	81.38	-1.73	1.05	0.85	24.79
RRB-10	77.32	83.92	0.96	0.99	0.85	22.24
RMR-18	57.43	83.60	-36.5	0.95	0.78	7.27
RRB-18	65.63	81.50	-16.45	0.97	0.78	5.88
RMR-44	3.26	47.46	-55.20	0.41	0.19	3.24
RRB-44	0.00	37.87	-50.83	0.41	0.15	3.62

The numbers behind RMR and RRB in the "set-up" column stand for the gas feed rate wit $10 = 10 \, \text{mL} \, \text{min}^{-1}$ (0.007 vvm), $18 = 18 \, \text{mL} \, \text{min}^{-1}$ (0.012 vvm), $44 = 44 \, \text{mL} \, \text{min}^{-1}$ (0.029 vvm). E_{H_2}, consumption ratio of hydrogen as consumed amount of hydrogen in per cent of total amount of ingoing hydrogen; E_{CO}, consumption ratio of carbon monoxide as consumed amount of carbon monoxide in per cent of total amount of ingoing carbon monoxide; E_{CO_2}, consumption ratio of carbon dioxide as consumed amount of carbon dioxide in per cent of total amount of ingoing carbon dioxide; $Y_{P/S}{}^{*}$, product yield based on consumed substrates; $Y_{P/S}{}^{**}$, yield based on total fed substrates; HAc:EtOH, molar ratio of acetic acid to ethanol.

47.46 % of the total fed hydrogen and carbon monoxide respectively. The RRB set-up consumes only 37.87 % carbon monoxide. The better performance of the RMR set-up at 0.029 vvm is in my opinion due to the high recirculation of gas in the vortex zone as described above. The $Y_{P/S}^{*}$ values of the substrate consumption experiments show only small differences between both stirrer set-ups. The low value of 0.41 g g^{-1} at 0.029 vvm is in agreement with the maximum theoretical values for acetic acid and ethanol from CO which is 0.45 g g^{-1} at a molar acetic acid to ethanol ratio of 3. Of more significance in evaluating the overall process efficiency is the $Y_{P/S}^{**}$. Abubackar *et al.* [2016] used *C. autoethanogenum*, a close relative of *C. ljungdahlii*, in liquid batch culture fed with 0.008 vvm of pure CO with conditions favoring solventogenesis. Their data allows the calculation of $Y_{P/S}^{**}$ at the end of their process to 0.02 g g^{-1} which is 5 % of the theoretical maximum for ethanol from carbon monoxide and 6.26 % of the fed CO is consumed [Abubackar *et al.* 2016]. With a comparable gas feed rate we reach higher overall substrate consumption and $Y_{P/S}^{**}$ with a gas mixture consisting of equimolar amounts of hydrogen and carbon monoxide.

5.2   Elevated pressure for increased mass-transfer

Experiments in 1.5 L-scale are conducted at a $k_l a$ value of 10.2 10^{-3} s^{-1} (see section 4.1.1 RRB stirrer set-up) and since P/V_1 and $\dot{V}_g/V_1$ are kept constant, the mass transfer coefficient should have the same value in 2.5 L-scale [Schlüter et al., 1992]. Nevertheless, both scales do not show complete geometric similarity as outlined in the Methods section. Those discrepancies from geometric similarity may explain the observed deviations in product concentration and substrate consumption between 1.5 L-scale and 2.5 L-scale at 1 bar absolute pressure. Supporting this are the $Y_{P/S}$ values based on consumed substrates. For both scales, this yield is quite similar with the one from HPF-1 being only 4 % lower than the one found in 1.5 L-scale. That means that in both cases metabolic activity is similar since the same ratio of consumed substrates end up in products. Of far more interest in assessing the whole experimental set-up for 2.5 L-scale is the yield based on totally fed substrates during the fermentation. This value shows the overall conversion efficiency of the set-up and one aim of improving every process should be to bring this value as close to the yield based on consumed substrates as possible. For the case at hand, 15 % of gaseous substrates fed in 1.5 L-scale end up in products while in 2.5 L-scale only 5 % and at elevated pressures 4 % can be found in products. I interpret the high conformity of the values for 2.5 L-scale as indication that the found differences in substrate consumption and product concentration between scales at atmospheric conditions

are due to incomplete geometric similarity and independent of absolute process pressure. [Oswald *et al.* 2018a]

When looking at the product spectrum of the conducted experiments in Figure 3.7, the main thing that jumps the eye is that with increasing pressure the spectrum is shifted towards formic acid formation. At a total pressure of 7 bar almost no ethanol and only 0.8 g L^{-1} acetic acid is produced over the course of fermentation (see Figure 3.7) while a total of 3.2 g L^{-1} of formic acid is produced. Figure 5.3 shows the amount of substance ratios ($x_i = c_i/\Sigma c_i$) of the products at the end of the cultivations at elevated pressure. It seems that at a p_{H_2} of 2.13 bar (4 bar total pressure) formic acid and acetic acid are produced in equimolar amounts while at a p_{H_2} of 3.73 bar (7 bar total pressure) values of x for formic acid and acetic acid seem to be inverted compared to experiments at atmospheric conditions. The data also suggests that in the range of p_{H_2} from 0.5 to 3.37 bar (corresponding p_{CO_2} from 0.25 to 1.9 bar) there might be a linear relationship between x_i and the substrate partial pressure. Increased formic acid production at elevated pressures with H_2/CO_2 is described by Bleichert and Winter [1994] for pure cultures of *Methanobacterium formicum* and *M. palustre* as well as for mixed cultures
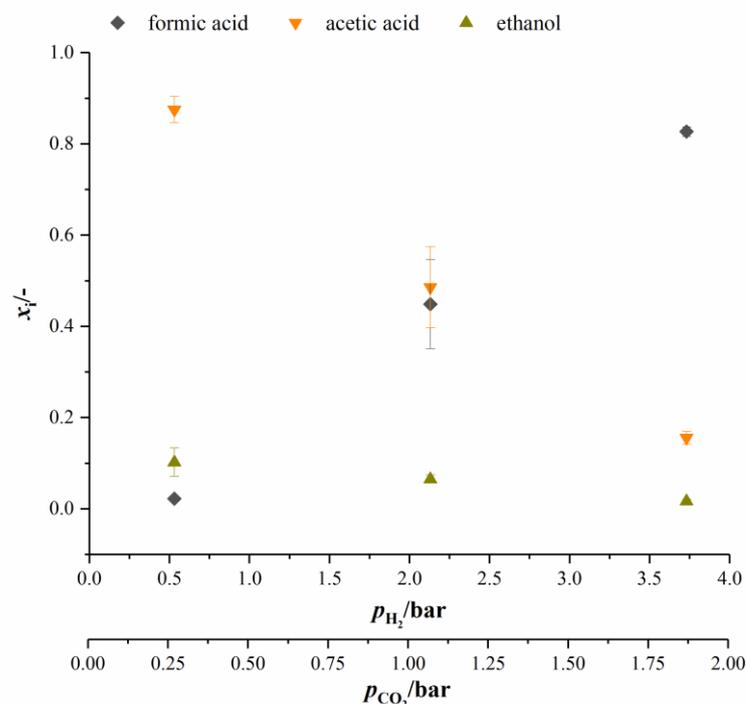
Figure 5.3 – Amount of substance ratio for products at the end of cultivations at elevated pressure. dark grey diamonds, formic acid; orange upturned triangles, acetic acid; dark yellow triangles, ethanol. [Oswald *et al.* 2018a]

from sewage sludge at hydrogen partial pressures of more than 2 bar. Kantzow and Weuster-Botz [2016] and before them Peters et al. [1999] show that formic acid formation is linked to the hydrogen partial pressure in *A. woodii*. By shifting the hydrogen partial pressure from 1.4 bar to 2.1 bar, they increased final formic acid concentration after 74.4 h of cultivation from 4.2 g L^{-1} to 7.3 g L^{-1} and increased the yield of formic acid per gram substrates fed of about 67 % [Kantzow and Weuster-Botz, 2016]. Peters et al. [1999] report an increase in formic acid production for bottle experiments of 0.5 mM per 0.1 bar increase in initial p_{H_2}. In *A. woodii*, the hydrogen dependent carbon dioxide reductase (HDCR) catalyzes the hydrogenation of CO_2 with molecular hydrogen [Schuchmann and Müller, 2013] while in *C. autoethanogenum*, a close relative to *C. ljungdahlii*, the direct hydrogenation of CO_2 with H_2 is one of three possible reactions of the hydrogenase-formate dehydrogenase complex funneling CO_2 into the methyl branch of the Wood-Ljungdahl pathway [Wang et al., 2013]. It might be that the ATP consuming reaction of formic acid and THF to formyl-THF is a possible bottleneck in the methyl branch and results in accumulation of formic acid at increased substrate partial pressures. At these conditions, ATP formation is not high enough to provide enough energy for formyl-THF formation [Yang and Drake, 1990; Kantzow and Weuster-Botz, 2016] and/or a limited pool of THF slows down the processing of formic acid. At biological standard conditions, the formation of formic acid is scratch feasible. Increasing the partial pressure of hydrogen and carbon dioxide makes the reaction more favorable [Daniels, 1982], which in my opinion favors the direct hydrogenation of CO_2 by the hydrogenase-formate-dehydrogenase complex. However, the results give that there is a nonlinear relationship between formic acid formation and p_{H_2}. Peters *et al.* report a linear relationship of 0.5 mM formic acid produced per 0.1 bar increase in p_{H_2} for *A. woodii* and *A. carbinolicu*. Calculating the increase in formic acid formation divided by the increase in hydrogen partial pressure in this work results in 17 mM bar^{-1} when increasing p_{H_2} to 2.13 bar (4 bar absolute pressure) and 25.6 mM bar^{-1} when increasing p_{H_2} further to 3.73 bar. [Oswald *et al.* 2018a]

Unfortunately, the only publications that state results from experiments with *C. ljungdahlii* at elevated substrate pressures so far do not report if formic acid production is increased at higher pressures. This may be because no formic acid is produced when working with CO containing gases at elevated pressures or more likely because the authors did not check for formic acid in their sample analytics. However, since no significant growth could be observed

at 4 bar and 7 bar, even without CO in the gas atmosphere, growth inhibition at elevated pressures seems not to be linked to inhibitory effects of carbon monoxide alone, as reported by Vega et al. [1989c] and the Department of Chemical Engineering and the University of Arkansas [1993]. Dissolved CO_2 is in balance with the concentration of HCO_3^-, it is likely that increased concentrations of CO_2/HCO_3^- cause similar effects in *C. ljungdahlii* as it is reported for *Saccharomyces cervisiae*. Shifts in CO_2/HCO_3^- concentration causes multiple intracellular responses, which in total result in prolonged lag phases during which the cells adapt to the increased concentrations. [Eigenstetter and Takors, 2017]

In the cultivations at 4 bar and 7 bar, p_{H_2} is 2.13 bar and 3.73 bar but volumetric power input and gas feed rate is lower than the ones used by Kantzow and Weuster-Botz [2016]. From the data in their publication a yield of formic acid per fed substrates of 0.002 g g^{-1} can be calculated which is 14 % of what is reported here at similar p_{H_2} with an overall $Y_{P/S}$ for formic acid of 0.015 g g^{-1}. This indicates that, despite the differences between 1.5 L-scale and 2.5 L-scale, working with constant $\dot{n}\,V_1^{-1}$ yields a more substrate efficient process at elevated pressure than the classical approach of keeping $\dot{V}_g/V_1^{-1}$ constant does. While the approach of constant volumetric gas feed rate ensures constant k_1a-values if P/V_L is kept constant as well [Schlüter et al., 1992] even at elevated pressure [Maier et al., 2001], $\dot{V}_g/V_1^{-1}$ decreases with increasing pressure when $\dot{n}\,V_1^{-1}$ is kept constant. The actual volumetric flow rates for each pressure stage in this work are 0.029 vvm (1 bar), 0.007 vvm (4 bar) and 0.004 vvm (7 bar). Under these conditions, the k_1a-value cannot assumed to be equal in all pressure stages. But since k_1 is independent from pressure, an approximation for k_1a at different pressures with $\dot{n}\,V_1^{-1}$ = constant can be calculated by [Linek and Sinkule 1991]

$$k_1a_{(p_2)} = \left(\frac{p_1}{p_2}\right)^{\frac{2}{3}} k_1a_{(p_1)}. \tag{5.5}$$

Approximation of k_1a-values for oxygen in medium with equation (5.5) results in 4.0 10^{-3} s^{-1} at 4 bar and 2.8 10^{-3} s^{-1} at 7 bar. k_1a-values for different gases are proportional to each other by the square root of the quotient of their diffusion coefficients [Kodama et al., 1976]. However, the formation of formic acid is more substrate efficient at higher pressures when $\dot{n}\,V_1^{-1}$ is kept constant although the gas-liquid mass transfer coefficient significantly decreases with increasing pressure. [Oswald *et al.* 2018a]

5.3 Influence of cyanide on growth and product formation of *Clostridium ljungdahlii*

5.3.1 Experiments with fructose as substrate

Cyanide is known to reversible inhibit the enzyme carbon monoxide dehydrogenase of acetogenic bacteria [Thauer *et al.* 1974, Ragsdale *et al.* 1983, Terlesky *et al.* 1986, Grahame and Stadtman 1987, Ha *et al.* 2007], but available literature deals only with the effect of cyanide on crude extract or isolated CODH. Table 5.2 summarizes the results of experiments under heterotrophic conditions. Since CODH is involved in the uptake of carbon dioxide, formed during glycolysis, it is not surprising to see inhibitory effects on growth on fructose. However, it is interesting to note that for cyanide concentrations of 0.025 mM to 0.1 mM the resulting maximum CDW is lower than in cyanide free cultures but at 1 mM cyanide it is within the same range as the control cultures. Though, when comparing the not-adapted with the adapted strain at 1.0 mM cyanide, the later grows to a maximum CDW lower than both strains without cyanide while the not-adapted strain, after 261 h lag-phase, reaches a CDW comparable to the control cultures. The reason for this remains unknown. Although the lag-

Table 5.2 – Results for CDW, growth rate, lag-phase and product yield of heterotrophic cultures in presence of different concentrations of cyanide [Oswald *et al.* 2018b]

Culture	$\beta_{\text{CDW, max}}$	μ_{max}	$t_{\text{lag-phase}}$	$Y_{\text{P/S,aa}}$	$Y_{\text{P/S,etOH}}$
	g L^{-1}	h^{-1}	h	g g^{-1}	g g^{-1}
Non-adapted Cultures					
0 mM cyanide[*]	0.73	0.10	0	0.76	0.03
0.025 mM cyanide	0.54	0.08	0	0.61	0.05
0.05 mM cyanide	0.46	0.05	0	0.65	0.11
0.1 mM cyanide[*]	0.60	0.04	49	0.65	0.10
1.0 mM cyanide[*]	0.75	0.05	227	0.09	0.42
Adapted Cultures					
0 mM cyanide	0.78	0.10	0	0.63	0.08
0.1 mM cyanide	0.87	0.10	0	0.65	0.28
1.0 mM cyanide	0.53	0.06	20	0.23	0.35

[*], Mean values from the initial experiments and the experiments where adapted and non-adapted strain are compared with each other; $Y_{\text{P/S,aa}}$, yield of acetic acid per substrate; $Y_{\text{P/S,etOH}}$, yield of ethanol per substrate.

phase of the adapted strain in presence of 1.0 mM cyanide is prolonged compared to 0.1 mM, the cultures start to grow after 24 h. This is less than a 10th of the time the not-adapted strain needs to start growing under these conditions, which shows that *C. ljungdahlii* can be conditioned to grow in presence of cyanide. Once adapted, growth happens with the same growth rate than without cyanide (0.1 h^{-1}) up to CN$^-$ concentrations of 0.1 mM. [Oswald *et al.* 2018b]

At heterotrophic growth conditions, the purpose of the Wood-Ljungdahl-Pathway (WLP) is to recycle NAD$^+$ and ferredoxin by capturing the CO_2 from decarboxylation of pyruvate. CODH is the central enzyme in the WLP and if it is inactivated by cyanide, capturing of CO_2 is no longer possible. However, the eight reducing equivalents gained from glycolysis need to be discarded to recycle NAD$^+$ and ferredoxin. With the WLP disabled by cyanide, one possibility for *C. ljungdahlii* to recycle NAD$^+$ and ferredoxin is to convert acetic acid to ethanol [Köpke et al. 2010]. This shifts the main product from acetic acid to ethanol. Figure 5.1 illustrates the molar ratio of products ($x_i = c_i\,(\Sigma c_{\text{Products}})^{-1}$) in both sets of experiments with fructose as a carbon source. It is evident, that with increasing cyanide concentration more ethanol is formed while the amount of acetic acid decreases. This indicates that with increasing cyanide concentration CODH activity is increasingly inhibited and NAD$^+$ and ferredoxin are recycled by conversion of acetic acid to ethanol. The overall product yield is supporting this as well.
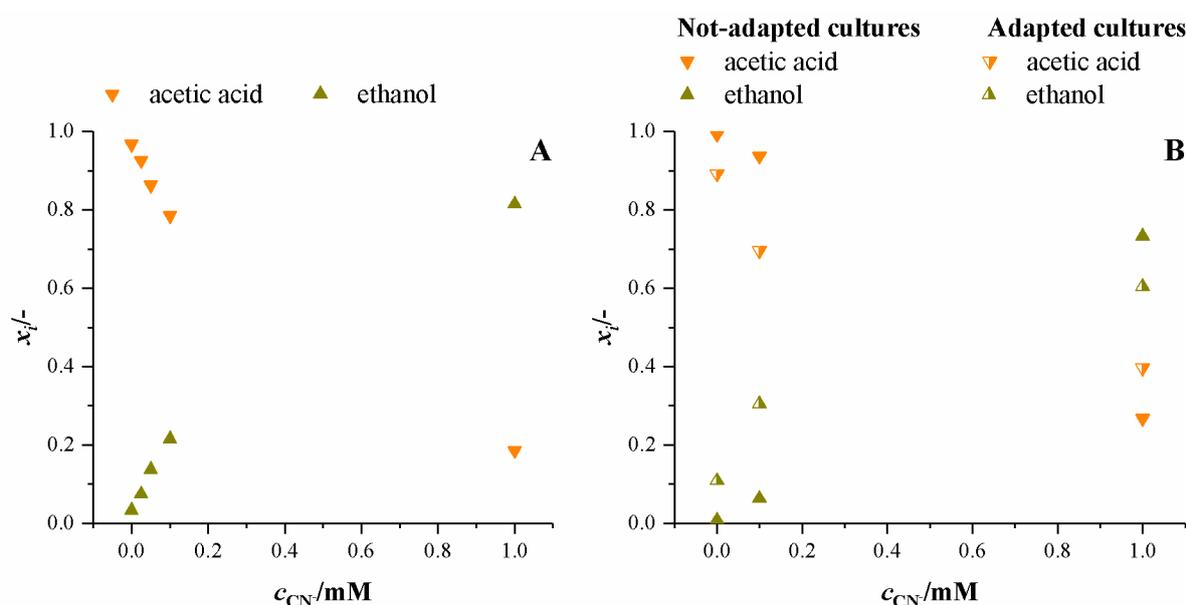
Figure 5.4 – Molar ratio of products formed by *C. ljungdahlii* in presence of increasing concentrations of cyanide with fructose as carbon source. A, experiments with not-adapted cultures only; **B**, experiments with not-adapted and adapted cultures; Orange, upturned triangles, acetic acid; dark yellow triangles, ethanol. [Oswald *et al.* 2018b]

With no CODH activity, the maximum possible product yield is $0.51 \, \mathrm{g \, g^{-1}}$. In our experiments, the $Y_{P/S}$ decreases from $0.79 \, \mathrm{g \, g^{-1}}$ at $0 \, \mathrm{mM}$ cyanide to $0.51 \, \mathrm{g \, g^{-1}}$ in the non-adapted cultures and $0.58 \, \mathrm{g \, g^{-1}}$ in the adapted cultures at $1.0 \, \mathrm{mM}$ cyanide. This indicates that at $1.0 \, \mathrm{mM}$ of cyanide the WLP is disabled by inhibition of CODH. [Oswald *et al*. 2018b]

5.3.2 Cultivations with syngas as carbon and energy source

Table 5.3 summarizes the results for CDW, maximum growth rate and lag-phase of the experiments under autotrophic conditions. Similar to the results with fructose as carbon source, the lag-phase is prolonged with increasing levels of cyanide. In contrast to the results at heterotrophic growth, no increase in CDW or consumption of substrates is measurable at $1.0 \, \mathrm{mM}$ cyanide. Autotrophic growth on CO or CO_2 is only possible with the WLP functional. Therefore, this result is in accordance with the findings from fructose grown cultures, where product spectrum and product yield indicate a loss of most of the CODH activity at $1.0 \, \mathrm{mM}$ cyanide. Inhibitory effects of cyanide on CODH will directly result in reduced growth and product formation. However, the final CDW and maximum growth rate seems unaffected by cyanide up to concentrations of $0.1 \, \mathrm{mM}$. Figure 5.5 shows the development of the partial pressures of hydrogen, carbon monoxide and carbon dioxide in the headspace of the culture bottles. At $0.1 \, \mathrm{mM}$ cyanide, the CO consumption in the adapted strain cultures starts after a

Table 5.3 – Results for CDW, growth rate and lag-phase of autotrophic cultures in presence of different concentrations of cyanide [Oswald *et al*. 2018b]

Culture	$\beta_{CDW, \, max}$	μ_{max}	$t_{lag\text{-}phase}$
	$\mathrm{g \, L^{-1}}$	$\mathrm{h^{-1}}$	h
Non-adapted Cultures			
0 mM cyanide[*]	0.17	0.06	32
0.025 mM cyanide	0.16	0.03	65
0.05 mM cyanide	0.20	0.04	160
0.1 mM cyanide[*]	0.21	0.04	221
1.0 mM cyanide[*]	no growth	no growth	no growth
Adapted Cultures			
0 mM cyanide	0.11	0.07	43
0.1 mM cyanide	0.14	0.06	66
1.0 mM cyanide	no growth	no growth	no growth

[*] Mean values from the initial experiments and the experiments where adapted and non-adapted strain are compared with each other
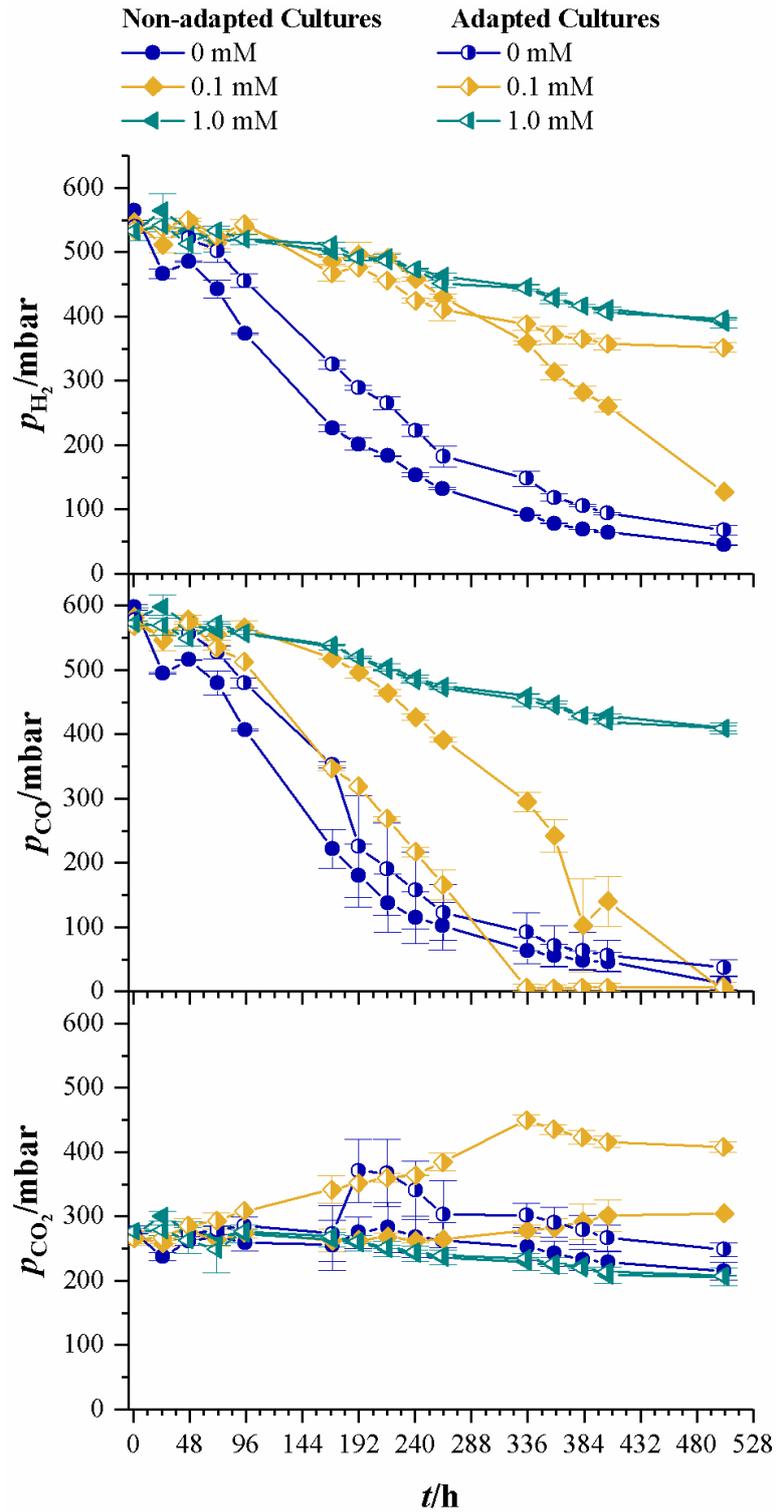
Figure 5.5 – Development of partial pressures of H₂, CO, and CO₂ for not-adapted *C. ljungdahlii* (full symbols) vs. the adapted cultures (half filled symbols) at different cyanide concentrations. Cyanide concentrations are 0 mM (blue dots), 0.1 mM (yellow diamonds) and 1.0 mM (petrol tilted triangles). [Oswald *et al.* 2018b]

lag-phase of 48 h and the non-adapted strain after 192 h. Both show no other signs of cyanide inhibition when compared with the cyanide-free cultures but completely consume the available carbon monoxide. This indicates that either cyanide is actively degraded, or the organism adapts to it in another way. Whatever the mechanism behind the adaption is, it seems to influence hydrogenase activity. Usually, in cultures growing on CO and H_2, hydrogenases are inhibited by CO until the liquid CO concentration is low enough to revoke the inhibition [Vega et al. 1989]. While for both strains hydrogen consumption starts at p_{CO} of 300 mbar, only about 50 mbar H_2 are consumed by the adapted strain (the difference between last measured partial pressure in 1.0 mM and 0.1 mM culture) whereas the non-adapted strain consumes 260 mbar H_2. [Oswald *et al.* 2018b]

Hydrogenases are usually not inhibited by cyanide [Adams et al., 1981] and since the non-adapted strain does consume 260 mbar of hydrogen in presence of 0.1 mM CN^-, an inhibitory effect of cyanide on hydrogenase activity in the adapted strain cultures seems unlikely.[Oswald *et al.* 2018b] However, cyanide not only inhibits CODH but is also known to inactivate formate dehydrogenases of several organisms [Barber *et al.* 1986, Ohyama and Yamazaki 1975] as well as interfering with the methanol metabolism of *Moorella thermoacetica* [Das *et al.* 2007]. Inactivation of formate dehydrogenase would prevent the formation of the methyl group in the WLP and therefore result in reduced need for hydrogen, product formation and growth. Still, carbon monoxide metabolism is unaltered at 0.1 mM cyanide compared to the control cultures of not-adapted and adapted strain. This and the fact that the development of products and CDW is also comparable to the control does make inhibition of formate dehydrogenase by cyanide unlikely. It is noteworthy that acetic acid concentration in cultures with the adapted strain and 0.1 mM cyanide reaches the highest value once CO is completely consumed. After this point (330 h) parts of the acetic acid are converted to ethanol, thus tripling the ethanol concentration from $0.1\,g\,L^{-1}$ to $0.3\,g\,L^{-1}$. The same late beginning of ethanol formation can be found in the not-adapted cultures at 0.1 mM cyanide. Although, with a higher final concentration.

How *C. ljungdahlii* is adapting to the applied cyanide concentration could not be identified during this study. Hydrocyanic acid in aqueous solution is known to slowly disintegrate into ammonia and formic acid [Roempp 2012]. While at first glance this could indicate that growth after a prolonged lag-phase is due to autocatalytic disintegration of cyanide, it is refuted by the fact that the adapted strain shows only effects of inhibition when exposed to

concentrations of 1 mM cyanide. Another possibility could be that *C. ljungdahlii* upregulates enzymes like cyanase, cyanidase, nitrilase or rhodanese to neutralize HCN [Dubey and Holmes]. However, none of these enzymes can be found in the published complete genome of *C. ljungdahlii* DSM 13528 (Köpke et al. 2010) and the product and yield data from heterotrophic cultures show no signs of cyanide degradation. Further investigation of the transcriptome and proteome at different cyanide concentrations is necessary to determine in what way *C. ljungdahlii* adapts to cyanide. [Oswald *et al*. 2018]

5.4   Process link-up: From syngas to malic acid

Utilization of acetic acid, the main product of acetogenic metabolism, by aerobic organisms would broaden the spectrum of products that can be made from syngas. Using the filamentous fungi *A. oryzae* to produce L-malic acid from the acetic acid in the broth of syngas fermentation is one option. The main challenges for such a process link-up are the involved organisms and their requirements in terms of reactor set-up, medium composition and product synthesis. When optimizing product yield and/or productivity of a certain process, common procedure is to address the needs of the involved organism. In this case two fermentation processes are interlinked by sequentially cultivating *A. oryzae* in culture broth of syngas fermentation with *C. ljundahlii*. Key aspect of the success of this process is either a medium compromise for both organisms or the compatibility of the first (optimized) medium for *A. oryzae* fermentation in terms of product synthesis. Furthermore, the second organism has to be able to use the product of the first process as a carbon source. The combination of both aspects must be fulfilled to achieve a successful process chain from syngas to malic acid. [Oswald *et al*. 2016]

The *Aspergillus* part of this study shows for the first time that *A. oryzae* can use acetic acid as a sole source of carbon to produce malic acid. For carbohydrate based malic acid production the metabolic pathways are largely understood. A partly reductive TCA cycle following on glycolysis and malic acid is then synthesized from pyruvic acid and oxaloacetic acid [Osmani and Scrutton 1983; Peleg *et al.* 1988, 1989; Bercovitz *et al.* 1990]. Not much is known for the pathways with other carbon sources. In terms of acetic acid, acetyl-CoA synthase is the central enzyme of ethanol and acetic acid metabolism, which converts acetic acid to acetyl-CoA in *Candita albicans* [Carman *et al*. 2008]. Acetyl-CoA may then enter the glyoxylate cycle, which is partly located in the peroxisome and contains malic acid as an intermediate.

This might be the pathway to form malic acid from acetic acid. The metabolic flux of this path is summarized by Strijbis and Distel [2010]. [Oswald *et al*. 2016]

Preliminary experiments with *A. oryzae*, conducted by Stefan Dörsam, indicated that if nitrogen is omitted from syngas medium, the yield of 0.37 gram L-malic acid per gram consumed acetic acid is comparable to the one in malic acid production medium with acetic acid as carbon source ($Y_{P/S} = 0.28 \, \text{g} \, \text{g}^{-1}$). Even though the yield of malic acid per gram consumed acetic acid is higher in syngas fermentation medium, the concentration of malic acid after 168 h of fermentation is only about half of the concentration in optimized malic acid production medium ($4.11 \pm 0.50 \, \text{g} \, \text{L}^{-1}$ compared to $8.62 \pm 1,15 \, \text{g} \, \text{L}^{-1}$). Malic acid production also seems to be influenced by the presence of biomass from syngas fermentation. Without removal of *C. ljungdahlii* cells, malic acid could already be detected after 48 h while in medium with removed cells no formation of malic acid could be observed. The biomass itself might serve as a source of nutrients and minerals. Ethanol is not used as carbon source, but the presence of ethanol (up to $1.24 \, \text{g} \, \text{L}^{-1}$) resulted in the highest $Y_{P/S}$ value. This may indicate a possible stimulation effect of ethanol on L-malic acid formation. Knuf *et al.* [2013] found that stress conditions are beneficial the production of L-malic acid. Overall, the preliminary experiments with *A. oryzae* show that the conversion of acetic acid to L-malic acid in broth from syngas fermentation is possible and that the link-up of the two processes is a promising approach. [Oswald *et al.* 2016]

Results from preliminary experiments with *C. ljungdahlii* indicate that reducing the ammonia concentration does not negatively affect acetic acid formation, substrate consumption and overall yield during syngas fermentation. The slightly lower biomass concentration in ammonia reduced medium is consistent with results from Xu *et al.* [2011] which also show slight differences of biomass concentration in this range of ammonia concentrations. Off-gas data and fructose measurements from the main process link-up experiment show that during the first 18 h of fermentation *C. ljungdahlii* is only consuming fructose and carbon monoxide but no hydrogen. Carbon monoxide is a known inhibitor of hydrogenase activity [Gray and Gest 1965; Chen and Blanchard 1978; Kim *et al.* 1984; Devarapalli *et al.* 2016] and therefore hydrogen consumption can only start if the carbon monoxide partial pressure in the broth is below a certain threshold which seems to be around 5 vol-% CO in the headspace of the bioreactor. Fuchs *et al.* [1974] report that concentrations of more than 5 % of CO inhibits growth of *C. pasteurianum* on glucose as carbon and energy source. This could also explain

that it takes *C. ljungdahlii* 18 h to completely consume the 0.77 g L^{-1} of fructose left from the preculture. Considerable formation of acetic acid is observed after fructose is depleted and hydrogen consumption starts. This point is accompanied by a temporary increase of the redox potential in the broth. [Oswald *et al.* 2016]

Acetic acid is continuously produced up to the moment when hydrogen consumption starts to decrease. At this point, ethanol formation can be observed. In case the decrease of hydrogen consumption is due to the increase in gas feed rate and therefore increased CO supply, we reduced the gas feed rate to stabilize the uptake rates again. This yielded only a temporary improvement and the rate of hydrogen consumption decreased for the rest of the experiment. The occurrence of sudden decrease in hydrogen consumption is a known phenomenon when cultivating *C. ljungdahlii* on syngas [Cotter *et al.* 2009, Maddipati *et al.* 2011]. However, the reason for this is still unknown. [Oswald *et al.* 2016]

The malic acid production in the main link-up experiment varied widely. Two out of three reactors showed malic acid production. With different production profiles. The high complexity of the medium composition after syngas fermentation makes finding an explanation for the very different behavior of the reactors in the *A. oryzae* stage of the link-up experiment is difficult. Small differences in syngas fermentation seem to have large effects on the following fungal fermentation. For preliminary experiments medium of syngas fermentations has been pooled to gain a similar medium for all experiments. Since in the main link-up experiment each reactor resulted in a possible different medium composition, the results should be seen as three different batches of link-up experiments. However, the results clearly show, that conversion of syngas to malic acid by means of sequential mixed culture is possible. The conversion efficiency of syngas into acetic acid and ethanol can be expressed by an overall $Y_{P/S}$ of 0.86 g g^{-1}. Combined with the $Y_{P/S}$ of 0.33 g g^{-1} for aerobic conversion of acetic acid to malic acid the overall conversion efficiency of syngas into malic acid is 28 %. This is achieved by complete conversion of CO and H$_2$ into products. [Oswald *et al.* 2016]

Due to the lack of other processes that converse CO, CO$_2$ and H$_2$ into dicarboxylic acids, yields are compared with anaerobic production of other C$_4$ molecules. Yields for anaerobic production of butanol from sugars of lignocellulosic substrates with *C. beijerinckii* or *C. acetobutylicum* are between 0.1 g g^{-1} to 0.3 g g^{-1} [Schiel-Bengelsdorf *et al.* 2013]. Using syngas for production of butanol yields 0.08 g butanol per gram of consumed carbon monoxide [Lewis *et al.* 2007]. Other processes described in literature for production of C$_4$-

molecules using anaerobic syngas fermentation do not state values for $Y_{P/S}$ and lack of proper information for calculation of yields by the reader. This prevents proper comparison. [Oswald *et al*. 2016] Approaches using synthetic biology to introduce new pathways or enhance existing pathways for production of C_4 and higher products are accompanied by 3 to 60-fold higher by-production of acetic acid or ethanol [Banerjee *et al*. 2014, Fernández-Naveira *et al*. 2017, Doll *et al.* 2018].

Sequential mixed cultures are used for centuries in food industry, e. g. sake production, applications for production of chemicals are rare. It could be shown, that this kind of biotechnological process is suitable to produce low price chemicals like single cell oils for biofuel production [Hu *et al*. 2016]. Other approaches co-cultivate a homoacetogen, e. g. *C. ljungdahlii* and an anaerobic organism that can grow on ethanol or acetate and produces butanol or butyrate [Datta and Reeves 2014]. Lagoa-Costa *et al*. [2017] sequentially link anaerobic syngas fermentation with *C. autoethanogenum* with aerobic formation of polyhydroxyalkanoates from acetic acid but do not name organism. Another approach uses *C. kluyveri* to convert ethanol-acetic acid mixtures from syngas fermentation into medium chain carboxylic acids [Gildemyn *et al*. 2017]. Other interlinking processes are a combination of algae and yeast fermentation [Dillschneider *et al*. 2014], dextran fermentation [Kim and Day 1994] and biogas production. [Oswald *et al*. 2016] Recently, Liebal *et al*. [2018] did a theoretical examination of possible routes from CO_2 to succinic acid. Their conclusion is, that the most economic route would be to link acetic acid formation by syngas fermentation with aerobic production of succinic acid by an *E. coli* strain [Liebal *et al*. 2018].

6.   Conclusions

Characterization of the 1.5 L-scale cultivation system with RMR and RRB stirrer set-up revealed that with the syngas mixture used, even at a volume-based gas feed rate of 0.029 vvm the process becomes inefficient in terms of substrate conversion into products. This is despite the six-fold and four-fold increase in $k_l a$ for the RMR and RRB stirrer set-up respectively when increasing the gas feed rate from 0.007 vvm to 0.029 vvm. The substrate conversion efficiency is much better at lower values. However, due to the nature of a batch process, it is possible that a continuous cultivation with cell retention could also achieve complete substrate consumption at 0.029 vvm and higher if a continuous running culture could circumvent the decrease in hydrogen consumption. Then a volume-based gas feed rate above 0.012 vvm would also be substrate efficient and result in higher titers of products. The other strategy discussed in literature to improve mass-transfer, increasing the absolute system pressure and therefore the partial pressure of gaseous substrates, does not result in higher product yields. However, in the work at hand the product spectrum shifts from 2.4 % formic acid, 86.5 % acetic acid and 11.1 % ethanol to 82.7 % formic acid, 15.6 % acetic acid and 1.7 % ethanol. Final CDW does decrease with increasing pressure. Whether this reduction of CDW is subject to an inhibitory effect of increased hydrogen partial pressure [Kantzow and Weuster-Botz 2016] or more likely due to inhibitory effects of increased intracellular dissolved carbon dioxide concentration [Eigenstetter and Takors 2017] remains a topic of interest for further investigations. When dealing with inhibition caused by increased dissolved carbon monoxide concentrations, a stepwise increase in process pressure avoided that problem [University of Arkansas 1993]. Using constant $\dot{n}\, V_1^{-1}$ results in a 7.5 times higher yield of formic acid per fed substrate than with the process published by Kantzow and Weuster-Botz [2016] where $\dot{V}_g/V_1$ is kept constant. However, at constant $\dot{n}\, V_1^{-1}$ the $k_l a$-value decreases with increasing pressure. [Oswald *et al.* 2018a]

The complete usage of substrates is a crucial point in increasing the overall efficiency of syngas fermentation processes. Therefore, further investigations on the influence of feed gas flow rate and substrate partial pressure on the substrate conversion efficiency are necessary to increase the efficiency of anaerobic syngas fermentation. [Oswald *et al.* 2018a]

To further increase the economics of syngas fermentation-based processes it is necessary to reduce gas purification efforts by using crude or partially purified syngas [Ahmed *et al* 2006,

Xu *et al*. 2011, Abubackar *et al*. 2011]. Typical cyanide loads of crude syngas from wood or straw are below 25 ppm for wood [Boerrighter *et al*. 2013] and 250 ppm for straw [Kurkela *et al*. 1996] but can also reach values up to 2500 ppm when gasifying switchgrass [Broer *et al*. 2015]. The resulting liquid concentrations range from 0.24 mM (straw) to 2.4 mM (wood) and 24.3 mM (switchgrass). Assuming a gas feed rate of 0.1 vvm it would take more than 41 h of gas sparging to reach saturation concentrations and the actual concentrations a culture has to deal with in the beginning of cultivation is much lower.

The results of this work show that maximum growth rates are unaffected by cyanide up to 0.1 mM cyanide with syngas as carbon source. Using cultures that are already adapted to cyanide will also decrease the lag-phase at the beginning of the cultivation. These results are the first to show that *C. ljungdahlii* can be adapted to cyanide, which is a huge step, since literature commonly states that if syngas is used as a substrate for fermentation, it needs to be as clean as possible to avoid inhibitory effects [Xu *et al*. 2011; Daniell *et al*. 2012; Liew *et al*. 2016]. Nevertheless, this work only shows the influence in bottle experiments and further investigation in bioreactors with continuous feed of cyanide containing gas is necessary to determine at which cyanide load the crude syngas needs to be purified. On the other hand, some impurities counter the effect of others or protect against inhibition when applied as a mixture. Unfortunately, the lack of studies using mixtures of impurities or crude syngas for cultivation of whole cells makes it difficult to give a common statement on that topic.

Together with Stefan Dörsam, it was possible to show that a process link-up of anaerobic syngas fermentation with aerobic fungal production of malic acid is possible. The linking metabolite is acetic acid. This is the second successful process of this kind described in literature. Further increase in yield is feasible since only wild type strains of *C. ljungdahlii* and *A. oryzae* are used and the medium is neither optimized for acetic acid production nor for malic acid production. Linking syngas fermentation with other processes offers the opportunity to extend the product portfolio of syngas fermentation. When interlinking with an aerobic process, such as Stefan Dörsam and I did, no further step is necessary other than changing the feed gas from syngas to air and addition of calcium carbonate to prepare the medium for fungal fermentation. In demonstrating the successful production of malic acid using a sequential mixed cultures of *C. ljungdahlii* and *A. oryzae* Stefan Dörsam and I not only broadened the feedstock for malic acid production from glycerol and sugars to the whole feedstock of gasification processes but also reported the highest yield to date for the production of C_4 components from syngas. [Oswald *et al*. 2016] As has recently be outlined

by Liebal *et al.* [2018] the production of succinic acid with continuous cultures of *C. ljungdahlii* and *E. coli* in series is economically superior to other ways of CO_2 to succinic acid conversion. In general, any organism capable of producing a valuable substance from acetic acid as carbon source is a potential candidate for further process link-up strategies.

References

Abubackar, H. N., Bengeldorf, F. R., Dürre, P., Veiga, M. C. and Kennes, C. 2016. Improved operation strategy for continuous fermentation of carbon monoxide to fuel-ethanol by clostridia. *Applied Energy*. 169:210-217.

Abubackar, H. N., Veiga, M. and Kennes, C. 2011. Biological conversion of carbon monoxide: rich syngas or wase gasest o bioethanol. *Biofuels, Bioproducts and Biorefining*. 5:93-114.

Adams, M. W. W., Mortenson, L. E. and Chen, J.-S. 1981. Hydrogenase. *Biochimica et Biophysica Acta*. 594:105-176.

Ahmed, A. and Lewis, R. S. 2006. Fermentation of Biomass-Generated Synthesis Gas: Effects of Nitric Oxide. *Biotechnology and Bioengineering*. 97(5):1080-1086.

Ahmed, A., Cateni, B. G., Huhnke, R. L. and Lewis, R. S. 2006. Effects of biomass-generated producer gas constituents on cell growth, product distribution and hydrogenase activity of *Clostridium carboxidivorans* P7[T]. *Biomass and Bioenergy*. 30(7):665-672.

Anderson, M. E., DeRose, V. J., Hoffman, B. M. and Lindahl, P. A. 1993. Identification of a Cyanide Binding Site in CO Dehydrogenase from *Clostridium thermoaceticum* Using EPR and ENDOR Spectroscopies. *Journal of the American Chemical Society*. 115(25):12204-12205.

Arnold, J. H. 1930. Studies in Diffusion. I – Estimation of Diffusivities in Gaseous Systems. *Industrial and Engineering Chemistry*. 22(19):1091-1095.

Bailey, J. E. and Ollis, D. F. 1991. *Biochemical engineering fundamentals*. McGraw-Hill: New York.

Banerjee, A., Leang, C., Ueki, T., Nevin, K. P. and Lovley, D. R. 2014. Lactose-Indicible System for Metabolic Engineering of *clostridium ljungdahlii*. *Applied and Environmental Microbiology*. 80(8):2410-2416. doi: 10.1128/AEM.03666-13.

Barber, M. J., Hal, D. and Ferry, J. G. 1986. Inactivation of Formate Dehydrogenase from *Methanobacterium formicum* by Cyanide. *Biochemistry*. 25:8150-8155.

Barik, S., Prieto, S., Harrison, S. B., Clausen, E. C. and Gaddy, J. L. 1988. Biological production of alcohols from coal through indirect liquefaction. *Applied Biochemistry*. 18(1):363-378.

Barker, H. A. and Kamen M. D. 1945. Carbon Dioxide Utilization in the Synthesis of Acetic Aceid by *Clostridium thermoaceticum*. *Proceedings of the National Academy of Sciences*. 31(8):219-225.

Bengelsdorf, F. R., Poehlein, A., Linder, S., Erz, C., Hummel, T., Hoffmeister, S. Daniel, R. and Dürre, P. 2016. Industrila Acetogenic Biocatalysis: A Comperative Metabolic and Genomic Analysis. *Frontiers in Microbiology*. 7:1036. DOI: 10.3389/fmicb.2016.01036.

Bengelsdorf, F., Straub, M. and Dürre, P. 2013. Bacterial synthesis gas (syngas) fermentation. *Environmental Technology*. 34(13-14):1639-1651.

Bercovitz, A., Peleg, Y., Battat, E., Rokem, J., S., and Goldberg, I. 1990. Localization of pyruvate carboxylase in organic acid-producing aspergillus strains. *Applied Environmental Microbiology*. 56:1594–1597.

Bertsch, J. and Müller, V. 2015. Bioenergetic constrains for cnversion of syngas to biofuels in acetogenic bacteria. *Biotechnology for Biofuels*. 8:210. doi: 10.1186/s13068-015-0393.

Bertsch, J., Siemund, A. L., Kremp, F. and Müller, V. 2016. A novel route forethanol oxidation on the acetogenic bacterium *Acetobacterium woodii*: the acetaldehyde/ethanol dehydrogenase pathway. *Environmental Microbiology*. 8(9):2913-2922. doi: 10.1111/1462-2920.13082

Bleichert, K. and Winter, J. 1994. Formate production and utilization by methanogens and by sewage sludge consortia – interference with the concept of interspecies formate transfer. *Applied Microbiology and Biotechnology*. 40:910-915.

Boerrighter, H., Uil, H. and Calis, H.-P. 2013. Green Diesel from Biomass via Fischer-Tropsch synthesis: New Insights in Gas Cleaning and Process Design. *Pyrolysis and Gasification of Biomass and Waste*. 371-383.

Bredwell, M. D. and Worden, R. 1998. Mass-Transfer Properties of Microbubbles. 1. Experimental Studies. *Biotechnology progress*. 14:31-38.

Bredwell, M. D., Srivastava, P. and Worden, R. M. 1999. Reactor Design Issues for Synthesis-Gas Fermentations. *Biotechnology Progress*. 15(5):834-844.

Broer, K. M., Woolock, P. J., Johnston, P. A. and Brown, R. C. 2015. Steam/oxygen gasification system for the production of clean syngas. *Fuel*. 140:282-292.

Carman, A. J., Vylkova, S. and Lorenz, M. C. 2008. Role of acetyl coenzyme a synthesis and breakdown in alternative carbon source utilization in *candida albicans*. *Eukaryotic Cell*. 7:1733–1741. doi: 10.1128/EC.00253-08.

Chen, J.-S. and Blanchard, D. K. 1978. Isolation and Properties of a unidirectional H2-oxidizing hydrogenase from strictly anaerobic N2-fixing bacteriumClostridiumpasteurianumW5. *Biochemical and Biophysical Research Communications*. 84:1144–1150. doi: 10.1016/0006-291X(78)91703-5

Chisti, Y. 2010. Mass transfer. In: M. C. Flickinger (ed.) *Encyclopedia of Industrial Biotechnology – Bioprocess, Bioseparation and Cell Technology*. New York: Wiley. 3241-3276.

Daniell, J., Köpke, M. and Simpson, S. D. 2012. Commercial Biomass Syngas Fermentation. *Energies*. 5(12):5372-5417. doi: 10.3390/en5125372.

Daniels, L. 1982. Comments on Enzymatic Synthesis of Organic Acids and Alcohols from H_2, CO_2 and CO. Communications to the editor. *Biotechnoloy and Bioenineering*. 24:2099-2102.

Das, A., Fu, Z.-Q., Tempel, W., Liu, Z.-J., Chang, J., Chen, L., Lee, D., Zhou, W., Xu, H., Shaw, N., John, P. R., Ljungdahl, L. G. and Wang, B.-C. 2007. Characterization of a Corrinoid Protein Involved in the C1 Metabolism of Strict Anaerobic Bacterium *Moorella thermoacetica*. *Proteins: Structure, Funkction and Bioinformatics*. 67:167-176.

Datta, R. and Reeves, A. 2014. *Syntropic Co-Culture of Anaerobic Microorganism for Production of n-Butanol from syngas*. US patent no. US2014/0206066 A1.

Demler, M. 2012. *Reaktionstechnische Untersuchung zur autotrophen Herstellung von Acetat mit Acetobacterium woodii*. Dissertation, TU München.

Devarapalli, M., Atiyeh, H. K., Phillips, J. R., Lewis, R. S. and Huhnke, R., L. 2016. Ethanol production during semi-continuous syngas fermentation in a trickle bed reactor using Clostridium ragsdalei. *Bioresource Technology*. 209:56–65 doi: 10.1016/j.biortech.2016.02.086

Diekert, G. and Wohlfarth, G. 1994. Metabolism of homoacetogens. *Antonie van Leeuwenhoek*. 66(1-3):209-221.

Diekert, G. B. and Thauer, R. T. 1978. Carbon Monoxide Oxidation by *Clostridium thermoaceticum* and *Clostridium formicoaceticum*. *Journal of Bacteriology*. 136(2):597-606.

Dillschneider, R., Schulze, I., Neumann, A., Posten, C. and Syldatk, C. 2014. Combination of algae and yeasr fermentation for an integrated process to produce single cell oils. *Applied Microbiology and Biotechnology*. 98(18):7793-7802. doi: 10.1007/s00253-014-5867-4.

Doll, K. Rückel, A., Kämpf, P., Wende, M. and Weuster-Botz, D. 2018. Two stirred-tank bioreactors in series enable continuous production of alcohols from carbon monoxide with *Clostridium carboxidivorans*. *Bioprocess and Biosystems Engineering*. 41(10):1403-1416. doi: 10.1007/s00449-018-1969-1.

Drake, H. L. 1994. Acetogenesis, Acetogenic Bacteria, and the Acetyl-CoA "Wood/Ljungdahl" Pathway: Past and Current Perspectives. In: Harold L. Drake (ed.) *Acetogenesis*. Dordrecht: Springer Science and Business. 3-60.

Dubey, S. K. and Holmes, D. S. 1995. Biological cyanide destruction mediated by microorganisms. *World Journal of Microbiology & Biotechnology*. 11(5):257-265.

Eigenstetter, G. and Takors, R. 2017. Dynamic modeling reveals a three-step response of *Saccharomyces cervisiae* to high CO_2 levels accompanied by increasing ATP demands. *FEMS Yeast Research*. Doi: 10.1093/femsyr/fox008.

Ensing, S. A., Hyman, M. R. and Ludden, P. W. 1989. Nickel-Specific, Slow-Binding Inhibition of Carbon Monoxide Dehydrogenase from *Rhodospirillum rubrum* by Cyanide. *Biochemistry*. 28(12):4973-4979.

Evonik Industries 11/14/2013. Mehrstufiges Syntheseverfahren mit Synthesegas. Patent no.: DE 10 2012207 921 A1. 2013.11.14.

Fernández-Naveira, Á., Abubackar, H. N., Veiga, M. C. and Kennes, C. 2017. Production of chemicals from C1 gases (CO, CO_2) by *Clostridium carboxidivorans*. *World Journal of Microbiology and Biotechnology*. 33:43. doi: 10.1007/s11274-016-2188-z.

Fernández-Naveira, Á., Abubackar, H. N., Veiga, M. C. and Kennes, C. 2016. Efficient butanol-ethanol (B-E) production from carbon monoxide fermentation by *Clostridium carboxidivorans*. *Applied Microbiology and Biotechnology*. 100(7):3361-3370.

Fuchs, G., Schnitker, U. and Thauer, R. K. 1974. Carbon Monoxide Oxidation by Growing Cultures of Clostridium pasteurianum. European Journal of Biochemistry. 49(1):111-115.

Gaddis, E. S. 1999. Mass transfer in gas-liquid contactors. *Chemical Engineering and Processing*. 38(4):503-510.

Gildemyn, S., Molitor, B., Usack, J., Nguyen, M., Rabaey, K. and Angenent, L. T. 2017. Upgrading syngas fermentation effluent using *Clostridium kluyveri* in a continuous fermentation. *Biotechnology for Biofuels*. 10:83. doi: 10.1186/s13068-017-0764-6.

Gößner, A. S., Picardal, F., Tanner, R. S., Drake, H. L. 2008. Carbon metabolism of the moderate acid-tolerant acetogen *Clostridium drakei* isolated from peat. *FEMS Microbiology Letters*. 287(2):236-242.

Grahame, D. A. and Stadtman, T. C. 1987. Carbon Monoxide Dehydrogenase from *Methanosarcina barkeri*. Disaggregation, Purification, and Physicochemical Properties of the Enzyme. *The Journal of Biological Chemistry*. 262(8):3706-3712.

Gray, C. T. and Gest, H. 1965. Biological formation of molecular hydrogen. *Science*. 148:186–192.

Ha, S-W., Korbas, M., Klepsch, M., Meyer-Klaucke, W., Meyer, Ortwin and Svetlitchnyi, V. 2007. Interaction of Potassium Cyanide with the [Ni-4Fe-5S] Active Site Cluster of CO Dehydrogenase from *Carboxydothermus hydrogenoformans*. *The Journal of Biological Chemistry*. 282(14):10639-10646.

Hammerschmidt, A., Boukis, N., Hauer, E., Galla, U., Dinjus, E., Hitzmann, B., Larsen, T., Nygaard, S. D. 2011. Catalytic conversion of waste biomass by hydrothermal treatment. *Fuel*. 90(2):555-562.

Hannula I, Kurkela E 2013. Liquid transportation fuels via largescale fluidised-bed gasification of lignocellulosic biomass. *VTT Technology*. 91:114.

He, S.-H., Woo, S. B., DerVartanian, D. V., Le Gall, J. and Peck, H. D. 1989. Effects of Acetylene on Hydogenase from the Sulfate Reducing and Methanogenic Bacteria. *Biochemical and Biophysical Research Communications*. 161(1):127-133.

Henzler, H. 1982. Verfahrenstechnische Auslegungsunterlagen für Rührbehälter als Fermenter. *Chemie Ingenieur Technik*. 54(5):461-476.

Hofbauer H, Vogel A, Kaltschmitt M 2009. Vergasungstechnik. In: M. Kaltschmitt, Hartmann H, Hofbauer H (eds) *Energie aus Biomasse. Grundlagen, Techniken und Verfahren*. 2. neu bearbeitete und erweiterte Auflage. Heidelberg and others: Springer. 600–628

Hu, O., Chakraborty, S., Kumar, A., Woolston, B., Liu, H., Emerson, D. and Stephanopoulos, G. 2016. Integrated bioprocess for conversion of gaseous substrates to liquids. *Proceedings of the National Academy of Science*. 113(14):3773-3778.

Huang, H., Wang, S., Moll, J. and Thauer, R. K. 2012. Electron Bifurcation Involved in the Energy Metabolism of the Acetogenic Bacterium *Moorella thermoacetica* Growing on Glucose or H_2 plus CO_2. *Jouornal of Bacteriology*. 194(14):3689-3699.

Huber, C., Caldeira, J., Jongejan, J. A. and Simon, H. 1994. Further characterization of 2 different, reversible aldehyde oxidoreductases from *Clostridium formicoaceticum*, one containing tungsten and the other molybdenum. *Archives of Microbiology*. 162(5):303-309.

Huber, C., Skopan, H., Feich, R., White, H. and Simon, H. 1995. Pterin cofactor, substrate specificity, and observations on the kinetics of the reversible tungsten-containing aldehyde oxidoreductase from *Clostridium thermoaceticum*: preparative reductions of a series of carboxylates to alcohols. *Archives of Microbiology*. 164(2):110-118.

Huhnke, R. L., Lewis, R. S., Tanner, R. S. 04/27/2010. Isolation and Characterisation of Novel Clostridial Species. US-Patent no.: US 7,704,723 B2.

Hyman, M. R. and Arp, D. J. 1988. Acetylene Inhibition of Metaloenzymes. *Analytical Biochemistry*. 173(2):207-220.

Hyman, M. R., Ensing, S. A., Arp, D. J. and Ludden, P. W. 1989. Carbonyl Sulfide Inhibition of CO Dehydrogenase from *Rhodospirillum rubrum*. *Biochemistry*. 28(17):6821-6826.

Ju, L.-K. and Chase, G. G. 1992. Improved scale-up strategies of bioreactors. *Bioprocess Engineering*. 8(1):49-53.

Judat, H. 1976. *Zum Dispergieren von Gasen*. Dissertation TU Dortmund.

Kantzow, C. and Weuster-Botz, D. 2016. Effects of hydrogen partial pressure on autotrophic growth and product formation of *Acetobacterium woodii*. *Bioprocess and Biosystems Engineering*. 39:1325-1330. Doi: 10.1007/s00449-016-1600-2.

Kapic, A., Jones, S. T. and Heindel, T. J. 2006. Carbon Monoxide Mass Transfer in a Syngas Mixture. *Industrial & Engineering Chemistry Research*. 45(26):9150-9155.

Kerby, R., Niemczura, W. and Zeikus, J. G. 1983. Single-Carbon Catabolism in Acetogens: Analysis of Carbon Flow in *Acetobacterium woodii* and *Butyribacterium methylotrophicum* by Fermentation and ^{13}C Nuclear Magnetic Resonance Measurement. *Journal of Bacteriology*. 155(3):1208-1218.

Kim, B. H., Bellows, P., Datta, R. and Zeikus, J. G. 1984. Control of carbon and electron flow in Clostridium acetobutylicum fermentations: utilization of carbon monoxide to inhibit hydrogen production and enhance butanol yields. *Applied Environmental Microbioloy*. 48:764–770.

Kim, D. and Day, D. F. 1994. A new process for the production of clinical dextran by mixed-culture fermentation of lipomyces starkeyi and *Leuconostoc mesenteroides*. *Enzyme and microbial Technology*. 16(10):844-848. doi: 10.1016/0141-0229(94)90058-2

Klasson, K. T., Ackerson, M. D., Clausen, E. C. and Gaddy, J. L. 1992. Bioliquefaction of coal synthesis gas. *American Chemical Society Division Fuel Chemistry*. 37:1977-1982.

Knuf, C., Nookaew, I., Brown, S. H., McCulloch, M., Berry, A., and Nielsen, J. 2013. Investigation of Malic Acid Production in Aspergillus Oryzae under Nitrogen Starvation Conditions. *Applied and Environmental Microbiology*. 79(19):6050–58. DOI: 10.1128/AEM.01445-13.

Ko, C. W., Vega, J. L., Clausen, E. C. and Gaddy, J. L. (1989). Effect of High Pressure on a Co-Culture for the Production of Methane from Coal Synthesis Gas. *Chemical Engineering Communications*. 77:155-169.

Kodama, T., Goto, E. and Minoda, Y. 1976. Determination of Dissolved Hydrogen Concentration and $[K_La]_{H2}$ in Submerged Culture Vessels. *Agricultural Biology and Chemistry*. 40(12):2373-2377.

Köpke, M., Held, C., Hujer, S., Liesegang, H., Wiezer, A., Wollherr, A., Ehrenreich, A., Liebl, W., Gottschalk, G. and Dürre, P. 2010. *Clostridium ljungdahlii* represents a microbial production platform based on syngas. *Proceedings of the National Academy of Sciences*. 107(29):13087-13092.

Köpke, M., Mihalcea, C., Liew, F., Tizard, J. H., Ali, M. S., Conolly, J. J., Al-Sinawi, B. and Simpson, S. D. 2011. 2,3-Butanediol Production by Acetogenic Bacteria, an Alternative Route to Chemical Synthesis, Using Industrial Waste Gas. *Appl. Environ. Microbiol*. 77:5467–5475

Krasna, A. I. and Rittenberg, D. 1954. The Inhibition of Hydrogenase by Nitric Oxide. *Proceedings of the National Academy of Sciences*. 40(4):225-227.

Kurkela, E., Laatikainen-Luntama, J., Stahlberg, P. and Moilanen, A. 1996. Pressurised fluidised-bed gasification experiments with biomass, peat and coal at VTT in 1991-1994. Part 3. Gasification of Danish wheat straw and coal. *VTT Technology*. 291.

Lagoa-Costa, B., Abubackar, H. N., Fernández-Romastana, M., Kennes, C. and Veiga, M. C. 2017. Integrated bioconversion of syngas into bioethanol and biopolymers. *Bioresource Technology*. 239:244-249.

Lane, J. 2014. On the Mend: Why INEOS Bio Isn't Producing Ethanol in Florida [online]. *BiofuelsDigest*. Available at: http://www.biofuelsdigest.com/bdigest/2014/09/05/on-the-mend-why-ineos-bio-isnt-reporting-much-ethanol-production/ [accessed June 13. 2017].

Lara Márquez, A., Wild, G. and Midoux, N. 1994. A review of recent chemical techniques for the determination of the volumetric mass-transfer coefficient $k_L a$ in gas-liquid reactors. *Chemical Engineering and Processing*. 33:247-260.

Lewis, R. S., Tanner, R. S. and Huhnke, R. L. 11/29/2007. Indirect or direct fermentation of biomass to fuel alcohol. US patent no.: US 2007/0275447 A1.

Liebal, U. W., Blank, L. M. and Ebert, B. E. 2018. CO_2 to succinic acid – Estimating the potential of biocatalytic routes. *Metabolic engineering Communications*.7:75. doi: 10.1016/j.mec.2018.e00075.

Liew, F. M., Köpke, M. and Simpson, S. D. 2013. Gas Fermentation for Commercial Biofuels Production. In: Zhen Fang (Ed.) *Liquid, Gaseous and Solid Biofuels – Conversion Techniques*. Rijeka: INTECH. 125-173.

Liew, F. M., Martin, M. E., Tappel, R. C., Heijstra, B. D., Mihalcea, C. and Köpke, M. 2016. Gas Fermentation – A Flexible Platform for Commercial Scale Production of Low-Carbon-Fuels and Chemicals from Waste and Renewable Feedstocks. *Frontiers in Microbiology*. 7:1-28. Doi: 10.3389/fmicb.2016.00694.

Linek, V. and Sinkule, V. 1991. The Influence of Gas and Liquid Axial Dispersion on Determination of $k_L a$ by Dynamic Method. *Transactions of the Institution of Chemical Engineers*. 69(A):308-312.

Linek, V. and Vacek, V. 1981. Chemical engineering use of catalyzed sulphite oxidation kinetics for determination of mass transfer characteristics of gas-liquids contactors. *Chemical Engineering Science*. 36(11):1747-1768.

Linek, V. Benes, P. and Vacek, V. 1989. Dynamic Pressure Method for $k_L a$ Measurement in Large-Scale Bioreactors. *Biotechnology and Bioengineering*. 33(11):1406-1412.

Linek, V., Vacek, V. and Bennes, P. 1987. A critical review and experimental verification of the correct use of the dynamic method for the determination of oxygen-transfer in aerated agitated vessels to water, electrolyte-solutions and viscous liquids. *The Chemical Engineering Journal*. 34(1):11-34.

Liu, K., Atiyeh, H. K., Stevenson, B. S., Tanner, R. S., Wilkins, M. R. and Huhnke, R. L. 2014. Continuous syngas fermentation for the production of ethanol, n-propanol and n-butanol. *Bioresource Technology*. 151:69-77.

Lohbeck, K., Haferkorn, H., Fuhrmann, W. and Fedtke, N. 2000. Meleic and fumaric acids. In: Elvers, B. (ed.) *Ullmann's Encyclopedia of Industrial Chemistry*. Weinheim: Wiley-VCH Verlag. 145-155.

Löser, C., Schröder, A., Deponte, S. and Bley, T. 2005. Balancing the Ethanol Formation in Continuous Bioreactors with Ethanol Stripping. *Engineering in Life Sciences*. 5(4):325-332.

Maier, B., Dietrich, C. and Büchs, J. (2001). Correct application of the sulphite oxidation methodology of measuring the volumetric mass transfer coefficient $k_L a$ under non-pressurized and pressurized conditions. *Transactions of the Institution of Chemical Engineers*. 79(2):107-113.

Maness, P.C. and Weaver, P. F. 2001. Evidence for three distinct hydrogenase activites in *Rhodospirillum rubrum. Applied Microbiology and Biotechnology*. 57(5-6):751-756.

Miltenberger, K. 2000. Hydroxycarboxylic acids, aliphatic. In: Elvers, B. (ed.) *Ullmann's Encyclopedia of Industrial Chemistry*. Weinheim: Wiley-VCH Verlag. 145-155.

Mock, J., Zheng, Y., Mueller, A. P., Ly, S., Tran, L., Segovia, S., Nagaraju, S., Köpke, M., Dürre, P. and Thauer, R. K. 2015. Energy Conservation Associated with Ethanol Formation from H_2 and CO_2 in *Clostridium autoethanogenum* Involving Electron Bifurcation. *Journal of Bacteriology*. 197(18):2965-2980.

Molitor, B., Marcellin, E. and Angenent, L. T. 2017. Overcoming the energetic limitations of syngas fermentation. *Current Opinion in Chemical Biology*. 41:84-92. doi: 10.1016/j.cbpa.2017.10.003.

Müller, V. 2003. Energy Conservation in Acetogenic Bacteria. *Applied and Environmental Microbiology*. 69(11):6345-6353.

Nagarajan, H., Sahin, M., Nogales, J., Latif, H., Lovley, D. R., Ebrahim, A. and Zengler, K. 2013. Characterizing acetogenic metabolism using a genome-scale metabolic reconstruction of *Clostridium ljungdahlii. Microbial Cell Factories*. 12(1):118-131.

Neumann, A., Dörsam, S., Oswald, F. and Ochsenreither, K. 2016. Microbial Production of Value-Added Chemicals from Pyrolysis Oil and Syngas. In: M. Xian (Ed.) *Sustainable Production of Bulk Chemicals. Integration of Bio-, Chemo-Resources and Processes*. Dordrecht: Springer Science+Business Media.

Ochsenreither, K., Fischer, C., Neumann, A. and Syldatk, C. 20014. Process characterisation and influence of alternative carbon sources and carbon-to-nitrogen ratio an organic acid production by *Aspergilus oryzae* DSM1863. *Applied Microbiology and Biotechnology*. 98(12):5449-5460. doi: 10.1007/s00253-014-5614-x.

Ohyama, T. and Yamazaki, I. 1975. Formate Dehydrogenase. Subunit and Mechanism of Inhibition by Cyanide and Azide. *The Journal of Biochemistry*. 77:845-852.

Orgill, J. J., Atiyeh, H. K., Devarapalli, M., Phillips, J. R., Lewis, R. S. and Huhnke, R. L. 2013. A comparison of mass transfer coefficients between trickle-bed, hollow fiber and stirred tank reactors. *Bioresource Technology*. 133:340-346.

Osmani, S. A. and Scrutton, M. C. 1983. The sub-cellular localisation of pyruvate carboxylase and of some other enzymes in *Aspergillus nidulans. Eur. J. Biochem*. 133:551–560. doi: 10.1111/j.1432-1033.1983.tb07499.x

Oswald, F., Dörsam, S., Veith, N., Zwick, M., Neumann, A., Ochsenreither, K. and Syldatk, C. 2016. Sequential Mixed Cultures: From Syngas to Malic Acid. *Frontiers in Microbiology*. 7:891. DOI: 10.3389/fmicb.2016.00891.

Oswald, F., Stoll, I. K., Zwick, M., Herbig, S., Sauer, J., Boukis, N. and Neumann, A. 2018a. Formic Acid Formation by *Clostridium ljungdahlii* at Elevated Pressures of Carbon Dioxide and Hydrogen. *Frontiers in Bioengineering and Biotechnology*. 6:6. doi: 10.3389/fbioe.20180006.

Oswald, F., Zwick, M., Omar, O., Hotz, E. H. and Neumann, A. 2018b. Growth and Product Formation of *Clostridium ljungdahlii* in Presence of Cyanide. *Frontiers in Microbiology*. 9:1213. doi: 10.3389/fmicb.2018.01213.

Peleg, Y., Barak, A., Scrutton, M. C. and Goldberg, I. 1989. Malic acid accumulation by *Aspergillus flavus*. III. 13CNMR and isoenzyme analysis. 30:176–83. doi: 10.1007/BF00264008

Peleg, Y., Stieglitz, B. and Goldberg, I. 1988. Malic acid accumulation by *Aspergillus flavus* - I. biochemical aspects of acid biosynthesis. *Applied Microbiology and Biotechnology*. 28:69-75. doi: 10.1007/BF00250501

Peters, V., Janssen, P. H. and Conrad, R. (1999). Transient Production of Formate During Chemolithothrophic Growth of Anaerobic Microorganisms on Hydrogen. *Current Microbiology*. 38:285-289.

Ragsdale, S. W. and Wood, H. G. 1985. Acetate Biosynthesis by Acetogenic Bacteria. *Journal of Biological Chemistry*. 260(7):3970-3977.

Ragsdale, S. W., Clark, J. E., Ljungdahl, L. G., Lundie, L. L. and Drake, H. L. 1983a. Properties of Purified Carbon Monoxide Dehydrogenase from *Clostridium thermoaceticum*, a Nickel, Iron-Sulfur Protein. *The Journal of Biological Chemistry*. 258(4):2364-2369.

Ragsdale, S. W., Ljungdahl, L. G. and DerVartanian, D. V. 1983b. Isolation of Carbon Monoxide Dehydrogenase from *Acetobacterum woodii* and Comparison of Its Properties with Those of the *Clostridium thermoaceticum* Enzyme. *Journal of Bacteriology*. 155(3):1224-1237.

Roempp 2012. Article on the search term „Blausäure". Available at: https://roempp.thieme.de/roempp4.0/do/data/RD-02-01881 [last called at 25th of November 2017, 5:32 pm].

Rokni, M. 2015. Thermodynamic analyses of municipal solid waste gasification plant integrated with solid oxide fuel cell and Stirling hybrid system. *International Journal of Hydrogen Energy*. 40(24):7855-7869.

Schiel-Bengelsdorf, B., Montoya, J., Linder, S. and Dürre, P. 2013. Butanol fermentation. *Environmental Technology*. 34(13-14):1691-1710.

Schlüter, V., Yonsel, S. and Deckwer, W.-D. 1992. Korrelation der O_2-Stoffübergangskoeffizienten ($k_L a$) in Rührreaktoren mit niederviskosen Fermentationsmedien. *Chemie Ingenieur Technik*. 64(5):474-475.

Schmidt, R. L. and Cooney, C. L. 1986. Production of acetic acid from hydrogen and carbon dioxide by *Clostridium* species ATCC 29797. *Chemical Engineering Communications*. 45(1-6):61-73.

Schuchmann, K. and Müller, V. 2013. Direct and Reversible Hydrogenation of CO_2 to Formate by a Bacterial Carbon Dioxide Reductase. *Science*. 342:1382-1385.

Schuchmann, K. and Müller, V. 2014. Autotrophy at the thermodynamic limit of life: a model for energy conservation in acetogenic bacteria. *Nature Reviews Microbiology*. 12:809–821. doi: 10.1038/nrmicro3365.

Seravalli, J. and Ragsdale, S. W. 2000. Channeling of carbon monoxide during anaerobic carbon dioxide fixation. *Biochemistry*. 39(6):1274-1277.

Sikkema, J., De Bont, J. A. M. and Poolman, B. 1995. Mechanisms of Membrane Toxicity of Hydrocarbons. *Microbiological Reviews*. 59(2):201-222.

Simankova, M. V., Kotsyurbenko, O. R., Stackebrandt, E., Kostrikina, N. A., Lysenko, A. M., Osipov, G. A. and Nozhevnikova, A. N. 2000. *Acetobacterium tundra* sp. nov., a new psychrophilic acetogenic bacterium from tundra soil. *Archives of Microbiology*. 174(6):440-447.

Smith, E. T., Ensing, S. A., Ludden, P. W. and Feinberg, B. A. 1992. Direct electrochemical studies of hydrogenase and CO dehydrogenase. *Biochemical Journal*. 285(1):181-185.

Straub, M. 2012. Fermentative Acetatproduktion durch Homoacetat-Gärung bzw. Acetatbildung. Dissertation. Institute for Microbiology and Biotechnology. University of Ulm.

Strijbis, K., and Distel, B. 2010. Intracellular Acetyl Unit Transport in Fungal CarbonMetabolism. *Eukaryotic Cell*. 9:1809–1815. doi: 10.1128/EC.00172-10.

Tanner, R. 2007. Cultivation of Bacteria and Fungi. In: C. J. Hurst et al. (ed.) *Manual of Enviromental Microbiology*. 3rd Edition. Washington, D. C.: ASM Press. 69-78.

Tanner, R. S. and Laopaiboon, R. 1997. Invited Abstracts of The Art of Anaerobes Conference. Metabolism of *Clostridium ljungdahlii*, an acetogen in the clostridial RNA homology group I. *BioFactors*. 6(1):53-81.

Tanner, R., Miller, L. M. and Yang, D. 1993. *Clostridium ljungdahlii* sp. Nov., an Acetogenic Species in Clostridial rRNA Homology Group I. *International Journal of Systematic Bacteriology*.43(2):232-236.

Terlesky, K. C., Nelson, M. J. K. and Ferry, J. 1986. Isolation of an Enzyme Complex with Carbon Monoxide Dehydrogenase Activity Containing Corrinoid and Nickel from Acetate-Grown Methanosarcina thermophila. *Journal of Bacteriology*. 168(3)1053-1058.

Thauer, R. K., Fuchs, G., Käufer, B. and Schnitker, U. 1974. Carbon-Monoxide Oxidation in Cell-Free Extracts of *Clostridium Pasteurianum*. *European Journal of Biochemistry*. 45(2):343-349.

Tremblay, P-L., Zhang, T., Dar, S. A., Leang, C. and Lovley, D. R. 2012. The Rnf Complex of *Clostridium ljungdahlii* Is a Proton-Translocating Ferredoxin:NAD⁺ Oxidoreductase Essential for Autotrophic Growth. *mBio*. 4(1): e00406-12. doi:10.1128/mBio.00406-12.

University of Arkansas, Department of Chemical Engineering 1993. *High Pressure Synthesis Gas Conversion*. Final Report for the United States Department of Energy.

Van't Riet, K. 1979. Review of Measuring Methods and Results in Nonviscous Gas-Liquid Mass Transfer in Stirred Vessels. *Industrial & Engineering Chemistry Process Design and Development*. 18(3):357-364.

Vega, J. L., Antorrena, G. M., Clausen, E. C. and Gaddy, J. L. 1989a. Study of Gaseous Substrate Fermentations: Carbon Monoxide Conversion to Acetate. 2. Continous Culture. *Biotechnology and Bioengineering*. 34:785-793.

Vega, J. L., Clausen, E. C. and Gaddy, J. L. 1989b. Study of Gaseous Substrate Fermentations: Carbon Monoxide Conversion to Acetate. 1. Batch Culture. *Biotechnology and Bioengineering*. 34:774-784.

Vega, J. L., Klasson, K. T., Kimmel, D. E., Clausen, E. C. and Gaddy, J. L. 1990. Sulfur Gas Tolerance and Toxicity of CO-Utilizing and Methanogenic Bacteria. *Applied Biochemistry and Biotechnology*. 24-25(1):329-340.

Vega, J. L., Prieto, S., Elmore, B. B., Clausen, E. C. and Gaddy, J. L. 1989c. The Biological Production of Ethanol from Synthesis Gas. *Applied Biochemistry and Biotechnology*. 20/21:781-797.

Wang, S., Huang, H., Kahnt, A., Mueller, A. P., Köpke, M. and Thauer, R. K. 2013. NADP-Specific Electron-Bifurcating [FeFe]-Hydrogenase in a Functional Complex with Formate Dehydrogenase in *Clostridium autoethanogenum* Grown on CO. *Journal of Bacteriology*. 195(19):4373-4386.

Wang, S., Huang, H., Moll, J. and Thauer, R. K. 2010. NADP⁺ Reduction with reduced Ferredoxin and NADP⁺ Reduction with NADH Are Coupled via an Electron-Bifurcating Enzyme Complex in *Clostridium kluyveri*. *Journal of Bacteriology*. 192(19):5115-5123.

Werpy, T. and Petersen, G. 2004. Top *Value Added Chemicals from Biomass Volume I. Results of Screening for Potential Candidates from Sugars and Synthesis Gas*. Washington: U. S. Department of Energy.

White, H., Huber, C., Feich, R. and Simon, H. 1993. On a reversible molybdenum-containing aldehyde oxidoreductase from *Clostridium formicoaceticum*. *Archives of Microbiology*. 159(3)244-249.

Wilke, C. and Chang, P. 1955. Correlation of Diffusion Coefficients in Dilute Solutions. *AIChE Journal*. 1(2):264-270.

Wood, H. G. 1952. A Study of Carbon Dioxide Fixation by Mass Determination of Types of C¹³-Acetate*. *Journal of Biological Chemistry*. 194(2):905-932.

Wood, H. G. 1991. Life with CO or CO_2 and H_2 as a source of carbon and energy. *FASEB*. 5(2):156-163.

Worden, R. M., Bredwell, M. D. and Grethlein, A. J. 1997. Engineering Issues in Synthesis Gas Fermentations. In: Saha, B. (Ed.) *Fuels and Chemicals from Biomass*. ACS Symposium Series. Washington, DC: American Chemical Society. 320-335.

Xu, D., Tree, D. R. and Lewis, R. S. 2011. The effects of syngas impurities on syngas fermentation to liquid fuels. *Biomass and Bioenergy*. 35(7):2690-2696.

Yang, H. and Drake, H. 1990. Differential Effects of Sodium on Hydrogen- and Glucose-Dependent Growth of Acetogenic Bacterium *Acetogenium kivui*. *Applied and Environmental Microbiology*. 56:81-86.

Zlokarnik, M. 1973. Rührleistung in begasten Flüssigkeiten. *Chemie Ingenieur Technik*. 45(9-10):689-692.

Zlokarnik, M. 1979. Sorption characteristics of slot injectors and their dependency on the coalescence behaviour [!] of the system. *Chemical engineering Science*. 34(10):1265-1271.

Zlokarnik, M. 1981. Verfahrenstechnische Grundlagen der Reaktorgestaltung. *Acta Biotechnologica*. 1(4):311-325.

Zlokarnik, M. 1999. *Rührtechnik. Theorie und Praxis*. Berlin a. o.: Springer-Verlag.

List of figures

List of tables

Appendix

List of chemicals and vendors

Table 0.1 – List of Chemicals and their respective vendors used throughout this thesis.

Name	Elemental formula	Vendor
2-(N-morpholino) ethansulfonic acid (MES)	$C_6H_{13}NO_4S$	Carl-Roth, Germany
Yeast extract	n. a.	BD, USA
Sodium chloride	$NaCl$	Carl-Roth, Germany
Ammonium chloride	NH_4Cl	Carl-Roth, Germany
Potassium chloride	KCl	Carl-Roth, Germany
Potassium dihydrogen phosphate	KH_2PO_4	Carl-Roth, Germany
Magnesium sulfate heptahydrate	$MgSO_4 \cdot 7\ H_2O$	Carl-Roth, Germany
Calcium chloride dihydrate	$CaCl_2 \cdot 2\ H_2O$	Carl-Roth, Germany
Resazurin sodium salt	$NaC_{12}H_6NO_4$	Sigma-Aldrich, Germany
Nitrilotriacetic acid	$C_6H_9NO_6$	Sigma-Aldrich, Germany
Manganese(II) sulfate monohydrate	$MnSO_4 \cdot H_2O$	Sigma-Aldrich, Germany
Iron(II) sulfate heptahydrate	$FeSO_4 \cdot 7\ H_2O$	Carl-Roth, Germany
Cobalt(II) chloride hexahydrate	$CoCl_2 \cdot 6\ H_2O$	Riedel de haën, Germany
Zinc(II) sulfate heptahydrate	$ZnSO_4 \cdot 7\ H_2O$	Carl-Roth, Germany
Copper(II) chloride dihydrate	$CuCl_2 \cdot 2\ H_2O$	Carl-Roth, Germany
Nickel(II) chloride hexahydrate	$NiCl_2 \cdot 6\ H_2O$	Sigma-Aldrich, Germany
Sodium molybdate dihydrate	$Na_2MoO_4 \cdot 2\ H_2O$	Sigma-Aldrich, Germany
Sodium selenite pentahydrate	$Na_2SeO_3 \cdot 5\ H_2O$	Sigma-Aldrich, Germany
Sodium tungstate dihydrate	$Na_2WO_4 \cdot 2\ H_2O$	Sigma-Aldrich, Germany
Biotin (vitamin B_7)	$C_{10}H_{16}N_2O_3S$	Sigma-Aldrich, Germany
Folic acid (vitamin B_9)	$C_{19}H_{19}N_7O_6$	Sigma-Aldrich, Germany
Pyridoxine (vitamin B_6)	$C_8H_{11}NO_3$	Alfa Aesar, Germany
Thiamine-HCl (vitamin B_1)	$C_{12}H_{18}Cl_2N_4OS$	Carl-Roth, Germany

Table 0.1 – continuation

Name	Elemental formula	Vendor
Riboflavin (vitamin B$_2$)	$C_{17}H_{20}N_4O_6$	Sigma-Aldrich, Germany
Niacin (vitamin B$_3$)	$C_6H_5NO_2$	Sigma-Aldrich, Germany
Ca-pantothenate (vitamin B$_5$)	$C_{18}H_{32}CaN_2O_{10}$	Sigma-Aldrich, Germany
Cobalamin (vitamin B$_{12}$)	$C_{72}H_{100}CoN_{18}O_{17}P$	Sigma-Aldrich, Germany
4-aminobenzoic acid	$C_7H_7NO_2$	Sigma-Aldrich, Germany
Lipoic acid	$C_8H_{14}O_2S_2$	Cayman Chemical, USA
Contraspum A5040	n. a.	Zschimmer und Schwarz, Germany
Cysteine-HCl	$C_3H_7NO_2S \cdot HCl$	Carl-Roth, Germany
Calcium carbonate	$CaCO_3$	Carl-Roth, Germany
Ethanol	C_2H_6O	Carl-Roth, Germany
Sodium acetate	$C_2H_3NaO_2$	Carl-Roth, Germany
Isobutanol	$C_4H_{10}O$	Carl-Roth, Germany
Hydrochloric acid	HCl	Carl-Roth, Germany
Potassium cyanide	KCN	Sigma-Aldrich, Germany
Potassium hydroxide	KOH	Carl-Roth, Germany
Orthophosphoric acid	H_3PO_4	Carl-Roth, Germany

Results of third reactor from substrate consumption experiments

Table 0.2 – Results of substrate consumption experiments with *C. ljungdahlii* growing with syngas as sole carbon and energy source for the third bioreactor

Set-up	RMR-10	RRB-10	RMR-18	RRB-18	RMR-44	RRB-44
β_{CDW}/g L^{-1}	0.77	0.77	0.83	0.81	0.51	0.24
$\beta_{acetic\ acid}$/g L^{-1}	12.47	11.76	22.32	20.33	5.33	6.11
β_{EtOH}/g L^{-1}	0.90	1.09	1.36	1.11	4.47	2.75
$\beta_{fructose}$/g L^{-1}	0.71	0.45	0.61	0.53	0.72	0.76
$c_{H2,R}$/mol L^{-1}	0.38	0.42	0.56	0.65	0.05	-0.03
$c_{CO,R}$/mol L^{-1}	0.42	0.43	0.54	0.77	1.02	0.77
$c_{CO2,R}$/mol L^{-1}	-0.015	-0.01	-0.15	-0.07	-0.62	-0.51
$V_{gas,\ total}$/L	58.39	60.03	103.50	102.42	254.81	254.15
t/h	96.35	96.20	95.83	94.83	96.30	96.05
E_{H2}/%	69.17	75.27	60.02	68.16	1.99	-1.35
E_{CO}/%	77.59	81.19	83.86	81.00	42.26	32.11
E_{CO2}/%	-7.05	-2.67	-34.74	-15.82	-56.99	-47.80

The numbers behind RMR and RRB in the table header stand for the gas feed rate with $10 = 10.3$ mL min^{-1}, $18 = 17.8$ mL min^{-1}, $44 = 44.4$ mL min^{-1}. β_{CDW}, maximum concentration of CDW; $\beta_{Fructose}$, concentration of fructose at beginning of fermentation; $\beta_{acetic\ acid}$, final concentration of acetic acid; β_{EtOH}, final concentration of ethanol; $c_{H2,R}$, consumed amount of hydrogen per liter reactor volume; $c_{CO,R}$, consumed amount of carbon monoxide per liter reactor volume; $c_{CO2,R}$, consumed amount of carbon dioxide per liter reactor volume; $V_{gas,\ total}$, total volume of used syngas over the course of fermentation; t, total process time; E_{H2}, consumption ratio of hydrogen as consumed amount of hydrogen in per cent of total amount of ingoing hydrogen; E_{CO}, consumption ratio of carbon monoxide as consumed amount of carbon monoxide in per cent of total amount of ingoing carbon monoxide; E_{CO2}, consumption ratio of carbon dioxide as consumed amount of carbon dioxide in per cent of total amount of ingoing carbon dioxide. Negative Values in the columns $c_{CO2,R}$ and E_{CO2} mean that more CO_2 has left the reactor than has gone in.

Table 0.3 – Product yields based on consumed and used substrate as well as average durations of complete substrate consumption for the third bioreactor.

Set-up	RMR-10	RRB-10	RMR-18	RRB-18	RMR-44	RRB-44
$Y_{P/S}^{*}$/g g^{-1}	0.98	0.93	0.95	0.90	0.32	0.40
$Y_{P/S}^{**}$/g g^{-1}	0.76	0.76	0.79	0.73	0.13	0.12
$t_{eH2 \geq 97\%}$/h	38.5	49.5	12.00	15.13	0.00	0.00
$t_{eCO \geq 97\%}$/h	68.10	72.30	29.78	33.30	0.00	0.00

*, based on consumed H$_2$ and CO; **, based on totally fed H$_2$ and CO; $t_{eH2 \geq 97\%}$, duration of complete hydrogen consumption; $t_{eCO \geq 97\%}$, duration of complete carbon monoxide consumption.
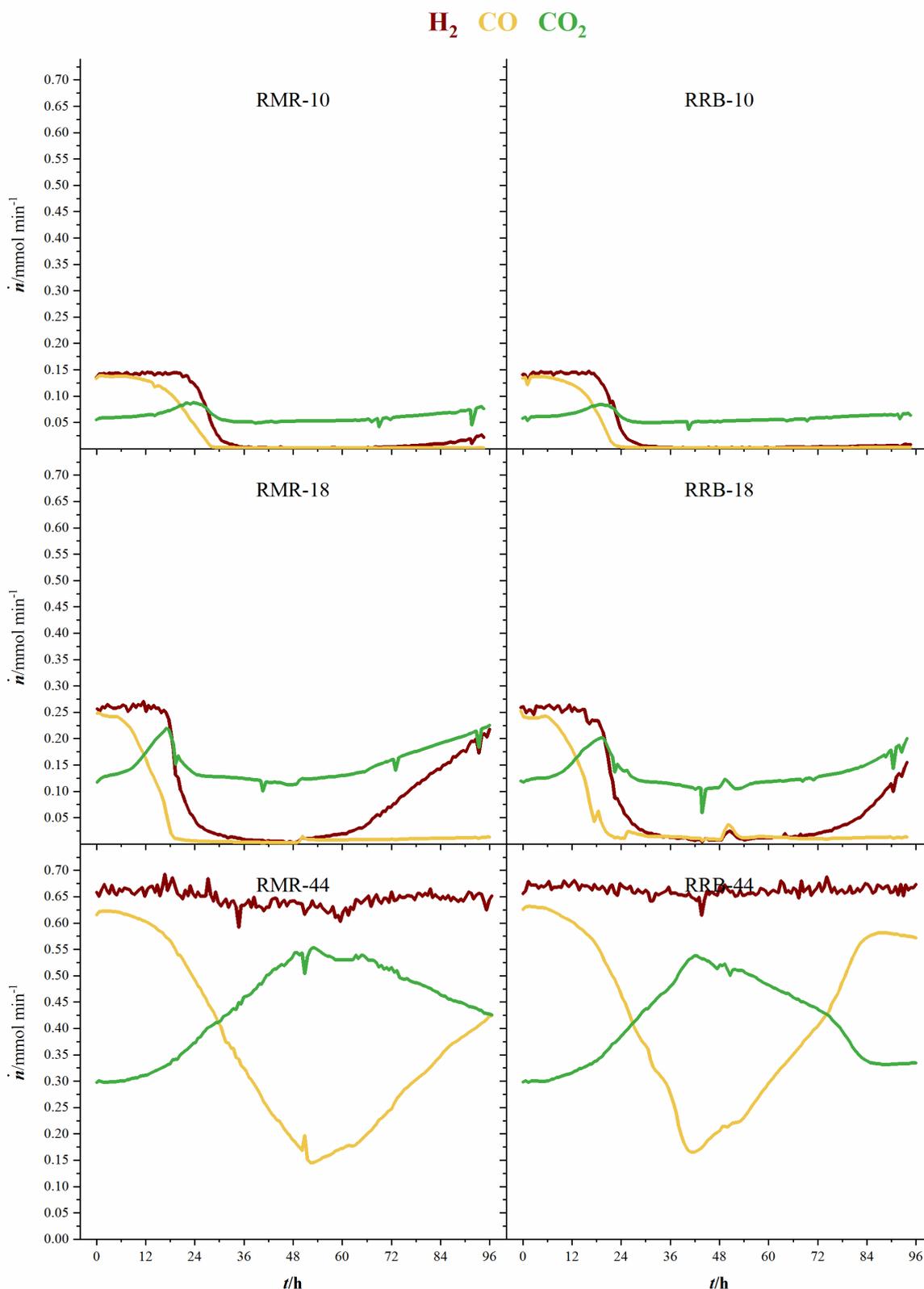
Figure 0.1 - amount of substance flow rates per liter medium in the off-gas of substrate consumption experiments for the third bioreactor. Results of experiments with RMR (left) and RRB stirrer set-up (right) at average gas flow rates of 10.33 ± 0.21 mL min^{-1}, 17.78 ± 0.22 mL min^{-1} and 44.38 ± 0.26 mL min^{-1} (top to bottom). Hydrogen (red line), carbon monoxide (yellow line) and carbon dioxide (green line).